



8-2001

Characterization of the tumor suppressor activity of the FHIT gene in association with application of innovative detection technologies

Minoo Askari Dermenaki Farahani

Follow this and additional works at: https://trace.tennessee.edu/utk_graddiss

Recommended Citation

Farahani, Minoo Askari Dermenaki, "Characterization of the tumor suppressor activity of the FHIT gene in association with application of innovative detection technologies. " PhD diss., University of Tennessee, 2001.

https://trace.tennessee.edu/utk_graddiss/8497

This Dissertation is brought to you for free and open access by the Graduate School at TRACE: Tennessee Research and Creative Exchange. It has been accepted for inclusion in Doctoral Dissertations by an authorized administrator of TRACE: Tennessee Research and Creative Exchange. For more information, please contact trace@utk.edu.

To the Graduate Council:

I am submitting herewith a dissertation written by Mino Askari Dermenaki Farahani entitled "Characterization of the tumor suppressor activity of the FHIT gene in association with application of innovative detection technologies." I have examined the final electronic copy of this dissertation for form and content and recommend that it be accepted in partial fulfillment of the requirements for the degree of Doctor of Philosophy, with a major in Biomedical Sciences.

Tuan Vo-Dinh, Major Professor

We have read this dissertation and recommend its acceptance:

Jeffery Becker, Stephen Kennel, Stephen Oliver

Accepted for the Council:

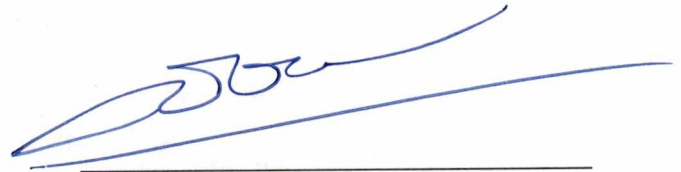
Carolyn R. Hodges

Vice Provost and Dean of the Graduate School

(Original signatures are on file with official student records.)


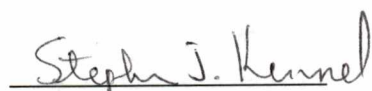
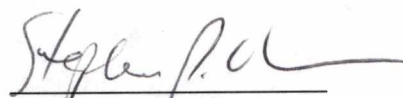
To the Graduate Council:

I am submitting herewith a dissertation by Minoos Askari Dermenaki Farahani entitled "Characterization of the Tumor Suppressor Activity of the FHIT Gene in Association with Application of Innovative Detection Technologies". I have examined the final copy of this dissertation for form and content and recommend that it be accepted in partial fulfillment of the requirements for the degree of Doctor of Philosophy, with a major in Biomedical Sciences.



Tuan Vo-Dinh, Ph.D., Major Professor

We have read this dissertation
and recommend its acceptance:


Jeffery Becker, Ph.D.
Stephen Kennel, Ph.D.
Stephen Oliver, Ph.D.

Accepted for the Council:



Interim Vice Provost and
Dean of the Graduate School

**Characterization of the Tumor Suppressor Activity of the
FHIT Gene in Association with Application of
Innovative Detection Technologies**

A Dissertation
Presented for the
Doctor of Philosophy Degree
The University of Tennessee, Knoxville

Minoo Askari Dermenaki Farahani

August 2001

DEDICATIONS

This dissertation is dedicated to

My Parents

Yadollah Askari Dermenaki Farahani
&
Mehri Yazdani

For teaching me to believe in myself and
without whom this would not have been possible

My Husband

Mahmoud Hassanalizadeh Haghghi

For his ever-present love and
a life time of support and encouragement

My Beloved Children

Bahbak Hassanalizadeh Haghghi
&
Orchideh Hassanalizadeh Haghghi

Lights of my life and my reasons for existence

ACKNOWLEDGEMENTS

I have been granted an opportunity at this obscure concept called life. I do not know if I am the one running the experiments or if I, myself, am an element in the study.

Nonetheless, I feel fortunate for the array of experiences that have sustained and guided me in my perpetual growth as a human being.

I extend my deepest gratitude to my family for giving me root and nourishing my soul. To my sister Mina who has always taught by example with love and kindness; to my brothers: Maziar, for teaching me everything is possible, and Ali, who shows me the daily power of faith; and to Kamran and Arash and Ashkon for their love and interest. I present my heartfelt thanks to all members of my extended family, Yazdani, Asiaban, Mirkarimi, Poor Mirzah, Haghighi, Askari, and all those who befriended me along the way. You all have significantly improved the quality of my life and provided me with valuable life lessons.

I offer my appreciation to my research advisor, Dr. Tuan Vo-Dinh, for supporting my research project. I am grateful to members of my committee, Professors Jeff Becker and Stephen Oliver and specifically Dr. Stephen Kennel, for their guidance and commitment to oversee this investigation. My appreciation is also extended to my colleagues at the Oak Ridge National Laboratory and the University of Tennessee at Knoxville for their assistance and fellowship during my tenure as a graduate student.

ABSTRACT

In early 1996, the Fragile Histidine Triad (FHIT) gene was cloned and shown to straddle the most active of the fragile human chromosome sites at chromosome band 3p14.2. The exceptionally large FHIT locus encompasses a hereditary renal carcinoma-associated chromosome translocation breakpoint. The size of the FHIT gene is about 1 megabase of genomic DNA, encoding a 1.1 kb mRNA message and a 16.8 kDa protein with diadenosine triphosphate hydrolase activity.

Early studies of a number of important human tumors such as breast, gastric, renal, and lung carcinoma and pancreatic adenocarcinoma have revealed that FHIT RNA expression was frequently altered and these alterations correlated with deletions in the FHIT gene, suggesting a role for this gene in development of cancer. There has also been a correlation between complete absence of Fhit protein and the early clinical stages of cancer. Such observations implicated FHIT as a putative tumor suppressor gene. Nonetheless, several lines of evidence have called into question the role of FHIT as a "classical" tumor suppressor gene, and raised the question of whether its apparent involvement simply reflects its location within an unstable region of the genome. Observation of biallelic deletions rather than mutations of the FHIT gene in cancers prompted a number of investigators to reject FHIT as a suppressor gene. In addition, consistent effects of exogenous FHIT on growth in cultures had not been observed. Additionally, experiments transfecting wild-type (*wild*) FHIT into tumor cell lines with FHIT abnormalities have

produced conflicting results regarding suppression of tumorigenesis *in vivo*.

The primary objective of this project was to investigate whether the FHIT gene was indeed a tumor suppressor gene. The goal was to establish a representation of the underlying molecular and cellular mechanisms of action of FHIT gene in suppression of tumorigenesis. The results demonstrate that the FHIT gene is indeed a tumor suppressor gene and that Fhit expression plays a possible role in induction of apoptosis. Our data indicates that Fhit protein alters the mitochondrial flux and efflux of molecules causing alterations in the transmembrane potential in the presence of apoptotic stimuli. We observed that induction of apoptosis in cells expressing the Fhit protein also involved the release of mitochondrial cytochrome c from the mitochondria and its subsequent translocation into the cytoplasmic compartment.

This investigation was also aimed at developing and applying novel spectroscopic and biosensing techniques and protocols designed to provide alternative methods for gene and protein identification, and defining gene function at the cellular and molecular levels for applications in biological research and clinical diagnosis laboratories. For the design of these systems, we took advantage of optical spectroscopy techniques including fluorescence, and synchronous luminescence spectroscopy, the biochip technology, and various microscopy methods. These modern technologies, developed at ORNL, have the potential to be selective, as well as sensitive, in providing information to understand how gene expression impacts a specific biological system.

TABLE OF CONTENTS

PART		PAGE
1.	INTRODUCTION AND PROJECT OVERVIEW	
1.1	Introduction	2
1.1.1	Historical Perspective	2
1.1.2	Fragile Histadine Triad, FHIT Gene	5
1.1.2.1	Deletions in the FHIT Gene	8
1.1.2.2	FHIT Transcription and Protein Expression	9
1.2	Hypothesis	11
1.2.1	Issues and Problem Statement	11
1.2.2	Objective and Specific Goals	13
1.3	Experimental Design	13
1.3.1	Generation of the Working Model	13
1.3.2	Technical Approach	14
1.3.3	Project Overview	15
1.3.4	Significance of the Proposed Research	17
1.3.5	Contributions to Future Research	19
	References	21
	Appendix	30
2.	SIMULTANEOUS DETECTION OF THE TUMOR SUPPRESSOR FHIT GENE AND PROTEIN USING THE MULTI-FUNCTIONAL BIOCHIP	35
2.1	Abstract	36
2.2	Introduction	37
2.3	Materials and Methods	39
2.3.1	Cell Lines	39
2.3.2	Fhit Protein Extraction and Quantification	40

2.3.3	Coomassie Brilliant Blue Analysis	40
2.3.4	Western Blot Analysis	41
2.3.5	FHIT Gene Amplification, Purification and Quantification.....	42
2.3.6	Fluorescent Labeling of Proteins	42
2.3.7	Microarray Sample Platform	43
2.3.8	Biochip Protein Assay	44
2.3.9	Biochip DNA Assay	44
2.3.10	Biochip Protein-DNA Assay	45
2.3.11	Instrumentation	45
2.3.11.1	Biochip Signal Detection System	45
2.3.11.2	Photometric Charge Coupled Device	46
2.4	Results and Discussion	47
2.4.1	Analysis of Fhit Protein Expression	48
2.4.1.1	Characterization of Fhit Expression in the Transfected Cell Lines	48
2.4.1.2	Analysis of Multiplex Protein Microarrays	50
2.4.1.3	Quantitative Fhit Protein Analysis	51
2.4.2	Analysis FHIT DNA	52
2.4.2.1	Analysis of FHIT DNA in the Transfected Cell Lines	52
2.4.2.2	Simultaneous Analysis of Multiple DNA Targets.....	53
2.4.2.3	Quantitative Analysis of FHIT DNA	55
2.4.3	Simultaneous FHIT Gene and Protein Multiplex Detection: The Multifunctional Biochip	55
2.5	Conclusion	56
2.6	Acknowledgements	57
	References	58
	Appendix	63

3.	ANALYSIS OF HYDROLYSIS ACTIVITY OF THE FHIT PROTEIN : APPLICATION OF SYNCHRONOUS LUMINESCENCE SPECTROSCOPY	76
3.1	Abstract	77
3.2	Introduction	78
3.3	Materials and Methods	79
	3.3.1 Fhit Hydrolysis Assay	79
	3.3.2 Synchronous Luminescence Spectroscopy	80
3.4	Results and Discussion	80
	3.4.1 Selection of Wavelength Interval	80
	3.4.2 Fhit Hydrolysis Reaction	81
	3.4.3 Quantitative Analysis of the Hydrolysis Assay	83
	3.4.4 Inhibition of the Enzymatic Reaction in Presence of ZnCl ₂	85
3.5	Conclusion	85
3.6	Acknowledgements	86
	References	87
	Appendix	90
4.	INVESTIGATION OF TUMOR SUPPRESSOR ACTIVITY AND APOPTOSIS-RELATED PROCESSES IN FHIT TRANSFECTED CELLS	98
4.1	Abstract	99
4.2	Introduction	100
4.3	Materials and Methods	103
	4.3.1 Cell Culture	103
	4.3.2 Western Blot Analysis	104
	4.3.3 Biochip DNA Analysis	105
	4.3.4 Growth Kinetics Analysis	106
	4.3.5 Murine Model for Tumorigenicity Assay	107
	4.3.6 Analysis of DNA Content for Cell Cycle Progression	107
	4.3.7 Analysis of Early Apoptotic Events	108

4.3.8	Analysis of DNA Fragmentation for Late Apoptotic Evaluation	108
4.3.9	Analysis of Production of Apoptotic Bodies	109
4.3.10	Alterations in the Mitochondrial Transmembrane Potential	110
4.4	Results and Discussion	110
4.4.1	Status of the FHIT Gene and Fhit Protein Expression in Cells ..	111
4.4.2	Phenotypic Effects of FHIT Expression on Cell Proliferation <i>In vitro</i>	112
4.4.3	Cell Cycle Kinetics	113
4.4.4	Tumor Suppressor Activity of the FHIT Expression <i>In vivo</i> ...	114
4.4.5	Potential Role of FHIT Gene in Apoptosis	115
4.4.6	Morphologic Analysis of Apoptosis	117
4.4.7	Alterations in the Inner Mitochondrial Transmembrane Potential	118
4.5	Conclusion	120
4.6	Acknowledgements	120
	References	122
	Appendix	129
5.	IMPLICATION OF MITOCHONDRIAL INVOLVEMENT IN APOPTOTIC ACTIVITY OF THE FHIT GENE	144
5.1	Abstract	145
5.2	Introduction	146
5.3	Materials and Methods	148
5.3.1	Cell Culture	148
5.3.2	Apoptosis Assay	149
5.3.3	Visualization of Altered Mitochondrial Activity	150
5.3.4	Evaluation of the Alterations in the Mitochondrial Membrane Potential	150
5.3.5	Evaluation of the Effects of Cyclosporin A	151
5.3.6	Inhibitory Effects of CsA on Loss of Transmembrane Potential	151

5.3.7	Cytochrome c Translocation and Western Blot Analysis	152
5.4	Results and Discussion	153
5.4.1	Characterization of the <i>In vitro</i> Model System	154
5.4.2	Alterations in the Inner Mitochondrial Transmembrane Potential	155
5.4.3	Possible Involvement of Mitochondrial Pores and Channels	157
5.4.4	Cytochrome C Translocation	159
5.5	Conclusion	161
5.6	Acknowledgements	161
	References	163
	Appendix	174
6.	SUMMARY AND CONCLUSION	188
6.1	Summary	189
6.1.1	FHIT Gene	189
6.1.2	Biotechnology	193
6.1.2.1	Biochip Technology.	193
6.1.2.2	Synchronous Luminescence Spectroscopy	194
6.2	Conclusion	195
6.2.1	FHIT Gene	195
6.2.2	Biotechnology	196
6.2.2.1	Biochip Technology	196
6.2.2.2	Synchronous Luminescence Spectroscopy	196
6.3	Future Research Directions	197
	References	199
	VITA	204

LIST OF FIGURES

FIGURE	PAGE
PART ONE	
1.1	Schematic diagram of chromosome 3 containing the fragile 3p14 region. 31
1.2	Fragile Histadine Triad, FHIT, gene DNA and protein sequences. 32
1.3	The map of FRA3B/FHIT loci at 3p14.2. The solid area at p14.2 shows the FRA3B region. FHIT exons are numbered 1 through 10; coding exons are in black. Positions of viral integration sites and t(3;8) translocation are marked with arrows. Gaps in the lines represent FHIT locus in the tumor cell lines demonstrate deletions. 33
PART TWO	
2.1	Schematic diagram of a biochip concept. Light from a 6.4 mW, He-Ne laser (632.8 nm) was transmitted through a laser band pass filter, a collimating lens, a 4 x 4 optical diffractive element and focused onto sample spots situated directly above the phototransistor detection elements. The 4x4 sensing array is comprised of 16 individual photodiodes arranged in a square with 900- μ m edges and 1-mm center-to-center spacing between them. A GRIN lens array, and a 650 \pm 10 nm band pass filter was situated between the detector elements and the sample substrate to isolate the fluorescence of interest. The photocurrent of each sensing element of the amplifier/ phototransistor microchip was transmitted to a digital voltmeter linked to a multimeter for data recording. 64
2.2	Study of nonspecific binding effect. Background fluorescent signal inherent to the biochip optical set up and the membrane platform were measured. Levels of background fluorescence signals are low and uniform in intensity providing an excellent baseline. 65

2.3	The MKN/FHIT and MKN/E4 gastric carcinoma cell lines were tested for expression of the Fhit protein. Coomassiee blue staining (Fig.2.3 a) and Western immunoblot analysis of cell lysates using anti-Fhit polyclonal antibody (Fig.2.3 b) show expression of detectable Fhit protein only in the MKN/FHIT cell line. Conversely, No exogenous Fhit expression was detected in the MKN/E4 cell line (Fig.2.3 a,b). Pure Fhit protein was included as positive control in the Coomassiee stained gel along with protein markers in both gels.	66
2.4	Biochip fluorescent signal measurement and analysis for detection of Fhit protein. Using Cy5-labeled polyclonal antibody against Fhit protein, fluorescent signals were detected from MKN/FHIT lysate row of spots. No significant fluorescence was observed from MKN/E4 lysate spots.	67
2.5	Simultaneous detection of multiple protein molecules was achieved using the biochip. Fluorescence signals were detected from the MKN/FHIT spots on the third row and p53 spots on the first row of the microarray. No signal was observed from MKN/E4 row of spots.	68
2.6	Fhit protein quantitative analysis. Biochip capability for quantitative analysis of different concentrations of the Fhit protein is demonstrated. The relative fluorescence signal detected by the biochip increased in response to increases in concentration of immobilized target MKN/FHIT lysate immobilized on the microarray in a curvilinear fashion.....	69
2.7	Genomic DNA was isolated from MKN/FHIT and MKN/E4 cell lysates using a guanidine- based lysing solution detected by gel electrophoresis (a). Extracted genomic DNAs were PCR amplified using sequence-specific primers for the FHIT gene and subjected to detection using fluorescently labeled FHIT DNA probes. As determined by the biochip, the MKN/FHIT cell line, PCR products, demonstrated significantly increased fluorescence signal over background as a result of retaining the FHIT gene. Presence of an intact FHIT gene did not present itself in the MKN/E4 cell line and the observed fluorescence signal was at the same level of the background fluorescence (b). Comparable biochip measurements were observed where targets were mixed with human serum (c).	70

2.8	Application of CCD system for detection of FHIT DNA. The CCD captured histogram of the row corresponding to the immobilized MKN/FHIT DNA (a) displayed a higher fluorescence signal as compared to MKN/E4 DNA spots (b). The CCD imaging results correlated well with the results from the biochip study and reconfirmed the absence of the FHIT gene in MKN/E4 cell line genomic extracts.	72
2.9	Application of the biochip for concurrent detection of various DNA molecules on the same microarray was accomplished. The biochip system simultaneously detected both immobilized target DNAs, the FHIT DNA and tuberculosis DNA (TB) on the same membrane using Cy5-labeled oligonucleotide probes for detection of both genes. Meanwhile, no fluorescence was detected from non-target MKN/E4 DNA row of spots. These results demonstrated the potential of the biochip for detection of a variety of distinct gene/ DNA probe molecules at one time.	73
2.10	FHIT DNA quantitative analysis. Biochip capability for quantitative analysis of FHIT DNA was illustrated by a relative increase in the signal output in response to increases in concentration of the membrane immobilized, FHIT DNA.....	74
2.11	Study of multi-target detection. Biochip device permitted simultaneous detection of immobilized MKN/FHIT lysate protein and PCR amplified FHIT DNA target molecules spotted in the same microarray using Cy5 labeled polyclonal Fhit antibody, and fluorescently labeled FHIT DNA probe. Biochip measurements demonstrated significant fluorescent signals from MKN/FHIT lysate spots row and the row where PCR amplified MKN/FHIT DNA was dispensed.	75

PART THREE

3.1	Deletions within the FHIT gene and absence of expression of Fhit protein occur in several common cancers.	91
3.2	The excitation, emission and SL spectra of tryptophan.	92

3.3	All spectroscopic measurements were performed using a single integrated workstation spectrofluorimeter with computer interfacing capabilities.	93
3.4	A representative SL spectrum ($\Delta\lambda = 50$ nm) for individual components of the hydrolysis reaction (a-c), the complete reaction (d) and confirmation of AMP formation (e) as a result of Ap_4A hydrolysis by Fhit protein are presented. Fluorescence spectrum of the hydrolysis solution (a) demonstrated absence of any distinguishable peaks. The spectrum of Ap_4A substrate (b) exhibited low fluorescence intensity with two broad peaks at 320 nm and 360 nm. The spectrum of Fhit protein (c) had higher fluorescence intensity than the Ap_4A substrate and two broad peaks at 285 nm and 370 nm. Addition of Fhit protein to an Ap_4A containing solution resulted in (d) a spectrum profile where there was a noticeable increase in the ratio of 285 nm to 370 nm, when compared to the fluorescence scan of Fhit alone. Addition of AMP to the same reaction vial (e) exhibited an increase only in the fluorescence intensity of the by-product peak at 285 nm.	94
3.5	Synchronous Luminescence peak for AMP in the hydrolysis solution occurred at 285 nm ($\Delta\lambda = 50$ nm).	95
3.6	The quantitative ability of the SL technique to measure fluorescence intensity associated with increased AMP production at constant Fhit protein concentration and increasing concentrations of Ap_4A (10-50 μM) are illustrated.	96
3.7	Inhibitory effects of $ZnCl_2$ (100 μl) on hydrolysis activity of Fhit protein are demonstrated. Fluorescence intensity of the 285 nm peak did not increase relative to the intensity of the second peak in presence of $ZnCl_2$. This alteration in the fluorescence profile was expected if Fhit protein had maintained its hydrolysis activity in the presence of Zn^{2+}	97

PART FOUR

4.1	Stable transfection of FHIT gene. Genomic DNAs isolated from MKN/FHIT and MKN/E4 cell lysates were PCR amplified using sequence-specific primers for the FHIT gene and subjected to detection using fluorescently labeled FHIT DNA probes. As determined by the
-----	---

biochip, the MKN/FHIT cell line demonstrated significantly increased fluorescence signal over the background as a result of retaining the FHIT gene. Presence of an intact FHIT gene did not present itself in the MKN/E4 cell line and the observed fluorescence signal was at the same level of background fluorescence in the MKN/FHIT cell line is demonstrated. 130

4.2 Fhit protein expression in cell lines. The MKN/FHIT, MKN/E4, 293 and AGS cell lines were tested for expression of Fhit protein. Western immunoblot analysis of cell lysates using anti-Fhit polyclonal antibody showed expression of detectable Fhit protein only in MKN/FHIT and 293 cell lines. Conversely, no exogenous Fhit expression was detected in MKN/E4 or AGS cell lines. 131

4.3 Effects of Fhit expression on the ability of cells to proliferate. MKN/FHIT transfected cell line and FHIT-positive 293 cell line along with Fhit-minus MKN/E4 and AGS cell lines were maintained continuously in their growth media. Significant difference in growth rates of each of the four cell lines were found. The MMC-treated (a) and EMS-treated (b) cells with stable Fhit expression demonstrated decreased proliferation rates as evidenced by their increased doubling time compared with FHIT-minus cells grown under the same conditions. 132

4.4 Distribution of nuclear DNA contents measured by flow cytometry. Distribution of nuclear DNA contents in MKN/FHIT cells (a) and MKN/E4 cells (b) grown under normal tissue culture conditions harvested 3 days after seeding. Different DNA contents and variation in percentages of cells in each stage of the cell cycle were observed. 134

4.5 Demonstration of *in vivo* tumor suppressor activity of the FHIT gene. (a) Transfected cells from MKN/FHIT and MKN/E4 cultures were harvested by trypsinization and resuspended in PBS at 2.5×10^7 /ml. A population of 5×10^6 cells in 0.2 ml of PBS were injected subcutaneously into the right flank of 6-week-old female nude mice, five mice per cell line. A group of 5 control mice were injected only with 0.2 ml of PBS. Inoculated animals were monitored twice weekly for tumor formation. Stable Fhit wild-type expression in transfected cancer cell clones suppressed tumor growth in nude mice. (b) The H&E stained tumors excised from mice. 136

- 4.6 Representative MKN/FHIT and MKN/E4 tumors were excised from mice. Western immunoblot analysis of MKN/FHIT and MKN/E4 tumor lysates demonstrated presence of Fhit protein only in MKN/FHIT tumors (a). Genomic DNA was isolated from these tumors and PCR amplified for the FHIT gene. Using the biochip, presence of the FHIT gene in the MKN/FHIT tumors and its absence in the MKN/E4 tumors was demonstrated (b)..... 137
- 4.7 Apoptosis among transfected MKN cells were analyzed by staining profiles of PE-conjugated Annexin-V for identification of early apoptotic cells and 7-AAD for identifying dead cells. Flow cytometric comparisons among the MKN/E4 cells (a) and MKN/FHIT cells (b) indicated a significantly higher number of apoptotic cells in MKN/FHIT cells. 138
- 4.8 In situ TUNEL staining of MKN/FHIT and MKN/E4 cells. Higher percentage of MKN/FHIT cells than MKN/E4 cells showed condensed and fragmented nuclei illustrated by higher number of MKN/FHIT cells incorporating the fluorescein-labeled dUTP. This indicates a higher ratio of apoptosis-induced DNA strand breaks in these cells. 139
- 4.9 Transmission electron micrograph of MMC-treated MKN/FHIT cells. Formation of typical apoptotic bodies that contain intact intracellular organelles is demonstrated (x 5000)..... 141
- 4.10 Confocal microscopy of MKN/FHIT and MKN/E4 cells incubated in media containing Rhodamine 123. Increased in the mitochondrial uptake of rhodamine 123 by MMC-treated MKN/FHIT is observed. 143

PART FIVE

- 5.1 Mitochondrial and the death receptor pathways are the two major apoptotic pathways that converge on cleavage of the cell death effector procaspases..... 175
- 5.2 Mitochondria induce apoptosis by releasing cytochrome c from intermembrane space to the cytosol. Cytosolic cytochrome c interacts with apoptotic protease activating factor 1 and procaspase 9 to form the apoptosome. In presence of ATP, the apoptosome cleaves procaspase 9 to the active form caspase 9, which, in turn, cleaves procaspase 3 to active caspase. 176

5.3	Expression of FHIT significantly inhibited apoptosis induced by MMC treatment for 20 h and analyzed by in situ TUNEL staining. Comparison of staining profiles of the MKN/FHIT (a) expressing Fhit protein with that of FHIT-minus MKN/E4 cells indicated a higher percentage of apoptotic MKN/FHIT with condensed and fragmented nuclei incorporating fluorescein-labeled dUTP.	177
5.4	Apoptotically-induced and untreated MKN/FHIT and MKN/E4 cells were incubated in growth media containing rhodamine123 which is a mitochondria specific lipophilic cation fluorescent dye. The dye is taken up in proportion to $\Delta\Psi_m$. The increase in rhodamine 123 uptake by MMC-treated cells was visually confirmed by fluorescent light microscopy (c,d) over untreated cells (a,b). However, MMC-treated MKN/FHIT cell-staining (c) was significantly enhanced as compared to staining of FHIT-negative MKN/E4 cells (d).	178
5.5	Confocal microscopy of MKN/FHIT and MKN/E4 cells incubated in media containing rhodamine 123 after induction of programmed cell death. Loss of mitochondrial membrane potential was demonstrated by increased uptake of rhodamine 123 by MKN/FHIT over MKN/E4 cells.	179
5.6	Excitation (a) and emission (b) spectra of rhodamine 123 which was taken up by mitochondria of MKN/FHIT cells.	180
5.7	Excitation, emission and synchronous spectra of R123 in PBS with a peak at 510 nm (a), and Synchronous spectra of cellular R123 uptake as a result of alterations in mitochondrial membrane potential of the MMC-treated and untreated MKN/FHIT (b) are illustrated.	181
5.8	Loss of $\Delta\Psi_m$ in the mitochondrial transmembrane of apoptotically-induced cells as a function of time (a). A steady increase in the cellular uptake of R123 was observed for the first 30 min after which the cells reached a steady state of equilibrium (b).	182
5.9	Effects of Fhit protein expression on cell proliferation in presence or absence of apoptotic inhibitor was investigated. The proliferation rate of MKN/FHIT cells maintained in growth media supplemented with MMC (second group of bar graphs) was significantly decreased in comparison with the growth rate of	

	cells cultured in the unsupplemented growth media (first group of bar graphs). Effects of the megachannel antagonist CsA blocked decrease in the doubling time of cells (third group of bar graphs) (c).	183
5.10	Synchronous luminescence spectroscopy revealed prevention of $\Delta\Psi_m$ -dependent uptake of R123 in apoptotically induced MKN/FHIT cells in presence of CsA.	184
5.11	Ultraviolet fluorescence microscopy of MKN/FHIT cells after rhodamine 123 incubation. MMC treatment (b) induced loss of membrane potential in mitochondrial organelles and increased rhodamine 123 uptake over untreated cells (a). Cyclosporin A inhibited loss of membrane potential as indicated by a lower level of rhodamine 123 uptake by cells.	185
5.12	Protein immunoblot analysis of cytochrome c expression in lysates of apoptotically induced MKN/FHIT and MKN/E4 cells. Samples of whole cell lysates or mitochondria extracted lysates were subjected to PAGE electrophoresis, western blotting, cytochrome c antibody probing and chemiluminescence visualization. Cytochrome c was detected in whole cell lysates of both MKN/FHIT and MKN/E4 cells (lanes 1 and 3). However, treatment of MKN/FHIT cells with MMC resulted in translocation of cytochrome c from the mitochondria into the cytosol (lane 2), indicated by equivalent concentration of the cytochrome c in the sample where mitochondria was present in the cytosol (lane 1). Detectable cytochrome c in MKN/E4 cell lysate did not translocate into the cytoplasm as was indicated by diminished protein band in the mitochondria removed lane (lane 4) as compared with the lane containing total expressed cytochrome c (lane 3).	187

LIST OF TABLES

TABLE		PAGE
PART ONE		
1.1	Estimated new cancer cases and deaths for 2001, all races, by case.	34
PART FOUR		
4.1	Percentages of cells in different stages of the cell cycle.	135
4.2	Percentage of the MMC induced MKN/FHIT and MKN/E4 apoptotic cells analyzed by TUNEL assay.....	140
4.3	Observed percentage of apoptotic cells in MMC-induced MKN/FHIT and MKN/E4 cell lines determined by transmission electron microscopy.	142

LIST OF ABBREVIATIONS

7-AAD	7-amino actinomycin D
AIF	apoptosis-inducing factor
AMP	adenosine monophosphate
AP₃A	diadenosine 5-prime,5-triple prime-P(1),P(3)-triphosphate
AP₄A	diadenosine 5-prime,5-triple prime-P(1),P(4)-triphosphate
APAF-1	apoptotic protease activating factor 1
ATP	adenosine triphosphate
BSA	bovine serum albumin
CCD	charge-coupled devices
CLSM	confocal laser scan microscopy
CMV	cytomegalovirus
CsA	cyclosporin A
Da	Dalton
DMEM	Delbecco's modified eagles medium
EMS	ethyl methane sulfonyl
FBS	fetal bovine serum
FHIT	fragile histidine triad gene
Fhit	fragile histidine triad protein
HIT	Histidine Triad
HRCA1	hereditary renal cancer associated 1
HNSCC	head and neck cancers
HMGIC	High Mobility Group Protein Isoform-C

LINE	long interspersed nuclear element
LOH	loss of heterozygosity
MMC	mitomycin c
PBS	phosphate buffered saline
PCR	polymerase chain reaction
PE	phycoerythrin
PI	propidium iodide
PT	permeability transition
R123	rhodamine 123
RT-PCR	reverse-transcription polymerase chain reaction
SDS	sodium dodecyl sulfate
SL	synchronous luminescence spectroscopy
TEM	transmission electron microscopy
TNF	tumor necrosis factor
TUNEL	terminal deoxynucleotidyl transferase labeling
VHL	von Hippel-Lindau gene
wt	wild type
YAC	yeast artificial chromosome
$\Delta\lambda$	wavelength interval
$\Delta\Psi_m$	mitochondrial transmembrane potential

LIST OF PROJECT RELATED PUBLICATIONS

M. Askari, T. Vo-Dinh. 2001. Involvement of the Mitochondria in Apoptotic Activity of the FHIT gene; Application of Synchronous Luminescence Spectroscopy (In preparation)

M. Askari, T. Vo-Dinh. 2001. Investigations of the Tumor Suppressor Activity and Apoptosis-related Processes in FHIT Transfected Cell Lines (In preparation)

M. Askari, G. Miller, T. Vo-Dinh. 2001. Simultaneous Detection of the Tumor Suppressor FHIT Gene and Protein Using the Multi-functional Biochip. *Cancer* (Submitted)

M. Askari, G. Miller, T. Vo-Dinh. 2001. Synchronous Luminescence: A Simple Technique for the Analysis of Hydrolysis Activity of the FHIT Protein. *Biotechnology Letters* (In press)

T. Vo-Dinh, M. Askari. 2001. Microarrays and Biochips: Applications and Potential in Genomics and Proteomics. *Current Genomics* (In press)

L.R. Allain, M. Askari, D.L. Stokes, T. Vo-Dinh. 2001. Microarray Sampling Platform Fabrication Using Bubble-Jet Technology for a Biochip System. *Fresenius J Anal Chem.* (In press)

M. Askari, J.P. Alarie, M. Moreno-Bondi, T. Vo-Dinh. 2001. Application of an Antibody Biochip for P53 Detection and Cancer Diagnosis. *Biotechnology Progress*, 17(3):543-552

LIST OF ABBREVIATIONS

7-AAD	7-amino actinomycin D
AIF	apoptosis-inducing factor
AMP	adenosine monophosphate
AP₃A	diadenosine 5-prime,5-triple prime-P(1),P(3)-triphosphate
AP₄A	diadenosine 5-prime,5-triple prime-P(1),P(4)-triphosphate
APAF-1	apoptotic protease activating factor 1
ATP	adenosine triphosphate
BSA	bovine serum albumin
CCD	charge-coupled devices
CLSM	confocal laser scan microscopy
CMV	cytomegalovirus
CsA	cyclosporin A
Da	Dalton
DMEM	Delbecco's modified eagles medium
EMS	ethyl methane sulfonyl
FBS	fetal bovine serum
FHIT	fragile histidine triad gene
Fhit	fragile histidine triad protein
HIT	Histidine Triad
HRCA1	hereditary renal cancer associated 1
HNSCC	head and neck cancers
HMGIC	High Mobility Group Protein Isoform-C

LINE	long interspersed nuclear element
LOH	loss of heterozygosity
MMC	mitomycin c
PBS	phosphate buffered saline
PCR	polymerase chain reaction
PE	phycoerythrin
PI	propidium iodide
PT	permeability transition
R123	rhodamine 123
RT-PCR	reverse-transcription polymerase chain reaction
SDS	sodium dodecyl sulfate
SL	synchronous luminescence spectroscopy
TEM	transmission electron microscopy
TNF	tumor necrosis factor
TUNEL	terminal deoxynucleotidyl transferase labeling
VHL	von Hippel-Lindau gene
wt	wild type
YAC	yeast artificial chromosome
$\Delta\lambda$	wavelength interval
$\Delta\Psi_m$	mitochondrial transmembrane potential

LIST OF PROJECT RELATED PUBLICATIONS

M. Askari, T. Vo-Dinh. 2001. Involvement of the Mitochondria in Apoptotic Activity of the FHIT gene; Application of Synchronous Luminescence Spectroscopy (In preparation)

M. Askari, T. Vo-Dinh. 2001. Investigations of the Tumor Suppressor Activity and Apoptosis-related Processes in FHIT Transfected Cell Lines (In preparation)

M. Askari, G. Miller, T. Vo-Dinh. 2001. Simultaneous Detection of the Tumor Suppressor FHIT Gene and Protein Using the Multi-functional Biochip. *Cancer* (Submitted)

M. Askari, G. Miller, T. Vo-Dinh. 2001. Synchronous Luminescence: A Simple Technique for the Analysis of Hydrolysis Activity of the FHIT Protein. *Biotechnology Letters* (In press)

T. Vo-Dinh, M. Askari. 2001. Microarrays and Biochips: Applications and Potential in Genomics and Proteomics. *Current Genomics* (In press)

L.R. Allain, M. Askari, D.L. Stokes, T. Vo-Dinh. 2001. Microarray Sampling Platform Fabrication Using Bubble-Jet Technology for a Biochip System. *Fresenius J Anal Chem.* (In press)

M. Askari, J.P. Alarie, M. Moreno-Bondi, T. Vo-Dinh. 2001. Application of an Antibody Biochip for P53 Detection and Cancer Diagnosis. *Biotechnology Progress*, 17(3):543-552

PART ONE

INTRODUCTION AND OVERVIEW

1.1 INTRODUCTION

1.1.1 Historical Perspective

In 1979 a family in which members with an inherited chromosomal translocation, $t(3;8)(p21;q24)$, were predisposed to renal cancer was described (1). In 1982, direct cytogenic studies on chromosome preparations of the renal cell carcinoma cells and the cultured peripheral blood lymphocytes of a patient with familial renal cell carcinoma were performed. The results revealed a specific, acquired translocations ($3p;11p$) present in the majority of metaphases of the tumor, indicating that the development of renal cell carcinoma was associated with a deletion in the proximal end of 3p (2). Later on in 1984, scientists used high resolution prometaphase G-banding analysis to demonstrate that the breakpoints occurred at the subbands 3p14.2 (not 3p21) and 8q24.1 translocation carriers from the $t(3;8)$ hereditary renal cell carcinoma family. It was clearly illustrated that the chromosomal rearrangement was reciprocal with breakpoints occurring at the sub-bands 3p14.2 and 8q24.1 (3).

Although the breakpoint of the balanced, reciprocal constitutional chromosome translocations, $t(3;8)(p21;q24)$, segregating with early onset multifocal renal carcinoma, was believed to mark the site of an oncogene or a tumor suppressor gene, more recent speculations suggested otherwise. In 1993 following up on the family reported (1) in 1979, investigators noticed that the tumors from 3 family members consistently showed

loss of the entire derivative chromosome 8, which bore the segment 3pter-p14. In contrast, no genetic change was detected in the derivative chromosome 3 or in normal chromosomes 3 and 8. One interpretation from these findings was that the breakpoints in chromosomes 3 and 8, *per se*, had no relevance to the renal carcinoma (4). Instead, other observations (1994) suggested that the breakpoint simply supplied a mechanism for the tumor to lose an allele between 3p14.2 and 3pter, and that, the occurrence of renal carcinoma was related to the tendency toward loss of the terminal part of 3p containing the von Hippel-Lindau gene (VHL). Further research demonstrated that the VHL gene was mutated in the germline of individuals with familial renal carcinoma reported by Cohen *et al.*, and that these same tumors retained one copy of a mutated VHL gene at 3p25 (5).

If the constitutional 3p14.2 break point had inactivated a tumor suppressor gene, then the tumors might be expected to lose the normal chromosome 3, to follow the established paradigm of the retinoblastoma model. This model suggests that a germline suppressor gene allele be mutated in all cells, so that the familial tumor cell need only mutate, or more often lose, the remaining normal allele (4-7,9). However, faced with many examples of chromosome translocations as initiators of tumorigenesis in soft tissues and hematopoietic cells, these accounts, though not without merit, were not necessarily imposing.

The search continued for a gene affected by the t(3;8) translocation. Positional cloning of the 3p14.2 breakpoint in the family reported in 1979 was accomplished in 1993 (6).

By positioning a chromosome 3 probe between the t(3;8) breakpoint and an aphidicolin-induced 3p14 breakpoint, a subsequent chromosome walk using yeast artificial chromosome (YAC) and use of a lambda sublibrary allowed isolation of clones spanning the t(3;8) rearrangement. Screening a kidney cDNA library by incorporation of unique and evolutionarily conserved DNA sequences, they identified a gene, referred to as HRCA1 (hereditary renal cancer associated 1), that mapped immediately adjacent to the breakpoint. On the basis of its chromosomal position, HRCA1 was considered to be a candidate tumor suppressor Gene (6,7).

Later in 1996, scientists pointed out that a 200-300-kb region of 3p14.2, including the fragile site locus FRA3B, closely telomeric to the t(3;8) breakpoint, was deleted homozygously in multiple tumor-derived cell lines (Fig. 1.1). By use of exon amplification from cosmids covering this deleted region, and defining of the smallest region of overlap of these homozygous deletions, they identified a portion of the human gene called FHIT (Fig. 1.2) for 'fragile histidine triad gene.' The gene was composed of 10 exons (Fig. 1.3) distributed over at least 500 kb, with three 5-prime untranslated exons centromeric to the renal carcinoma-associated 3p14.2 breakpoint, with the remaining exons telomeric to the t(3;8) translocation breakpoint, and exon 5 within the homozygously deleted fragile region (8,9).

In the same study, aberrant transcripts of the FHIT locus were found in approximately 50% of esophageal, stomach, and colon carcinoma cells (9). Analysis of the FHIT gene structure and transcription in a large series of normal and cancerous lung tissues in 1996,

revealed loss of heterozygosity for microsatellite markers internal to, and flanking the FHIT locus (10). It was postulated that in these tumors inactivation of the FHIT gene occurred by a mechanism consisting of loss of one allele and altered expression of the remaining allele (10). Examination of 26 head and neck cancers (HNSCC) cell lines for (a) deletions within the FHIT locus, (b) for allelic loss of specific exons of FHIT, and (c) for integrity of the FHIT transcripts was completed in 1996 (11). When the data were combined, 22 of 26 cell lines showed alterations of at least 1 allele of the FHIT gene. Thus, it was concluded that loss of FHIT function might be important in the development and/or progression of head and neck cancers (11). Meanwhile, other researchers (1996) found that FHIT protein is a 147-amino acid, AP₃A hydrolase. The authors stated that the FHIT preferred substrate, AP₃A (diadenosine 5-prime,5-triple prime-P(1),P(3)-triphosphate), and the Ap₄A have various intracellular functions, including regulation of DNA replication and signaling stress responses (12).

1.1.2 Fragile Histidine Triad, FHIT Gene

The Fragile Histidine Triad gene, FHIT, is a putative gene at chromosome 3p14.2, which was identified in 1996 by positional cloning. The FHIT gene is transcribed to a 1.1 kb mRNA, which is translated into a 16.8 kDa protein with diadenosine triphosphate hydrolysis activity (9). The gene encompasses the site of the t(3;8) translocation breakpoint of familial renal clear cell carcinoma, straddling the fragile site locus FRA3B (9) which is the most active of the common human chromosomal fragile sites. The

FRA3B region is susceptible in most or all individuals to formation of apparent chromosome gaps induced by inhibitors of DNA replication (13,14). Homozygous deletions within the FHIT locus have been observed in DNAs extracted from cell lines derived from cancers of the esophagus, stomach, colon, breast, kidney, and lung. Aberrant FHIT transcripts have also been observed in a spectrum of important human primary tumors (9,10,15).

The "common" chromosomal fragile sites may be seen on all chromosomes as a constant feature. Chromosomal fragile sites are loci that are especially prone to forming gaps or breaks on metaphase chromosomes in cells that are cultured under conditions that inhibit DNA replication or repair. In addition to forming fragile sites on metaphase chromosomes, these loci have been shown to display a number of characteristics of unstable and highly recombinogenic DNA *in vitro*. These aberrations include chromosome rearrangements, sister chromatid exchanges and, intrachromosomal gene amplifications (13,14). The distribution of such gaps in the FRA3B locus, representing DNA breaks or exogenous DNA integration sites, parallels the positions of neoplasia-associated chromosomal rearrangements, prompting the hypothesis that fragility disposes to chromosomal rearrangements (16-19). Implicit in this hypothesis is that genes at the fragile sites can be altered by chromosomal rearrangements and thus contribute to neoplastic growth.

The hypothesis that chromosomal fragile sites may be 'weak links' that result in hotspots for cancer-specific chromosome rearrangements has been supported by the discovery that numerous homozygous deletions in cancer cells and a familial translocation, map within

the FHIT gene encompassing the common fragile site, FRA3B. By use of sequence analysis of 276 kb of the FRA3B/FHIT locus, and 22 associated cancer cell deletion endpoints, it was (1997) demonstrated that this locus was a frequent site of homologous recombinations. These homologous recombinations between long interspersed nuclear element (LINE) sequences, probably induced by carcinogen damage at the FRA3B fragile sites, result in internal deletions in the FHIT gene (20). Additionally, other investigators (1997) found that FHIT was involved in a translocation-derived fusion with High Mobility Group Protein Isoform-C (HMGIC), the causative gene in a variety of benign tumors (21).

To investigate the role of the FHIT gene in carcinogen induction of neoplasia, scientists (2000) inactivated one of the FHIT alleles in mouse embryonic stem cells to produce F1 mice with an inactivated FHIT allele (+/-). FHIT +/+ and +/- mice were treated intragastrically with nitrosomethylbenzylamine and observed for 10 weeks posttreatment. In 25% of the +/+ mice, adenoma or papilloma of the forestomach developed, whereas 100% of the +/- mice developed multiple tumors that were a mixture of adenomas, squamous papillomas, and invasive carcinomas of the forestomach, as well as tumors of sebaceous glands. The visceral and sebaceous tumors, which lacked Fhit protein, had characteristics similar to the Muir-Torre familial cancer syndrome (22).

1.1.2.1 *Deletions in the FHIT Gene*

Alterations such as hemizygous and homozygous deletions in the FHIT gene, in parallel with loss of heterozygosity (LOH), associated with absent or reduced Fhit protein expression, has been observed in a high percentage of human tumors and tumor derived cell lines, such as breast (23,24), pancreas (25), esophagus (26), blood (27) and lung (28) cancers (29,30). An interesting preliminary observation has been that the most commonly deleted region in the fragile sites at the FRA3B region is identified to be a 200 kb region located within introns 4 and 5 of the FHIT gene, which flanks the first FHIT coding exon. Analysis of this region in the cancer cell lines (15) demonstrated that this region contained only one of the 10 FHIT exons, while four other 5' untranslated exons mapped centromeric, and exons 6-10 mapped telomeric, to this commonly deleted region.

However, homozygous deletions that are entirely contained within the FHIT gene and which target the same region of the gene are unusual. Another puzzling point has been that some cell lines appear to have homozygous deletions that do not include any of the FHIT exons (9). These observations have called into question the role of FHIT as a tumor suppressor gene, and raised the question of whether its apparent involvement simply reflects its location within an unstable region of the genome. The above mentioned points, however, can be addressed partially by the probability that most frequent tumor break points correspond to sites of breaks in this most active of the fragile regions, directly flanking exon 5 (29). It has also been observed that these breaks (18) or integrations

(17,19) in the mapped fragile sites are frequently accompanied by deletions. Some cell lines have exhibited at least two different FHIT deleted alleles where the deletions, which include different exons, overlap in the distal intron 5, hence the homozygously deleted region. Independent deletions in two FHIT gene alleles, in the same cell, are also unusual.

Researchers (20) believe that the mechanism of inactivation of FHIT will almost always involve deletions rather than mutations because breaks and deletions in this fragile gene are more frequent events than mutations. The inactivation occurs due to either, deletions within both FHIT alleles, or deletion of an entire FHIT locus plus some loss within the other. In a supporting study assessing the extent of homozygous deletion by evaluating more than 100 FHIT alleles, an amazing variety of missing or rearranged exons were identified, but no mutations were observed in these tumor cell lines.

1.1.2.2 FHIT Transcription and Protein Expression

Because the gene exhibits several of the hallmarks of a tumor suppressor gene, the transcription of its message and expression of its protein in tissues have been well characterized. Studies using northern blot analysis have demonstrated FHIT as a gene that has been broadly expressed in a spectrum of tissues. It has been demonstrated that the transcripts are absent, diminished or altered in some tumor cell lines with the homozygous deletions (30). Further analysis using reverse-transcription polymerase chain reaction (RT-PCR) has revealed tumors and tumor cell lines with (*i*) a mixture of normal and aberrant

products; *(ii)* with only aberrant, shorter than normal, products; or *(iii)* no product. These aberrant products have been found to be missing single or various exons, or contain small, unique or repetitive, insertions (9-11,31,32).

These aberrant RT-PCR products and the absence of Fhit protein expression in tumor derived cell lines and in primary tumors have been correlated with lesions at the DNA level (33). If the aberrant products are indicators of the presence of DNA lesions, then the mixture of normal and aberrant products would indicate that the originating cells containing one intact and one deleted allele or that the tumors are a mixed population of cells with different FHIT gene configurations. It has been demonstrated in many of these cell lines, where normal product was mixed in with the aberrant product, that at least one or both of FHIT alleles did not remain intact and that this heterogeneity persisted in tissue culture (11).

Results of these investigations on the integrity of the FHIT locus in many tumor types has pointed to some intriguing differences between FHIT gene profiles in tumor cells and the types of alterations found in nearly all tumor suppressor genes studied up to this point. Even though, FHIT does not fit the Knudson tumor suppressor paradigm, which proposes that individuals will develop cancer if they either inherit one mutated gene and incur a second mutation, or if they incur two mutations after conception, absence of Fhit protein has been prominent in cells with deleted coding or non-coding regions.

1.2 HYPOTHESIS

1.2.1 Issues and Problem Statement

Germline alteration of one allele in familial cancer and deletions within the gene in sporadic cancers are hallmarks of tumor suppressor genes. The preponderance of evidence suggests that the FHIT gene could indeed act as a tumor suppressor gene. Early studies of a number of important human tumor types such as breast, gastric, renal, and lung carcinoma and adenocarcinoma of pancreas have revealed that FHIT RNA expression frequently is altered (9,34,35). Alterations of RNA expression have since been shown to correlate with deletions in the FHIT gene (30), suggesting a role for this gene in carcinogenesis. Various investigators have implicated FHIT as a putative tumor suppressor gene (9,36). It has been suggested that inactivation of FHIT may promote cell cycle progression at G1/S by virtue of higher diadenosine oligophosphate levels (37). Of significant interest, there has been a correlation between complete absence of FHIT and the G1 morphological grade and early clinical stages of cancer (38). FHIT inactivation is suggested, therefore, to be a likely early event in stage 1 tumors and may be associated with progression in stage 2 and stage 3 tumors (38).

Despite these observations, *some DNA and RNA alterations exhibited by the FHIT gene in cancers have shown features not previously encountered for known tumor suppressor genes, prompting a number of investigators to reject FHIT as a suppressor gene.* They

(39-40) suggest that alterations in the gene are due to its location at the FRA3B active fragile site and that is why only allelic deletions are observed rather than mutations. In addition, no consistent effect of exogenous FHIT on cellular growth in cultures has been observed. These investigators have argued that FHIT alterations are not functionally important in tumorigenesis but simply result from its coincident location at an active fragile site (39). This “innocent bystander” hypothesis is plausible since most of the reported data are derived from human tumor cell lines. Aberrant FHIT transcripts observed in such cell lines may be an *in vitro* artifact in some cases. Indeed, aberrant FHIT transcripts have been observed in non-tumor tissues and are more common in aging cells (40).

Conversely, the frequent loss of heterozygosity at 3p14 in premalignant conditions argues for a role for FHIT in tumorigenesis (35). Experiments transfecting wild-type (*wt*) FHIT into tumor cell lines with FHIT abnormalities have produced conflicting results. Some investigators have found that stable overexpression of *wt* FHIT did not alter cell morphology, inhibit colony formation, or inhibit cell proliferation *in vitro* (41). In addition, overexpression of *wt* FHIT did not lead to altered cell cycle kinetics in dividing cells (41). Nevertheless, other studies have shown that reestablishment of *wt* FHIT expression in several FHIT negative tumor cell lines does suppress tumorigenesis *in vivo*. These studies have resulted in reduction of the frequency and smaller size of tumors developing after their transfer into nude mice (42).

1.2.2 Objective and Specific Goals

The objective of this project is to answer the question of whether the FHIT gene could be classified as a tumor suppressor gene. The specific goals of this study included:

- (i) Establishing a representation of the underlying molecular and cellular activity of the FHIT gene.
- (ii) Applying novel spectroscopic and biosensing techniques and protocols for biological research and clinical diagnosis

1.3 EXPERIMENTAL DESIGN

1.3.1 Generation of the Working Model

For analysis of the FHIT tumor suppressor activity, a model consisting of both *in vitro* and *in vivo* systems, each with subgroups with the ability to express or not to express the Fhit protein was established. There were two criteria for selection of cancer cell lines to be used in this study. First, the cell lines exhibit homozygous deletion of FHIT coding exons, and no detectable Fhit protein expression. Second, the chosen cell lines had to be tumorigenic in nude mice. The gastric carcinoma derived MKN74 cell lines (43), MKN/FHIT (transfected with a DNA fragment containing the human FHIT cDNA) and

MKN/E4 (containing the null vector) were kindly provided by Dr. Kay Huebner, Kimmel Cancer Center, Thomas Jefferson University. The parental MKN74 cell line forms tumors rapidly in nude mice (42). It had also been tested for deletion within the FHIT gene by PCR amplification of FHIT locus markers, encompassing mid intron 4 to distal intron 5, where homozygous deletion of markers in intron 5 had been observed. Control cell lines included 293 normal embryonic kidney cells which express Fhit protein and the AGS gastric cancer cell, which do not express Fhit protein were also incorporated in this study. Balb/c nude mice that were inoculated with the Fhit-expressing cells and Fhit-negative cells were employed to further investigate the role of Fhit protein in cancer development and to investigate mechanisms for a selective growth advantage of Fhit-negative tumors. The models allowed data acquisition via applications of conventional and novel biosensing technologies and provided systems to demonstrate their performance feasibility as detection tools.

1.3.2 Technical Approach

In this study, unique properties of advanced spectroscopy, biosensor and microscopy technologies along with proven conventional biological techniques have been employed. Designing the technical approach I incorporated an optical spectroscopy technique, the synchronous luminescence spectroscopy, which has the potential to be selective as well as sensitive with respect to detection of various molecular species (44,45). I used this technology for detection of the enzymatic activity of the Fhit protein. Biochips,

incorporating biochemical compounds such as DNA and antibodies as the sensing elements, have been applied for molecular identification and selective measurement of biochemical quantities in biological matrices. In this study, light, ultra violet, confocal and electron microscopy techniques evolved from qualitative imaging tools (46,47) to probes of critical dimensions for visualization and investigations of submicron, dynamic properties of biomolecules inside living cells.

1.3.3 Project Overview

The current section of this, Part 1, thesis has introduced and presented a comprehensive background, including a historical perspective leading to the discovery and cloning of the FHIT gene. Also, included in this section are the design of the working model and the incorporation of the novel and conventional detection technologies that were used for the assessment of the tumor suppressor activity of the FHIT gene (presented in Parts 2-5).

In Part 2, the suitability of the working model for the proposed research was analyzed by confirming the presence of the FHIT gene and the expression of the Fhit protein in cell lines using the biochip detection technology. In this study, the performance and feasibility of the biochip as a potential detection technology for biological applications was evaluated. Measurements were designed to: (a) detect the presence of FHIT DNA and develop a calibration curve in PCR amplified genomic DNA, (b) verify the expression and quantify the concentration of the Fhit protein in cellular lysates, and (c) simultaneously

identify both the FHIT gene and protein on the same sampling platform.

Analysis of the Fhit protein function, using synchronous luminescence (SL) spectroscopy is described in Part 3. The ability of the SL technique to analyze the hydrolysis of the Ap₄A substrate by the Fhit protein, through identification of reaction byproducts was investigated. An additional goal of this study was to develop a simple, yet highly sensitive spectrometric technique for detection of enzymatic activity of proteins without the need for use of radioactively modified or fluorescently labeled substrates.

Part four of this investigation deals with establishing the *in vivo* and *in vitro* tumor suppressor activity of the Fhit protein. This part provides an analysis of the effects of FHIT gene function and Fhit protein expression on cell cycle kinetics, structural modifications, and disease manifestations at both organism and cellular levels. The outcome of this study pointed to a probable proapoptotic role for the FHIT gene.

In Part five the apoptotic activity of the FHIT gene is further demonstrated. The results implicated the involvement of the mitochondria as an early event in the programmed cell death process. The proapoptotic role of the FHIT gene on disruption of the inner mitochondrial transmembrane potential ($\Delta\Psi_m$) and the release of apoptogenic cytochrome c protein into the cytoplasm, as characteristic biochemical events in the apoptotic program were evaluated.

Finally in part six, a summary of the results of this investigation and the conclusions that have been drawn from these observations along with future research direction regarding inhibitory effects of FHIT function in carcinogenic manifestations are presented.

1.3.4 Significance of Proposed Research

It is estimated that cancer affects three out of four families in the United States. In 2001, an estimated 1,268,100 people in the United States will be diagnosed with cancer (Table 1.1) and 553,400 will die of these diseases (48). Cancer is not only one but many diseases arising from changes in genes and their functioning within cells. The disease causes substantial mortality and morbidity, prompting intense interest in the exact changes cells undergo as they become malignant (49). In the last decade biologists have sorted through an ensemble of genes, as well as their expressed mRNAs and proteins to evaluate specific problems. However, our knowledge of components and events leading to carcinogenesis is not complete. It is therefore necessary to enhance our understanding of this devastating disease. Studies such as this, focused on dissecting the mechanism of the disease biology, will provide a much better understanding of the complex process of carcinogenesis at the molecular level by identifying more of the internal factors affecting the process.

Advances in our understanding of the complexity of these molecular alterations have provided an opportunity to enhance or alter the way research in human disease is carried out (50). Much of my interest in the biotechnology development stems from this explosive

increase in information and tremendous potential for diagnostics and therapy. Additionally, for sustained advancement of science, continued development of new and/or improved technologies for evaluation of large numbers of molecular alterations is extremely necessary. Grounded in scientists' rapidly evolving grasp of how alterations in the molecules within cells may lead to cancer, is the foundation for the design of these proposed technologies and methodologies.

These technologies aim to facilitate the evaluation of the relative contribution of specific molecular alterations to cancer and other disease processes. The novel technologies and protocols developed here have the potential to be applied to mutation detection at the gene and chromosomal level, and to evaluate gene expression, protein function, and assessment of many structural changes at both *in vivo* and *in vitro* levels. These technologies will initially be applicable in molecular and cellular biology research investigations and ultimately, would enable physicians to scan the human body for molecular changes that foreshadow diseases and detect early cellular changes typical of cancer. It is the hope of this study that these technologies ultimately will be appropriate for automation and adaptation to high-throughput applications in both research and clinical settings.

1.3.5 Contributions to Future Research

The most effective way to eradicate cancer is to prevent their occurrence. Individuals can significantly reduce their risk of cancer mortality through screening, early detection and monitoring of cancer (51,52). This search for answers on how to devise better ways to accomplish better detection presents exciting and intellectually rewarding challenges. This research was centered primarily on understanding the role of the FHIT gene in carcinogenesis and design, development and application of new detection devices.

These new tools and methods were designed and applied at various steps in the experimental lay out of this research. Used in place of or along with the conventional biological methods, these novel approaches have assessed the success of FHIT gene transfer, detected molecular level differences in protein expression, function and structure of FHIT transfected cells *in vivo* and *in vitro*. Elucidation of such differences might identify differences related to *in vivo* or *in vitro* expression of FHIT protein that might be contributing to its contradictory tumor suppressor activity in the two different systems.

Along with providing information regarding the tumor suppressor activity of the FHIT gene which is of great importance in cancer studies, these series of newly developed techniques and applications indicated the significant impact that state-of-the-art analytical techniques can have on understanding biology, from structure elucidation to probing biomolecular interactions. Development of these innovative technologies for diagnosis and

monitoring purposes of various transformations was intended to make contributions to the field of human health research in the clinical process. This study helps to realize the tremendous potential of these novel technologies as efficient, cost effective, sensitive tools at both *in vivo* and *in vitro* levels, to permit simultaneous, rapid evaluation of the spectrum of molecular alterations in single cells, tissue specimens, and whole organism.

REFERENCES

1. Cohen, A. J., Li, F. P., Berg, S., Marchetto, D. J. Tsai, S., Jacobs, S. C. & Brown, R. S. Hereditary renal-cell carcinoma associated with a chromosomal translocation (1979) *N. Engl. J. Med.*, 301(11), 592-5
2. Pathak, S., Strong, L. C., Ferrell, R. E. & Trindade, A. Familial renal cell carcinoma with a 3;11 chromosome translocation limited to tumor cells. (1982) *Science*, 217(4563), 939-941
3. Wang, N., & Perkins, K. L. Involvement of band 3p14 in t(3;8) hereditary renal carcinoma. *Cancer. (1984) Genet. Cytogenet.*, (4), 479-81
4. Li, F. P., Decker, H. J. H., Zbar, B., Stanton, V. P., Jr., Kovacs, G., Seizinger, B. R., Aburatani, H., Sandberg, A. A., Berg, S., Hosoe, S. & Brown, R. S. Clinical and genetic studies of renal cell carcinomas in a family with a constitutional chromosome 3;8 translocation: genetics of familial renal carcinoma. (1993) *Ann. Intern. Med.*, 118, 106-111
5. Gnarr, J. R., Tory, K., Weng, Y., Schmidt, L., Wei, M. H., Li, H., Latif, F., Liu, S., Chen, F., Duh, F. M., Lubensky, I., Duan, D. R., Florence, C., Pozzatti, R., Walther, M. M., Bander, N. H., Grossman, H. B., Brauch, H., Pomer, S., Brooks, J. D., Isaacs, W. B., Lerman, M. I., Zbar, B. & Linehan, W. M. Mutations of the VHL tumour suppressor gene in renal carcinoma. (1994) *Nature Genet.*, 7, 85-90
6. Boldog, F. L., Gemmill, R. M., Wilke, C. M., Glover, T. W., Nilsson, A.-S., Chandrasekharappa, S. C., Brown, R. S., Li, F. P. & Drabkin, H. A. Positional cloning of the hereditary renal carcinoma 3;8 chromosome translocation breakpoint. (1993) *Proc. Nat. Acad. Sci.* 90, 8509-8513

7. Roche, J., Whisenant, E., Boldog, F., Loeb, D., Vance, J.M., Drabkin, H. Dinucleotide repeats flanking the renal carcinoma breakpoint at 3p14. (1994) *Hum. Mol. Genet.*, 3(1), 215
8. <http://www.ncbi.nlm.nih.gov/LocusLink/refseq.html>
9. Ohta, M., Inoue, H., Cotticelli, M. G., Kastury, K., Baffa, R., Palazzo, J., Siprashvili, Z., Mori, M., McCue, P., Druck, T., Croce, C. M. & Huebner, K. The FHIT gene, spanning the chromosome 3p14.2 fragile site and renal carcinoma-associated t(3;8) breakpoint, is abnormal in digestive tract cancers. (1996) *Cell*, 84, 587-597
10. Sozzi, G., Veronese, M. L., Negrini, M., Baffa, R., Cotticelli, M. G., Inoue, H., Torielli, S., Pilotti, S., DeGregorio, L., Pastorino, V., Pierotti, M. A., Ohta, M., Huebner, K. & Croce, C. M. The FHIT gene 3p14.2 is abnormal in lung cancer. (1996) *Cell*, 85, 1726
11. Virgilio, L., Shuster, M., Gollin, S. M., Veronese, M. L., Ohta, M., Huebner, K. & Croce, C. M. FHIT gene alterations in head and neck squamous cell carcinomas. (1996) *Proc. Nat. Acad. Sci.*, 93, 9770-9775
12. Barnes, L. D., Garrison, P. N., Siprashvili, Z., Guranowski, A., Robinson, A. K., Ingram, S. W., Croce, C. M., Ohta, M. & Huebner, K. FHIT, a putative tumor suppressor in humans, is a dinucleoside 5',5'''-P1,P3-triphosphate hydrolase. (1996) *Biochemistry*, 35, 11529-11535
13. Glover, T. W., Coyle-Morris, J. F., Li, F. P., Brown, R. S., Berger, C. S., Gemmill, R. M., & Hecht, F. Translocation t(3;8)(p14.2;q24.1) in renal cell carcinoma affects expression of the common fragile site at 3p14(FRA3B) in lymphocytes. (1988) *Cancer*

Genet. Cytogenet., 1, 69-73

14. Glover, T. W., Berger, C., Coyle, J., & Echo, B. DNA polymerase alpha inhibition by aphidicolin induces gaps and breaks at common fragile sites in human chromosomes. (1984) *Hum. Genet.*, 67(2), 136-42
15. Kastury, K., Baffa, R., Druck, T., Ohta, M., Cotticelli, M. G., Inoue, H., Negrini, M., Rugge, M., Huang, D., Croce, C. M., Palazzo, J. & Huebner, K. Potential gastrointestinal tumor suppressor locus at the 3p14.2 FRA3B site identified by homozygous deletions in tumor cell lines. (1996) *Cancer Res.*, 56, 978-983
16. Huebner, K., Garrison, P. N., Barnes, L. D., & Croce, C. M. The role of the FHIT/FRA3B locus in cancer. (1998) *Annu. Rev. Genet.*, 32, 7-31
17. Wilke, M. C., Hall, B. K., Hoge, A., Paradee, W., Smith, D. I. & Glover, T. W. FRA3B extends over a broad region and contains a spontaneous HPV16 integration site: direct evidence for the coincidence of viral integration sites and fragile sites. (1996) *Hum. Mol. Genet.*, 5, 187-195
18. Paradee, W., Wilke, C. M., Wang, L., Shridhar, R., Mullins, C. M., Hoge, A., Glover, T. W. & Smith, D. I. A 350-kb cosmid contig in 3p14.2 that crosses the t(3;8) hereditary renal cell carcinoma translocation breakpoint and 17 aphidicolin-induced FRA3B breakpoints. (1996) *Genomics*, 35, 87-93
19. Rassool, F. V., LeBeau, M. M., Shen, M. L., Neilly, M. E., Espinosa, R., III, Ong, S. T., Boldog, F., Drabkin, H., McCarroll, R. & McKeithan, T. W. Direct cloning of DNA sequences from the common fragile site region at chromosome band 3p14.2. (1996) *Genomics*, 35, 109-117

20. Inoue, H., Ishii, H., Alder, H., Snyder, E., Druck, T., Huebner, K. & Croce, C. M.
Sequence of the FRA3B common fragile region: implications for the mechanism of
FHIT deletion. (1997) *Proc. Nat. Acad. Sci.*, 94, 14584-14589
21. Geurts, J. M., Schoenmakers, E. F., Roijer, E., Stenman, G. & van de Ven, W. J. M.
Expression of reciprocal hybrid transcripts of HMGIC and FHIT in a pleomorphic
adenoma of the parotid gland. (1997) *Cancer Res.*, 57: 13-17
22. Fong, L. Y. Y., Fidanza, V., Zanesi, N., Lock, L. F., Siracusa, L. D., Mancini, R.,
Siprashvili, Z. Ottey, M., Martin, S. E., Druck, T., McCue, P. A., Croce, C. M. &
Huebner, K. Muir-Torre-like syndrome in Fhit-deficient mice. (2000) *Proc. Nat. Acad.
Sci.*, 97, 4742-4747
23. Ingvarsson, S., Agnarsson, B. A., Sigbjornsdottir, B. I., Kononen, J., Kallioniemi, O.
P., Barkardottir, R. B., Kovatich, A. J., Schwarting, R., Hauck, W. W., Huebner, K.
& McCue, P. A. Reduced Fhit expression in sporadic and BRCA2-linked breast
carcinomas. (1999) *Cancer Res.*, 59(11), 2682-9
24. Huiping, C., Jonasson, J. G., Agnarsson, B. A., Sigbjornsdottir, B. I., Huebner, K. &
Ingvarsson, S. Analysis of the fragile histidine triad (FHIT) gene in lobular breast
cancer. (2000) *Eur. J. Cancer*, 36(12), 1552-7
25. Mangray, S. & King, T. C., Molecular pathobiology of pancreatic adenocarcinoma.
(1998) *Front. Biosci.*, 3, D1148-60
26. Mueller, J., Werner, M. & Siewert, J. R., Malignant progression in Barrett's
esophagus: pathology and molecular biology. (2000) *Recent Results Cancer Res.*, 155,
29-41

27. Gartenhaus, R. B. Allelic loss determination in chronic lymphocytic leukemia by immunomagnetic bead sorting and microsatellite marker analysis. (1997) *Oncogene*, 14(3), 375-8
28. Sozzi, G., Pastorino, U., Moiraghi, L., Tagliabue, E., Pezzella, F., Ghirelli, C., Tornielli, S., Sard, L., Huebner, K., Pierotti, M. A., Croce, C. M. & Pilotti, S. Loss of FHIT function in lung cancer and preinvasive bronchial lesions. (1998) *Cancer Res.*, 58(22), 5032-7
29. Zimonjic, D. B., Druck, T., Ohta, M., Kastury, K., Popescu, N. C. & Huebner, K. Positions of chromosome 3p14.2 fragile sites (FRA3B) within the FHIT gene. (1997) *Cancer Res.*, 57, 1166-1170
30. Druck, T., Hadaczek, P., Fu, T. B., Ohta, M., Siprashvili, Z., Baffa, R., Negrini, M., Kastury, K., Veronese, M. L., Rosen, D., Rothstein, J., McCue, P., Cotticelli, M. G., Inoue, H., Croce, C. M. & Huebner, K. Structure and expression of the human FHIT gene in normal and tumor cells. (1997) *Cancer Res.*, 57, 504-512
31. Panagopoulos, I., Pandis, N., Thelin, S., Petersson, C., Mertens, F., Borg, A., Kristoffersson, U., Mitelman, F. & Aman, P. The FHIT and PTPRG genes are deleted in benign proliferative breast disease associated with familial breast cancer and cytogenetic rearrangements of chromosome band 3p14. (1996) *Cancer Res.*, 56(21), 4871-5
32. Negrini, M., Monaco, C., Vorechovsky, I., Ohta, M., Druck, T., Baffa, R., Huebner, K. & Croce, C. M. The FHIT gene at 3p14.2 is abnormal in breast carcinomas. (1996) *Cancer Res.*, 56(14), 3173-9

33. Baffa, R., Veronese, M. L., Santoro, R., Mandes, B., Palazzo, J. P., Rugge, M, Santoro E, Croce, C. M. & Huebner, K. Loss of FHIT expression in gastric carcinoma. (1998) *Cancer Res.*, 58(20), 4708-14
34. Shridhar, V., Wang, L., Rosati, R., Paradee, W., Shridhar, R, Mullins, C., Sakr, W., Grignon, D., Miller, O. J., Sun, Q.C., Petros, J. & Smith, D. I. Frequent breakpoints in the region surrounding FRA3B in sporadic renal cell carcinomas.(1997) *Oncogene*, 14(11), 1269-77
35. Mao, L., Fan, Y. H., Lotan, R. & Hong, W. K. Frequent abnormalities of FHIT, a candidate tumor suppressor gene, in head and neck cancer cell lines. (1996) *Cancer Res.*, 56(22), 5128-31
36. Simon, B., Bartsch, D., Barth, P., Prasnikar, N., Munch, K., Blum, A., Arnold, R. & Goke, B. Frequent abnormalities of the putative tumor suppressor gene FHIT at 3p14.2 in pancreatic carcinoma cell lines. (1998) *Cancer Res.*, 58(8), 1583-7
37. Kisselev, L. L., Justesen, J., Wolfson, A. D. & Frolova, L.Y. Diadenosine oligophosphates (Ap(n)A), a novel class of signalling molecules? (1998) *FEBS. Lett.*, 27(2), 157-63
38. Hadaczek, P., Siprashvili, Z., Markiewski, M., Domagala, W., Druck, T., McCue, P. A., Pekarsky, Y., Ohta, M., Huebner, K. & Lubinski, J. Absence or reduction of Fhit expression in most clear cell renal carcinomas. (1998) *Cancer Res.*, 58(14), 2946-51
39. Mao, L. Tumor suppressor genes: does FHIT fit? (1998) *J. Natl. Cancer Inst.*, 90(6), 412-4

40. Carapeti, M., Aguiar, R. C., Sill, H., Goldman, J. M. & Cross, N. C. Aberrant transcripts of the FHIT gene are expressed in normal and leukaemic haemopoietic cells. (1998) *Br. J. Cancer*, 78(5), 601-5
41. Otterson, G. A., Xiao, G. H., Geradts, J., Jin, F., Chen, W. D., Niklinska, W., Kaye, F. J. & Yeung, R. S. Protein expression and functional analysis of the FHIT gene in human tumor cells. (1998) *J. Natl. Cancer Inst.*, 90(6), 426-32
42. Siprashvili, Z., Sozzi, G., Barnes, L. D., McCue, P., Robinson, A.K., Eryomin, V., Sard, L., Tagliabue, E., Greco, A., Fusetti, L., Schwartz, G., Pierotti, M. A., Croce, C. M. & Huebner, K. Replacement of Fhit in cancer cells suppresses tumorigenicity. (1997) *Proc. Natl. Acad. Sci. USA*, 94(25),13771-6
43. Sambrook, J., Fritsch, E. F., Maniatis, T. Molecular cloning. A laboratory manual. Second edition. Cold Spring Harbor Press, NY, 2nd edition,. (1989) 6.53-6.54
44. Helmenstine, A., Uziel, M. & Vo-Dinh, T. Measurement of DNA adducts using surface-enhanced Raman spectroscopy. (1993) *J. Toxicol. Environ. Health.*, 40(2-3),195-202
45. Xie, B., Ramanathan, K. & Danielsson, B. Principles of enzyme thermistor systems: applications to biomedical and other measurements. (1999) *Adv. Biochem. Eng. Biotechnol.*, 64, 1-33
46. Colton, R. J., Baselt, D. R., Dufrière, Y. F., Green, J. B. & Lee, G. U. Scanning probe microscopy. (1997) *Current Opinion in Chemical Biology*, 1, 370-377

47. Williams, R. M., Piston, D. W. & Webb, W. W. Two-photon molecular excitation provides intrinsic 3-dimensional resolution for laser-based microscopy and microphotochemistry. (1994) *FASEB J.*, 8(11), 804-813
48. Merrill, R. M., Kessler, L. G., Udler, J. M., Rasband, G. C. & Feuer E. J. Comparison of risk estimates for selected diseases and causes of death. (1999) *Prev. Med.*, 28(2), 179-93
49. National Cancer Institute: Cancer Control: Objectives for the Nation: 1985-2000 (1986) *J. Nat. Can. Inst. Monograph*, 2, 1-93
50. Sittampalam, G. S., Kahl, S. D. & Janzen, W. P. High-throughput screening: advances in assay technologies. (1997) *Curr. Opin. Chem. Biol.*, 1(3),384-9
51. Wingo, P. A., Ries, L. A., Rosenberg, H. M., Miller, D. S. & Edwards, B. K. 1973-1995: a report card for the U.S. Cancer. *Cancer incidence and mortality*, (1998) 82(6), 1197-207
52. Prorok, P. C. & Miller, A. B. Screening for Cancer: International Union Against Cancer Technical Report Series. (1984) Vol. 78

APPENDIX

Ideogram

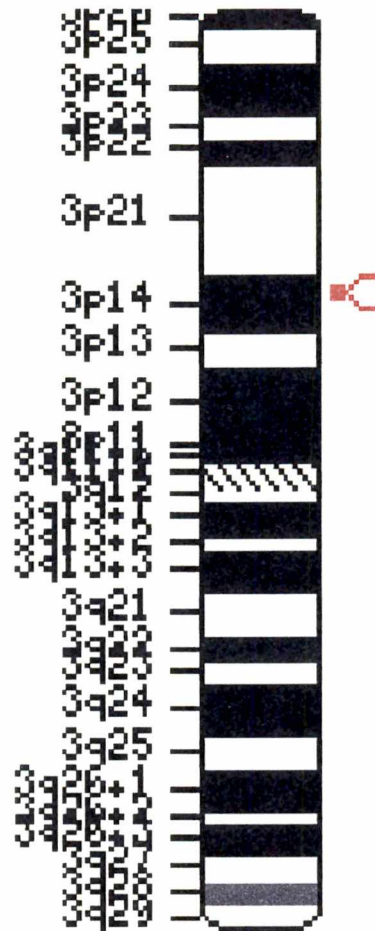


Figure 1.1 Schematic diagram of chromosome 3 containing the fragile 3p14 region.

Source: <http://www.ncbi.nlm.nih.gov/>

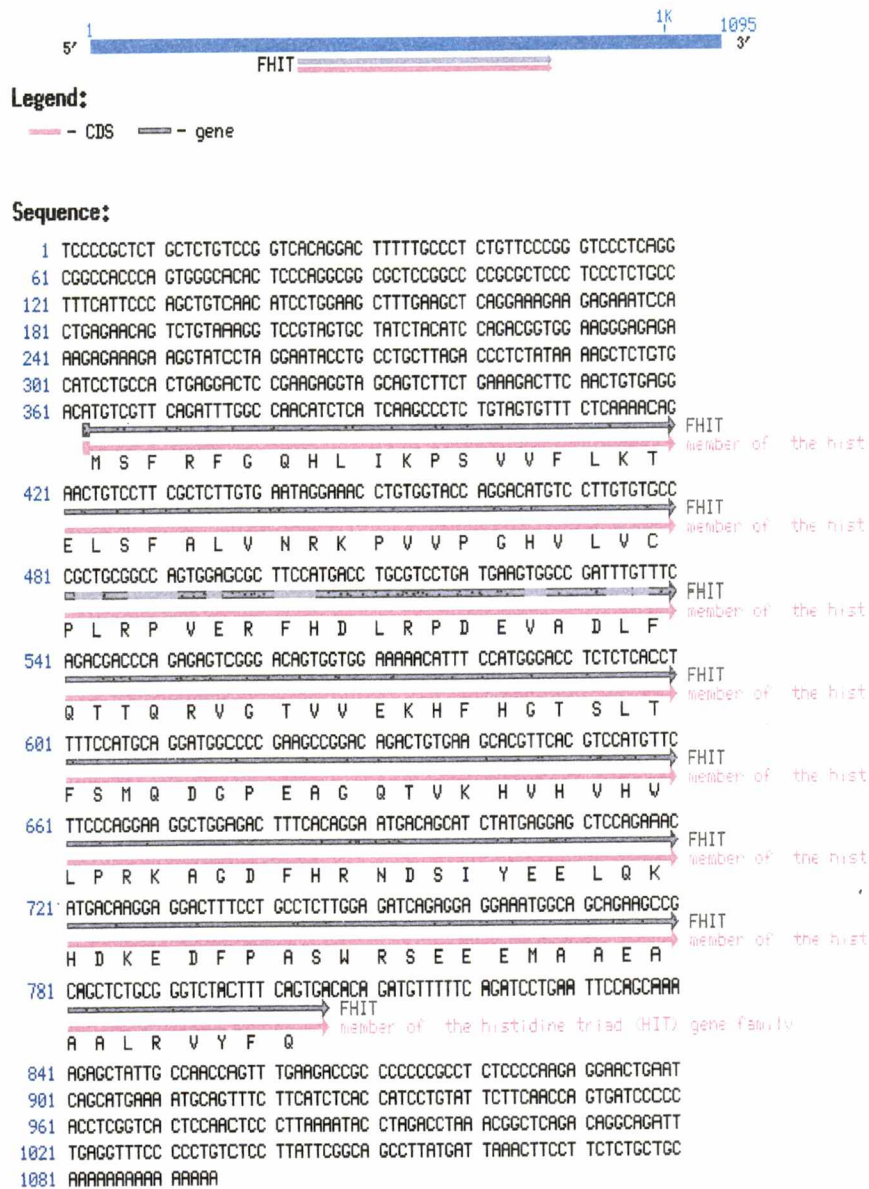


Figure 1.2 Fragile Histidine Triad, FHIT gene, DNA and protein sequences.

Source: <http://www.ncbi.nlm.nih.gov/LocusLink/refseq.html>

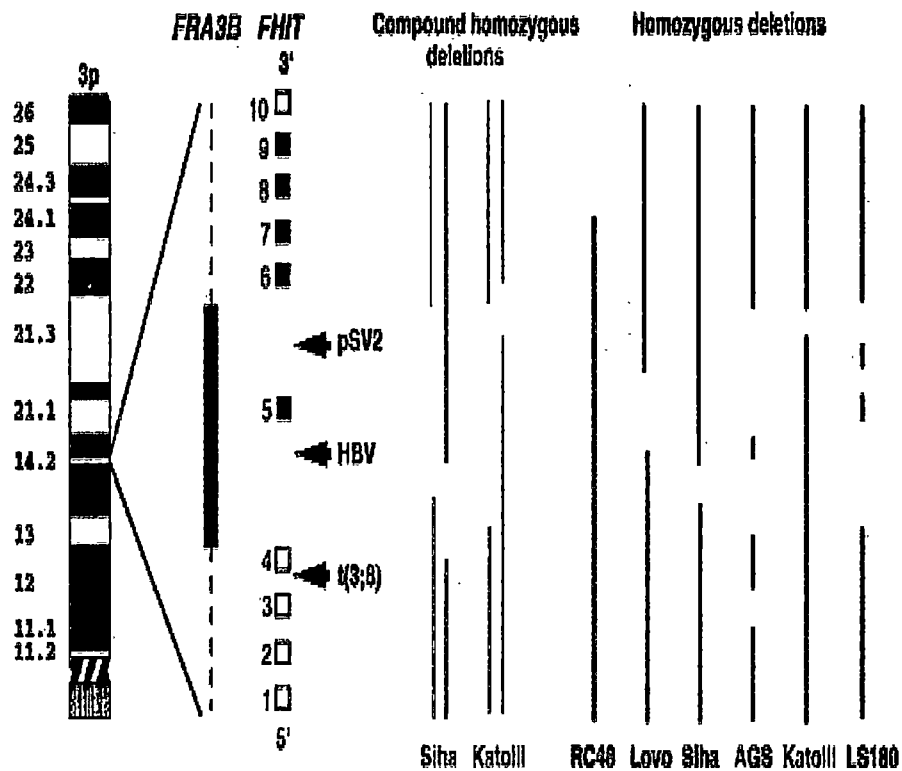


Figure 1.3 The map of FRA3B/FHIT loci at 3p14.2. The FRA3B region is shown by the solid area at p14.2. FHIT exons are numbered 1 through 10, coding exons are in black. Positions of viral integration sites and t(3;8) translocation are marked with arrows. Gaps in the lines represent FHIT locus in the tumor cell lines demonstrate deletions.

Source: Ohta, M., et al. (1996) *Cell*, 84(4), 587-597

Table 1.1

Estimated new cancer cases and deaths for 2001, all races, by case

<i>Estimated New Cases</i>			<i>Estimated Deaths</i>		
<i>Total</i>	Males	Females	<i>Total</i>	Males	Females
1,268,100	643,000	625,000	553,400	286,100	267,300

Source: Cancer Facts & Figures – 2001, American Cancer Society (ACS), Atlanta, Georgia, 2001. Excludes basal and squamous cell skin and in situ carcinomas except urinary bladder. Incidence projections are based on rates from the NCI SEER Program 1979-1997.

PART TWO

**SIMULTANEOUS DETECTION OF THE TUMOR SUPPRESSOR FHIT GENE
AND PROTEIN USING THE MULTIFUNCTIONAL BIOCHIP**

2.1 ABSTRACT

The tumor suppressor gene, FHIT, fragile histidine triad, encompasses the most common human chromosomal fragile site at 3p14.2. Detection of the FHIT gene is important in cancer diagnostics since its alterations have been associated with several human cancers. In this work, we used a unique multi-functional biochip for simultaneous detection of FHIT DNA and Fhit protein on the same platform. The biochip system design takes advantage of the miniaturization of photodiodes, where the functioning of multiple optical sensing elements, amplifiers, discriminators, and logic circuitry are integrated on a single integrated circuit (IC) board. The performance of the biochip is based on biomolecular recognition processes using both DNA and protein as bioreceptors, Cy5-labeled probes and laser excitation. Using the biochip system, we detected FHIT DNA in polymerase chain reaction (PCR) amplified genomic DNA and Fhit protein in cellular lysates. The linearity of response of the biochip necessary for quantitative and qualitative measurements of protein and DNA molecules at very low concentrations in different matrices was also demonstrated. Additionally, application of the biochip for concurrent detection of ligands which bind to various immobilized target DNA molecules (FHIT, tuberculosis DNAs), protein molecules (Fhit, p53 proteins) and multiplex of DNA and protein molecules (FHIT DNA, Fhit protein) spotted on the same microarray was accomplished. Levels of the background fluorescence signals were low and uniform in intensity providing an excellent baseline. These results demonstrated the utility of the multi-functional biochip as a useful detection technology with applications in biological research laboratories and in clinical settings.

2.2 INTRODUCTION

The recently cloned human tumor suppressor, Fragile Histidine Triad (FHIT) gene, spans a megabase of genomic region at chromosome band 3p14.2. The gene encompasses the most active of the common human chromosomal fragile regions, FRA3B (1). The FHIT gene includes 10 exons, and encodes a 1.1 kb transcript for a 16.8 kDa protein which has demonstrated dinucleoside 5', 5'''- P₁, P_n - polyphosphate hydrolase activity *in vitro* (2,3). In some systems, reconstitution of normal FHIT expression in FHIT-negative tumor cells abrogates their tumorigenicity *in vivo* and *in vitro* (4).

The human FHIT gene has recently received increasing interest among cancer researchers. A multitude of genetic aberrations within the FHIT gene have been observed in cancer cell lines, uncultured tumors, and even in preneoplastic lesions of a variety of cancers (5). Alterations such as hemizygous and homozygous deletions in the FHIT gene in parallel with loss of heterozygosity (LOH), associated with reduced FHIT expression, have been observed in a high percentage of human tumors, including breast (6,7), pancreas (8), esophagus (9), leukemia (10) and lung cancers (11). FHIT inactivation can occur as either an early event, as observed in the development of esophageal carcinoma (12), or as a late event possibly associated with progression to more aggressive neoplasia. Interestingly, loss of Fhit protein has been indicated to be the most frequent alteration in some cancers, occurring independently and more frequently than the p53 overexpression (11). Such observations, indicating reduced overall frequency of Fhit protein expression

or FHIT inactivation in premalignant and malignant tissues, suggest a potential use of this gene as a valuable biomarker for detection of FHIT associated cancers (13).

Recently, several optical biomarker detection technologies have been developed for clinical applications. The function of these immune and DNA- based diagnostic biosensing techniques has been based on direct monitoring of biomolecular recognition processes. Some of these biosensing devices include; single-target, fiber optic based biosensors (14,16), sol-gel-based biosensors for patient treatments (17) and planar array immunosensors for the detection of toxic agents (18). Our laboratory has recently developed a biochip, based on integrated circuit microchip technology with applications in medical diagnosis (19,20). A detailed description of the design of this integrated electro-optic system, developed at Oak Ridge National Laboratory, has been published previously (21). Briefly, this highly integrated biochip system is a self-contained fluorescence-detecting device, based on miniaturized phototransistors and photodiode array technology. This apparatus has multiple optical sensing elements, amplifiers, discriminators and logic circuitry that are fabricated on a single IC board. Size, performance, fabrication, analysis, and low production cost due to its integrated optical-sensing microchip are the principal advantages of this biochip over the currently available biosensor systems. The available detection technologies, for instance a confocal microscope, use external imaging systems such as photomultipliers, or charge-coupled devices (CCD) which greatly add to the size and dimensions of the instrument.

In the present study, we evaluated the performance of the biochip to quantitatively and qualitatively detect both targets, FHIT DNA and Fhit protein, immobilized on a single platform. Measurements were designed to (a) detect the presence of FHIT DNA and develop a FHIT DNA calibration curve in PCR amplified genomic DNA, (b) verify the expression and quantify the concentration of the Fhit protein in cellular lysates, and (c) simultaneously identify both the FHIT gene and the Fhit protein on the same sampling platform.

2.3 MATERIALS AND METHODS

2.3.1 Cell Lines

Two cell lines, MKN74-PRC-FHIT A66 (MKN/FHIT) and MKN74-PRC-E4 (MKN/E4) were kindly provided by Dr. Kay Huebner (Kimmel Cancer Center, Philadelphia, PA). These cell lines, derived from the same parental cell line, the MKN74 gastric carcinoma, were transfected either with a vector for expression of the FHIT gene, MKN/FHIT, or with null vectors, MKN/E4 (5). G418 resistant cultures were maintained at 37°C and 5% CO₂ in Dulbecco's modified Eagle's medium (DMEM) medium supplemented with 10% fetal bovine serum (FBS) and 200 µg/ml of geneticin (GIBCO/BRL, Grand Island, NY).

2.3.2 Fhit Protein Extraction and Quantification

Both cell lines were grown to about 75% subconfluent levels in several T175 tissue culture flasks, washed twice with phosphate buffered saline (PBS) and trypsinized using 1x trypsin-EDTA (Sigma immunochemicals, St. Louis, MO) for 7 minutes. Harvested cells were then suspended in 10 parts (v/v) lysis buffer (0.5 % NP-40 in PBS supplemented with 10 µg/ml leupeptin and 10 µg/mL PMSF (Sigma, St. Louis, MO)). Lysates were prepared by probe sonicating the cell suspensions for 30 sec, (Sonicator XL2020 Heat Systems, Inc.). The lysates were transferred into eppendorf tubes and centrifuged for 10 minutes at 10,000 rpm at 4° C to remove cellular debris. Protein concentration was determined using Pierce BCA Protein assay reagent (Rockford, IL) per manufacturer's instructions. Mouse ascities fluid containing monoclonal antibody to wild type p53 was obtained from Sigma immunochemicals (St. Louis, MO). Synthesized human p53 blocking peptide was obtained from Santa Cruz Biotechnologies (Santa Cruz, CA). Rabbit anti-goat IgG antibody and goat IgG along with human serum from clotted male blood were purchased from Sigma immunochemicals (St. Louis, MO).

2.3.3 Coomassie Brilliant Blue Analysis

The pure Fhit protein (kindly provided by Dr. Charles Brenner, Kimmel Cancer Center, Philadelphia, PA) and 15 µl (50 µg/lane) of each cell lysate were separated by electrophoresis on a 14% SDS-polyacrylamide (SDS-PAGE) gel (Novex, San Diego,

CA). Separated polypeptides were fixed and stained in a 0.25% solution of Coomassie brilliant blue in methanol-water-glacial acetic acid (45:45:10). Protein bands were detected after overnight destaining in methanol-water-glacial acetic acid solution.

2.3.4 Western Blot Analysis

Cellular lysates containing 25 µg (15 µl) of proteins were treated with SDS-reducing sample buffer, boiled for 5 min, and separated on a 14% SDS-PAGE gel (Novax, San Diego, CA) by electrophoresis. Proteins were transferred onto nitrocellulose membranes (Schleicher & Schuell, Keene, NH) using transfer buffer (25 mM Tris, 192 mM glycine, 20% v/v methanol, pH 8.3) at 100 V, 350 mA for 1hr. Membranes were then blocked for one hour in 10 ml of Blotto (5% nonfat dry milk (Kroger Co, Cincinnati OH) and 0.1% Tween-20 (Sigma, St. Louis, MO) in PBS) at room temp. Blots were further incubated in 10 ml of Blotto containing 1 µg/ml Fhit polyclonal antibody (Santa Cruz Biotechnologies, Santa Cruz, CA) for 2 hrs. After this primary antibody treatment, immunoblots were washed extensively in PBS/0.05% Tween-20, before incubation in a Blotto solution containing 1/1000 HRP-conjugated rabbit anti-goat IgG for 2 hrs at room temp. Membranes were again washed as in the PBS/0.05% Tween-20 and the Fhit proteins were detected using the Pierce DAB Super Signal System (Rockford IL) as described by the manufacturer.

2.3.5 FHIT Gene Amplification, Purification and Quantification

Genomic DNA contents of the two cell cultures, MKN/FHIT and MKN/E4, were extracted using DNAzol reagent (GIBCO/BRL, Grand Island, NY) by following the manufacturer-suggested protocol. Using 100 ng of extracted genomic DNA as the template and 50 μ M of primers corresponding to nucleotides 2 to 18 of the FHIT sequence, 5'-GTG GGA TCC ACA TGT CGT TCA GAT TTG GC-3' and nucleotides 445-427 of the FHIT sequence 5'-CCG CTC GAG TCA CTG AAA GTA GAC CCG-3' (Oligos etc., Wilsonville, OR), the exon 5 of the FHIT gene was PCR amplified. Thirty cycles of amplification were performed in a Perkin Elmer Cetus thermal cycler (Clearwater, MO) at 94° C for 60 sec, 55° C for 60 sec., and 72° C for 45 sec after an initial 5 min 95° C denaturation step. Picogreen dsDNA quantitation kit (Molecular Probes, Eugene, OR) was used for determination of DNA concentrations of PCR amplified products. The oligonucleotide sequence, 3'-ACT GGT CAG GTA GCC ACT AG-5' corresponding to a sequence in the Tuberculosis gene and its fluorescently labeled probe 5'-Cy5-TGA CCA GTC CAT CGG TGA TC-3', were obtained from Oligos etc. (Wilsonville, OR).

2.3.6 Fluorescent Labeling of Proteins

Polyclonal antibody to the Fhit protein and the p53 blocking peptide were fluorescently labeled with the Fluorolink Cy-5 Reactive Dye Pack (Biological Detection Systems, Inc.,

Pittsburgh, PA). The water soluble, bifunctional NHS-ester, Cy5 dye binds to the free amino group of the proteins, producing an intense fluorescence signal in the far-red region of the spectrum (Absorbance max = 649 nm and Emission max = 670 nm). Proteins were dissolved in a solution of 0.1 M sodium carbonate bicarbonate buffer (pH 9.3) to a final concentration of 1 mg/ml. A 1-ml aliquot of this protein solution was transferred to a vial containing 100 nM of the Cy5 dye and incubated for 30 min at room temperature. Labeled proteins were separated from the unconjugated dye using a Sephadex G-50 column. Optimal labeling occurred at pH 9.3 and increasing the protein concentration enhanced labeling efficiencies. Final concentrations of labeled proteins were determined by measuring absorbance at 280 nm.

2.3.7 Microarray Sample Platform

A WPI-PV830 pneumatic pico pump (World Precision Instruments, Sarasota, FL) was programmed and used for dispensing target molecules, both antibody and DNA, as microspot arrays on the membranes. Each membrane was secured on the nanopositioning stage of a Burleigh 6000 controller (Burleigh, Fisher, NY) in order to allow two-dimensional (XY) movements. Using a capillary-dispensing tip, a volume of 0.1 μ l of a solution containing the selected target molecules was deposited on the membrane to generate an individual spot. The translational stage was then programmed to move so as to achieve a 4 x 4-microarray spot arrangement dispensed in a 0.8-cm² area of the membrane with a constant, center-to-center, distance of 1.1 mm maintained between the spots in each row and column. The 4x4-array arrangement allowed positioning of spots

on the membrane to exactly match the spacing and arrangement of the 4x4 sensing elements on the biochip detection platform.

2.3.8 Biochip Protein Assay

Protein microarrays were generated on a surface modified, nylon, Immunodyne ABC membrane (Pall Corporation, Port Washington, NY), which has reactive groups that covalently bind the amino group of proteins. After spotting, protein arrays were allowed to stabilize by incubation at 25°C for 5 min, then unreacted sites were blocked in 4 ml of the blocking solution containing 2 mg of bovine serum albumin (BSA) (Sigma, St. Louis, MO) in 1 ml of phosphate buffered saline (PBS). After 30 min of the blocking procedure, the membranes were rinsed 3 times in PBS solution and further incubated for 1 hr at room temperature in the Cy5-labeled protein solution (250 µg/ml of either Cy5-labeled Fhit and/or Cy5-labeled p53 antibodies in PBS). Membranes were then washed twice for 1 minute each in 10 ml of washing solution (0.1% triton X-100 in PBS v/v) at room temperature to reduce background fluorescence signals. This step was followed by another rinse in 10 ml of PBS for 1 min and storage in PBS at 4°C until signal measurement.

2.3.9 Biochip DNA Assay

After generation of the microarray on Zeta probe membranes (BioRad Laboratories, Hercules, CA), DNAs were immobilized by 1 min of UV dimerization. Membranes were

then blocked in 5 ml of prehybridization solution (5X SSC, 1% Carnation non fat dry milk, and 0.02% sodium dodecyl sulfate (SDS)) for 1 hr at 37°C. The Cy5- labeled DNA probes (Oligos etc. Wilsonville, OR) were added to the prehybridization solution (100 ng/ml) and incubated at 37°C for 16 hrs. Membranes were then washed in 5 ml of wash solution (5X SSC, and 0.1% SDS) for 15 min at room temperature, followed by two 1-minute water rinses before detection.

2.3.10 Biochip Protein-DNA Assay

After generation of the DNA-protein array on the ABC Immunodyne membrane, samples were allowed to stabilize for 5 min at 25°C and then UV dimerized. The membrane was then blocked in 5 ml of prehybridization solution (6X SSC, 1% BSA and 0.02 % SDS) for 1 hr at 37°C and the Cy5- labeled FHIT DNA probe and Cy5 labeled Fhit antibody, as previously mentioned concentrations, were added simultaneously to the prehybridization solution. The ensuing steps, as in the DNA detection protocol, were followed.

2.3.11 Instrumentation

2.3.11.1 *Biochip Signal Detection System*

A schematic diagram of the biochip concept is presented in Fig. 2.1. The integrated electro-optic system of the biochip has been described previously (20). A basic biochip includes (1) an excitation source with its associated optics, (2) fluorescently labeled

probe molecules, (3) target molecules immobilized on a sample platform, (4) optical detectors and (5) signal amplification/processing systems. In these experiments, a Helium-Neon laser (632.8 nm, 6.4 mW, Spectra-Physics, Eugene, OR) was used as an excitation source. The laser light was passed through a Corion laser band pass filter (Franklin, MA), a collimating lens (Newport Optics; Irvine, CA), a 4 x 4 optical diffractive element and subsequently focused on the microarrays on the membranes. Membranes were placed directly above the photodiode detection element and fluorescence signals from the excited Cy5 labeled probes were passed through a Graded Index of Refraction (GRIN) lens, and a 650 nm-band pass filter onto the detectors. Optical filters were used to isolate the background membrane fluorescence and to filter out any scattered laser light from reaching the detectors. Direct quantification of the fluorescence intensity of signals was performed by the integrated components of the biochip and the photocurrent of each sensing element was transmitted to a digital multimeter for instant data recording.

2.3.11.2 *Photometric Charge-Coupled Device (CCD)*

Whereas the biochip is the device used for actual measurements, we also used a photometric charge-coupled device (CCD) with a Pentax 50-mm lens equipped with a Vivitar macro teleconverter (Japan) in order to record the intensity of fluorescence signals of the DNA microarrays. A Coherent Innova 70, Krypton laser (Palo Alto, Ca), was employed as the excitation source and a Raman holographic filter (Kaiser Optical

systems, San Jose, CA) and Corion filters (Franklin, MA) were utilized for beam alignment. The systems own software, CCDOPS performed the image analyses.

2.4 RESULTS AND DISCUSSION

Deletion mapping studies of various primary carcinomas have localized common regions of deletion to the 3p14.2 region where the putative tumor suppressor gene, FHIT, has been mapped. Previous studies have demonstrated allelic losses, reduced or aberrant FHIT transcripts and decreased or absent Fhit protein expression in a large percentage of cancer-derived cell lines and primary carcinomas (1-13). These observations suggest that analysis of FHIT, either at the genetic level or at the protein level, could serve as a useful marker in cancer detection or for cancer screening. In this series of experiments, we have evaluated the detection capabilities of the integrated biochip for either individual or simultaneous identification and quantification of the Fhit protein and the FHIT DNA.

As an initial step, it was important to determine the level of background fluorescence which is inherent to the biochip system itself, in combination with the fluorescence induced as a result of nonspecific adsorption of the Cy5-conjugated probes to the membrane. For this study, a membrane incubated in the blocking solution was incubated in a solution of Cy5-conjugated goat IgG, and contributions of the fluorescence signal from the optical setup and from the membrane were measured using the biochip. Results illustrated in Fig. 2.2 demonstrated that the sum of the inherent fluorescence signals from the biochip dark noise with that of the membrane fluorescence background were uniform

in nature, thus providing an excellent baseline. This study also demonstrated that exposure of the membranes to the Cy5-labeled probe resulted in only a 1 - 2 % increase in the background fluorescence signal (corresponding to signal incurred using < 2.5 pg of immobilized target molecules) when compared to control membranes incubated in solutions containing only BSA (data not shown).

2.4.1 Analysis of Fhit Protein Expression

2.4.1.1 Characterization of Exogenous Fhit Expression in the Transfected Cell Lines

The biochip was used to differentiate cells of the MKN/FHIT cell line that have been transfected with vectors containing the FHIT gene from the MKN/E4 cell line carrying the control vector, not containing the FHIT gene. The cell lines were tested for expression of the exogenous Fhit protein using both conventional biological methods and the novel biochip system. The Coomassie blue staining procedure (Fig. 2.3 a) and the immunoblot analysis of stable transfectant cell lysates, using anti-Fhit polyclonal antibody (Fig. 2.3 b) showed presence of a band, the same position as the position of the band, expected for the Fhit protein. This band was only detectable in the lysates prepared from the MKN/FHIT cell line. Conversely, no band indicating Fhit expression was detected in the lane for the MKN/E4 cell line (Fig. 2.3 a,b). Protein markers were used in these studies for protein size estimations, along with inclusion of the pure Fhit protein, as the positive control sample in the Coomassie blue stained gel.

The feasibility of the biochip to detect Fhit protein was evaluated. To ensure optimal immobilization, stabilization, and detection, 4x4 arrays of the MKN/FHIT and the MKN/E4 cell lysates were spotted on Immunodyne ABC membranes. Membranes were then processed, probed with the Cy5-labeled Fhit antibody, and the induced fluorescence signal from arrayed protein spots were individually detected using the biochip. Results for the specifically bound Cy5-labeled antibodies, scored by counting discrete fluorescent signals, arising from the fluorescently active spots are presented in Fig. 2.4. The data demonstrated expression of the Fhit protein in the MKN/FHIT transfected cell line (row 1) and lack of the Fhit protein expression in the MKN/E4 cell line (row 4) as detected by the biochip. Fluorescence signals from the MKN/E4 spots were as low as the background fluorescence. The 4x4-array configuration in these experiments, with each specific target molecule being dispensed four times in a row, provided quadruplicate measurements of the same sample for enhanced data collection and analysis. Fluorescence signals generated using the biochip technology correlated well with results obtained using Western blotting and Coomassie blue staining techniques.

Three observations were made from the results of these experiments. First, the fluorescence detection capability of the biochip to detect complex formation between the Fhit protein and its complementary Cy5-labeled anti-Fhit antibody was demonstrated. Second, the affinity and the selectivity of the Cy5-labeled Fhit antibody to identify its target molecule, the Fhit protein, were also demonstrated. Lastly, the absence of cross-reactivity between the Cy5-labeled Fhit antibody and other proteins present in the lysate

of the MKN/E4 cell line was illustrated. These results clearly demonstrate the feasibility of the biochip as a new protein chip detection technology.

2.4.1.2 *Analysis of Multiplex Protein Microarrays*

Simultaneous detection of multiple protein molecules would be a valuable feature in a detection technology to be used in a clinical or research laboratory. We next evaluated the performance of this immuno-biochip to serve potentially as a selective and sensitive detection tool by simultaneously detecting multiple and independent immunoassays on the same sampling platform. We evaluated the capability of the biochip to concurrently detect the p53 antibody along with the Fhit protein on the same membrane. Subsequent to demonstration of the absence of cross-reactivity between the Fhit and the p53 antibodies to each other's target proteins (data not shown), a multiarray containing sample spots of the p53 antibody on row 1, MKN/FHIT lysate on row 3, and MKN/E4 lysate on row 4 was produced. The membrane was then incubated in a solution containing both the Cy5-labeled p53 blocking peptide and the Cy5-labeled Fhit antibody probes. The results of the study, illustrated in Fig. 2.5, show fluorescence signals detected from both the MKN/FHIT spots dispensed on the third row, and the p53 antibody spots dispensed on the first row of the microarray. Again, no fluorescence signal over the background signal was detected in the MKN/E4 row of spots.

The biochip device allowed simultaneous detection of both immobilized target antibodies on the same membrane when using a probe solution containing more than one Cy5-

labeled probe, each complementary to only one of the target proteins. These results demonstrated the potential of the biochip for use with many different complementary antibody/antigen complexes. This valuable feature of the biochip should provide for a more comprehensive and versatile clinical diagnostic technology. Such observations demonstrate that as an impending detection technology, the biochip could become extendable to immunoassays employing a battery of different antigens and complementary antibodies each labeled with different and unique fluorescent labels.

2.4.1.3 *Quantitative Fhit Protein Analysis*

To serve as an effective detection technology, it is crucial for the biochip to have the capability for quantitative analysis of the protein of interest. To establish the ability of the biochip to discriminate between different concentrations of the Fhit protein, we carried out a quantitative calibration. A membrane spotted with Fhit protein solutions containing different concentrations of the Fhit protein ranging from 0 to 200 ng/ml was probed with Cy5-labeled Fhit antibody. The relative fluorescence signals obtained in response to changes in the concentration of the immobilized target protein are presented in Fig. 2.6. The magnitude of fluorescence signals detected by the biochip increased with the increase in the concentration of the membrane immobilized Fhit protein. The non-linear portion of the curve could be attributed to (a) surface saturation resulting in self absorption caused by vibrational dampening of the energy, (b) saturation of detectors and finally, (c) interaction between the molecules effecting the geometry of the binding sites. However, considering the linear portion of the curve, These results further demonstrated

the biochip to be a sensitive and effective technology for quantitative analysis, where evaluation of the information on increased expression of tumor marker proteins of interest is important in clinical analysis.

2.4.2 Analysis of FHIT DNA

The detection of exon 5 of the FHIT gene is important in early cancer diagnosis since alterations in this gene have been observed in several tissue types in humans. FHIT DNA is also a recently discovered serological parameter in individuals with lung cancer since in a study 61% of cases showing tumor alterations also displayed a change in Fhit plasma DNA (22). The convergence of these findings highlight new possibilities for early tumor detection based on analysis of FHIT genetic changes in cells and in plasma DNA.

2.4.2.1 Analysis of FHIT DNA in the Transfected Cell Lines

In this study we evaluated the performance of the biochip for detection of the FHIT tumor suppressor gene (exon 5) in the MKN/FHIT and the MKN/E4 cell lines in solution and in human serum. Using DNazol, a guanidine-detergent lysing solution that selectively precipitates DNA, genomic DNA was isolated from MKN/FHIT and MKN/E4 cells (Fig. 2.7 a) and subsequently used as template for PCR amplification of exon 5 of the FHIT gene. An intact FHIT DNA was not detected in the MKN/E4 cell line as demonstrated by low fluorescence signal obtained from the MKN/E4 spots. However, in the MKN/FHIT cell line, presence of the FHIT DNA was established by increased

fluorescence signal over the signals obtained from the MKN/E4 cell line (Fig. 2.7 b). In a similar study, where the PCR amplified DNA from the two cell lines were diluted in human serum, similar results were observed (Fig. 2.7 c). The present study demonstrated the feasibility of the biochip as a useful DNA-based analytical system for the detection of specific genes in the entire human genomic DNA in biological solutions and in human serum. These findings highlighted new prospects for future applications of this new biochip in noninvasive gene screening procedures.

For comparison purposes, specific target molecules arrayed on the membrane were also analyzed using the widely used laboratory-based CCD imaging device, which is about 20 times larger in size than the biochip system. Active membranes were placed on a microscope slide and positioned on the imaging platform of the CCD camera. The krypton laser beam, transmitted through a fiber and passed through a filter, was then focused on the active area of the membrane for generation of fluorescence signals. The fluorescence intensity of signal peaks obtained from spots of MKN/FHIT cell lysates were higher than the intensity of the MKN/E4 lysates spotted on membrane (Fig. 2.8 a, b). The biochip obtained information corroborated extensively with real-time quantitative CCD captured images and histograms.

2.4.2.2 *Simultaneous Analysis of Multiple DNA Targets*

In diagnosis of human diseases or in genetic screening procedures, it is at times desirable to obtain information on the status of more than one gene that might be involved in

manifestation of a disease or diseases. Specific examples include detection of different biomarkers associated with carcinogenesis in different human organs such as breast, lung and pancreas (23-27). Therefore, simultaneous detection of multiple DNA molecules would be a valuable feature in a detection technology to be used in clinical or research laboratories. We evaluated the capability of the biochip to detect concurrently the FHIT DNA and the tuberculosis (TB) DNA immobilized on the same membrane. A multiarray containing sample spots of TB DNA on the first row and the MKN/FHIT DNA on the third row along with the MKN/E4 DNA on the fourth row was generated and simultaneously probed with Cy5-labeled oligonucleotide probes for both the TB DNA and the FHIT DNA.

Results of the study illustrated in Fig. 2.9 showed fluorescence signals detected from the TB DNA dispensed on the first row and the MKN/FHIT DNA spotted on the third row. In contrast, the level of the induced fluorescence signal on the fourth row, where the MKN/E4 DNA was spotted, was as low as the background fluorescence. The biochip device allowed simultaneous detection of both immobilized targets, the TB DNA and the FHIT DNA from the non-target MKN/E4 DNA, using a probe solution containing more than one Cy5-labeled DNA. These results demonstrated the potential of the biochip for detection of a variety of distinct gene/DNA probe molecules. This valuable feature of the biochip should provide for a more comprehensive and versatile clinical diagnostic technology.

2.4.2.3 *Quantitative Analysis of FHIT DNA*

To evaluate the capability of the biochip to generate a concentration curve of FHIT DNA in solution, aliquots of different concentrations of PCR amplified FHIT DNA ranging from 0-400 ng/ml were spotted and UV dimerized onto the membranes. Results showed an increase in the fluorescence signal output in response to increased concentration of the FHIT DNA (Fig. 2.10 a). The ability of the biochip to develop a concentration curve for FHIT DNA in human serum was also demonstrated in a study where the induced fluorescence signal increased in accordance with the increase in the concentration of the FHIT DNA, ranging from 0-60 ug/ml, in human serum (Fig. 2.10 b). These findings are in agreement with detector-generated output signals, and therefore the sensitivity of the biochip, with respect to increases in the concentration of the target molecule. These observations substantiated the biochip as an effective technology for quantitative DNA analysis in biological solutions and in human serum.

2.4.3 *Simultaneous FHIT Gene and Protein Multiplex Detection:*

The Multifunctional Biochip

Genome analysis to monitor specific changes in gene activation is possible using the biochip technology. However, knowing the genetic sequence encoding a protein is not sufficient to predict the biological nature of a protein. This can be particularly important in cancer research where post-translational modifications of a protein can specifically lead to disease. As demonstrated in this study, immunoassay-based detection of proteins,

employing this biochip has been achieved. In this study, we combined the DNA and protein detection capabilities of the biochip to accomplish both gene detection and protein expression detection simultaneously.

To achieve this goal, we developed a novel and unique protocol, a “South-Western” assay, for simultaneous detection of proteins and DNA immobilized on the same substrate platform. The design of this bioassay involved a unique adaptation of traditional DNA and protein detection biochemistry. In a preliminary study, Fhit protein and FHIT DNA spots were generated in a microarray format and using this new protocol, the membrane was incubated in a solution containing both Cy5-labeled FHIT DNA probe and the Cy5-labeled complementary Fhit antibody. Successful detection of the fluorescent-signals induced in the different targets, the FHIT DNA and the Fhit protein, spotted on the first and the fourth rows of the same membrane are presented in Fig. 2.11. The fluorescence signal detection, afforded by the biochip in conjunction with the South-Western assay, enabled the immune- DNA assay to be carried out on multiplex samples, allowing simultaneous analyte detection with reliable sensitivity. These investigations illustrated the potential of the multifunctional biochip with an unprecedented capability for diverse molecule detection for applications in cancer diagnostics.

2.5 Conclusion

Cancer research would greatly benefit from innovative technologies that allow simultaneous screening of several unknown genes and proteins involved in

carcinogenic manifestations. The aim of development of this biochip was to design a dual modality, cancer diagnostic device, that performs processes that are currently carried out in biological research or clinical laboratories. These processes would require less initial sample and reagents, and would provide a reliable resolution of detection and specificity, all at a lower expense. The design of this highly efficient fluorescence detection technology with the capability for simultaneous DNA-protein detection is based on microelectronic fabrication and miniaturization technologies. The fluorescence-based, non-radioactive, detection method is convenient and inexpensive, permitting sensitive, selective and direct measurements of a variety of antigen-antibody complexes and double stranded DNA formations.

2.6 Acknowledgements

This research was jointly sponsored by the Office of Biological and Environmental Research, U.S. Department of Energy under contract DE-AC05-00OR22725 with UT-Battelle, LLC., and by the ORNL Laboratory Directed Research and Development Program (Advanced Nanosystems). The author would also like to thank Dr. Kay Huebner for providing the gift of cell lines (Kimmel Cancer Institute, Thomas Jefferson University) and Dr. Charles Brenner for contributing the gift of *w1* FHIT protein (Kimmel Cancer Institute, Thomas Jefferson University).

REFERENCES

1. Ohta, M., Inoue, H., Cotticelli, M. G., Kastury, K., Baffa, R., Palazzo, J., Siprashvili, Z., Mori, M., McCue, P., Druck, T., Croce, C. M. & Huebner, K. The FHIT gene, spanning the chromosome 3p14.2 fragile site and renal carcinoma-associated t(3;8) breakpoint, is abnormal in digestive tract cancers. (1996) *Cell*, 84(4), 587-597
2. Barnes, L. D., Garrison, P. N., Siprashvili, Z., Guranowski, A., Robinson, A. K., Ingram, S. W., Croce, C. M., Ohta, M. & Huebner, K. Fhit, a putative tumor suppressor in humans, is a dinucleoside 5',5'''-P1,P3-triphosphate hydrolase. (1996) *Biochemistry*, 35(36), 11529-35
3. Brenner, C., Garrison, P., Gilmour, J., Peisach, D., Ringe, D., Petsko, G. A. & Lowenstein, J. M. Crystal structures of HINT demonstrate that histidine triad proteins are GalT-related nucleotide-binding proteins. (1997) *Nat. Struct. Biol.*, 4, 231-238
4. Sard, L., Accornero, P., Tornielli, S., Delia, D., Bunone, G., Campiglio, M., Colombo, M. P., Gramegna, M., Croce, C.M., Pierotti, M. A. & Sozzi, G. C. The tumor-suppressor gene FHIT is involved in the regulation of apoptosis and in cell cycle control. (1999) *Proc. Natl. Acad. Sci.*, 96(15), 8489-8492
5. Huebner, K., Garrison, P. N., Barnes, L.D. & Croce, C. M. The role of the FHIT/FRA3B locus in cancer. (1998) *Annu. Rev. Genet.*, 32, 7-31
6. Ingvarsson, S., Agnarsson, B. A., Sigbjornsdottir, B. I., Kononen, J., Kallioniemi, O. P., Barkardottir, R.B., Kovatich, A.J., Schwarting, R., Hauck, W.W., Huebner, K. & McCue, P. A. Reduced Fhit expression in sporadic and BRCA2-linked breast carcinomas. (1999) *Cancer Res.*, 59(11), 2682-9

7. Huiping, C., Jonasson, J. G., Agnarsson, B. A., Sigbjornsdottir, B. I., Huebner, K. & Ingvarsson, S. Analysis of the fragile histidine triad (FHIT) gene in lobular breast cancer. (2000) *Eur. J. Cancer*, 36(12), 1552-7
8. Mangray, S., & King, T. C. Molecular pathobiology of pancreatic adenocarcinoma. (1998) *Front. Biosci.*, 3, D1148-60
9. Mueller, J., Werner, M., & Siewert, J. R. Malignant progression in Barrett's esophagus: pathology and molecular biology. (2000) *Recent Results Cancer Res.*, 155, 29-41
10. Gartenhaus, R. B. Allelic loss determination in chronic lymphocytic leukemia by immunomagnetic bead sorting and microsatellite marker analysis. (1997) *Oncogen*, 14(3), 375-8
11. Sozzi, G., Pastorino, U., Moiraghi, L., Tagliabue, E., Pezzella, F., Ghirelli, C., Tornielli, S., Sard, L., Huebner, K., Pierotti, M. A., Croce, C. M. & Pilotti, S. Loss of FHIT function in lung cancer and preinvasive bronchial lesions. (1998) *Cancer Res.*, 58(22), 5032-7
12. Mori, M., Mimori, K., Shiraishi, T., Alder, H., Inoue, H., Tanaka, Y., Sugimachi, K., Huebner, K., & Croce, C. M. Altered expression of Fhit in carcinoma and precarcinomatous lesions of the esophagus. (2000) *Cancer Res.*, 60(5), 1177-82
13. Sozzi, G., Musso, K., Ratcliffe, C., Goldstraw, P., Pierotti, M. A. & Pastorino, U. Detection of microsatellite alterations in plasma DNA of non-small cell lung cancer patients: a prospect for early diagnosis. (1999) *Clin. Cancer Res.*, 5(10), 2689-92

14. Schultz, S., Smith, D. R., Mock, J. J. & Schultz, D.A. Single-target molecule detection with nonbleaching multicolor optical immunolabels. (2000) *Proc. Natl. Acad. Sci. U S A*, 97(3), 996-1001
15. Spiker, J, O. & Kangm K, A. Preliminary study of real-time fiber optic based protein C biosensor. (1999) *Biotechnol. Bioeng.*, 66(3), 158-63
16. Narang, U. Anderson, G. P., Ligler, F. S. & Burans, J. Fiber optic-based biosensor for ricin. (1997) *J. Biosens. Bioelectron.*, 12(9-10), 937-45
17. Grant, S.A. & Glass, R. S. Sol-gel-based biosensors for use in stroke treatment. (1999) *IEEE Trans. Biomed. Eng.*, 46(10), 1207-11
18. Wadkins, R.M., Golden, J. P., Pritsiolas, L. M. & Ligler, F. S. Detection of multiple toxic agents using a planar array immunosensor. (1998) *Biosens. Bioelectron.*, 13(3-4), 407-15
19. Vo-Dinh, T., Wintenberg, A. L., Ericson, M. N., Isola, N. & Alarie, J. P. Development of a DNA biochip for gene diagnosis. Biomedical Sensing and Imaging Technologies, R. Lieberman et.al., Eds. (1998) SPIE Publishers, Bellingham, WA.
20. Vo-Dinh, T., Alarie, J. P., Isola, N., Landis, D., Wintenberg, A. L. & Ericson, M. N. DNA Biochip Using Phototransistor Integrated Circuit. (1999) *Anal. Chem.*, 71(2), 358-63
21. Vo-Dinh, T. Development of a DNA Biochip: Principle and Applications. (1998) *Sensors and Actuators*, B(51), 52-59
22. Sozzi, G., Musso, K., Ratcliffe, C., Goldstraw, P., Pierotti, M. A. & Pastorino, U. Detection of microsatellite alterations in plasma DNA of non-small cell lung cancer patients: a prospect for early diagnosis. (1999) *Clin. Cancer Res.*, 5(10), 2689-92

23. Inaji, H., Koyama, H., Motomura, K., Noguchi, S., Tsuji, N., Kimura, Y., Sato, H., Sugano, K. & Ohkura, H. Simultaneous Assay of ErbB-2 Protein and Carcinoembryonic Antigen in Cyst Fluid as an Aid in Diagnosing Cystic Lesions of the Breast. (1994) *Breast Cancer*, 1(1), 25-30
24. Sampietro, G., Tomasic, G., Collini, P., Biganzoli, E., Boracchi, P., Bidoli, P. & Pilotti, S. Gene product immunophenotyping of neuroendocrine lung tumors. No linking evidence between carcinoids and small-cell lung carcinomas suggested by multivariate statistical analysis. (2000) *Appl. Immunohistochem. Molecul. Morphol.*, 8(1), 49-56
25. Satoh, F., Umemura, S. & Osamura, R. Y. Immunohistochemical analysis of GCDFP-15 and GCDFP-24 in mammary and non-mammary tissue. (2000) *Breast Cancer*, 7(1), 49-55
26. Notohara, K., Hamazaki, S., Tsukayama, C., Nakamoto, S., Kawabata, K., Mizobuchi, K., Sakamoto, K. & Okada, S. Solid -pseudopapillary tumor of the pancreas: immunohistochemical localization of neuroendocrine markers and CD10. (2000) *Am. J. Surg. Pathol.*, 24(10), 1361-71
27. Kanavaros, P., Stefanaki, K., Vlachonikolis, J., Eliopoulos, G., Kakolyris, S., Rontogianni, D., Gorgoulis, V. & Georgoulis, V. Expression of p53, p21/waf1, bcl-2, bax, Rb and Ki67 proteins in Hodgkin's lymphomas. (2000) *Histol. Histopathol.*, 15(2), 445-53

APPENDIX

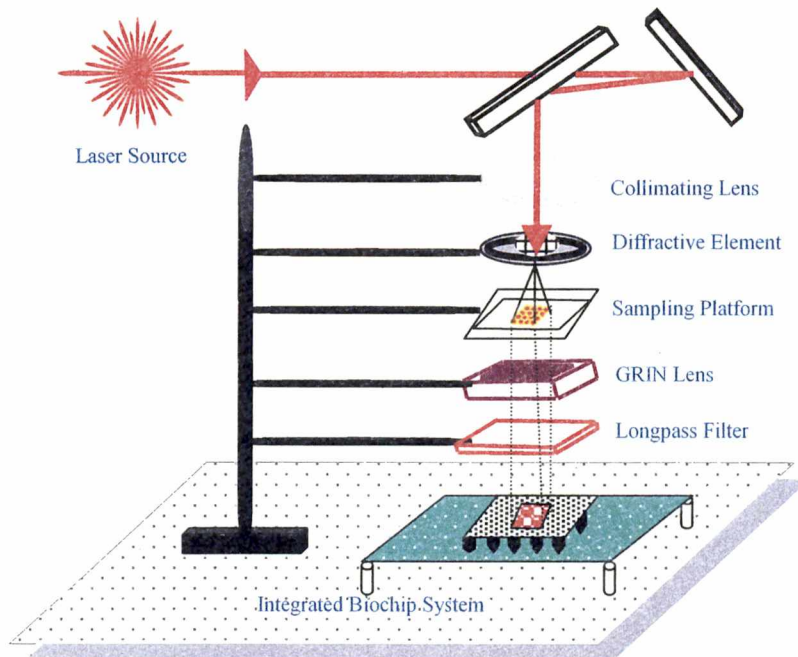
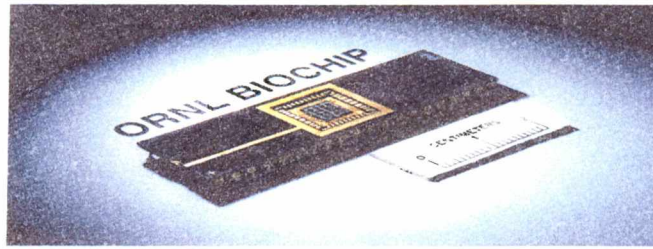


Figure 2.1 Schematic diagram of a biochip concept. Light from a 6.4 mW, He-Ne laser (632.8 nm) was transmitted through a laser band pass filter, a collimating lens, a 4 x 4 optical diffractive element and focused onto sample spots situated directly above the phototransistor detection elements. The 4x4 sensing array is comprised of 16 individual photodiodes arranged in a square with 900- μm edges and 1-mm center-to-center spacing between them. A GRIN lens, and a 650 ± 10 nm band pass filter was situated between the detector elements and the sample substrate to isolate the fluorescence of interest. The photocurrent of each sensing element of the amplifier/ phototransistor microchip was transmitted to a digital voltmeter linked to a multimeter for data recording.

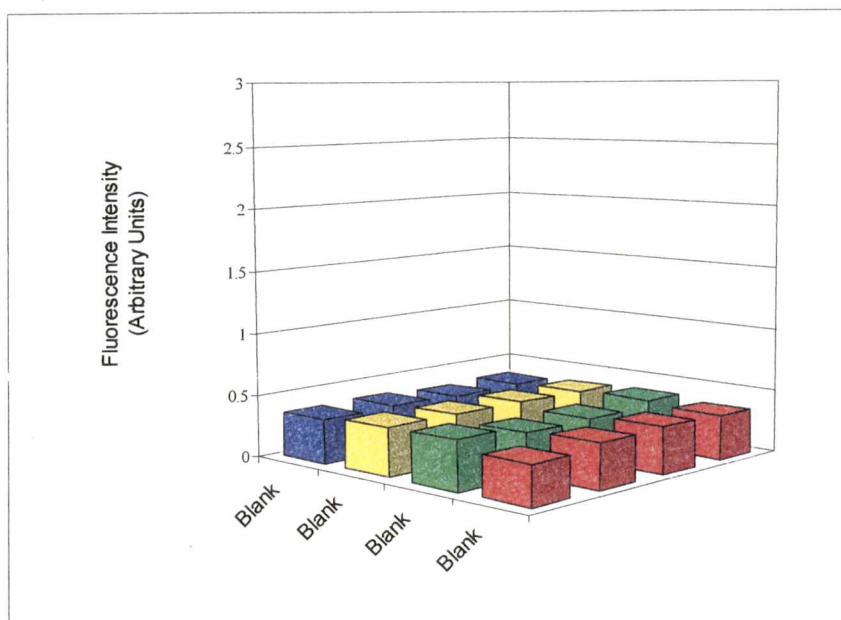


Figure 2.2 Study of nonspecific binding effect. Background fluorescent signal inherent to the biochip optical set up and the membrane platform were measured. Levels of background fluorescence signals are low and uniform in intensity providing an excellent baseline.

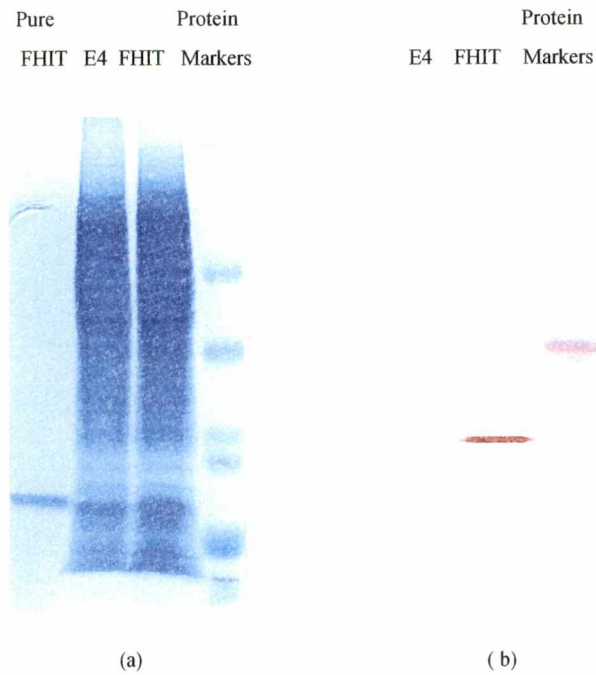


Figure 2.3 The MKN/FHIT and MKN/E4 gastric carcinoma cell lines were tested for expression of the Fhit protein. Coomassie blue staining (Fig.2.3 a) and Western immunoblot analysis of cell lysates using anti-Fhit polyclonal antibody (Fig.2.3 b) show expression of detectable Fhit protein only in the MKN/FHIT cell line. Conversely, no exogenous Fhit expression was detected in the MKN/E4 cell line (Fig.2.3 a,b). Pure Fhit protein was included as positive control in the Coomassie stained gel along protein markers in both gels.

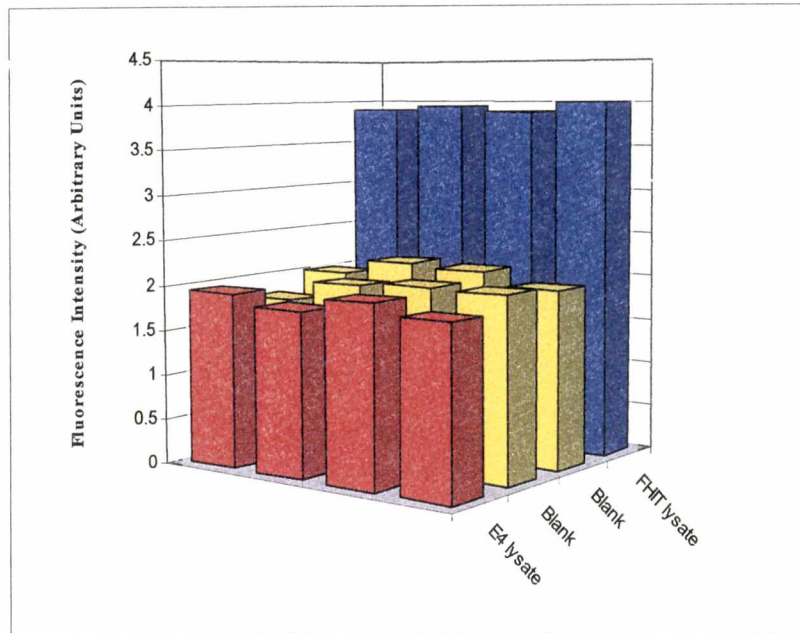


Figure 2.4 Biochip fluorescent signal measurement and analysis for detection of Fhit protein. Using Cy5-labeled polyclonal antibody against Fhit protein, fluorescent signals were detected from MKN/FHIT lysate row of spots. No significant fluorescence was observed from MKN/E4 lysate spots.

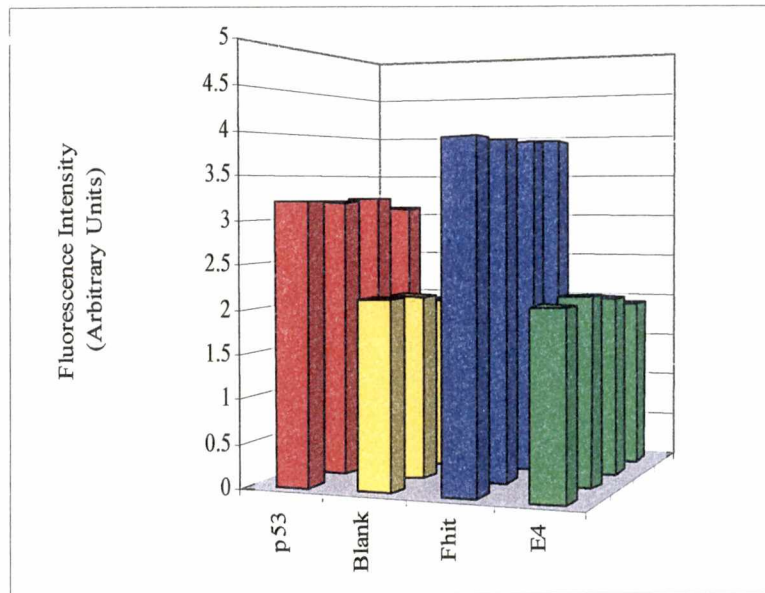


Figure 2.5 Simultaneous detection of multiple protein molecules was achieved using the biochip. Fluorescence signals were detected from MKN/FHIT spots on the third row and the p53 spots on the first row of the microarray. No signal was observed from MKN/E4 row of spots.

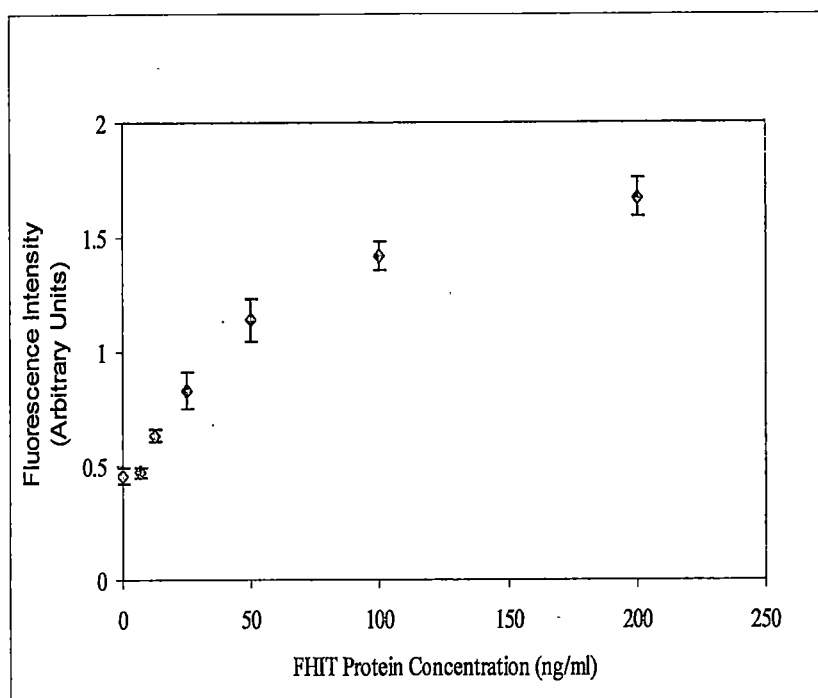
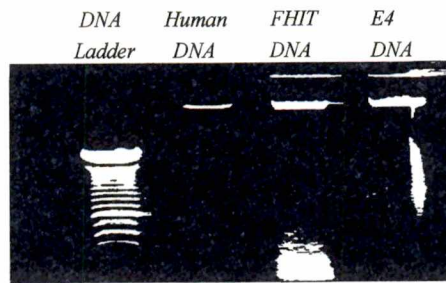
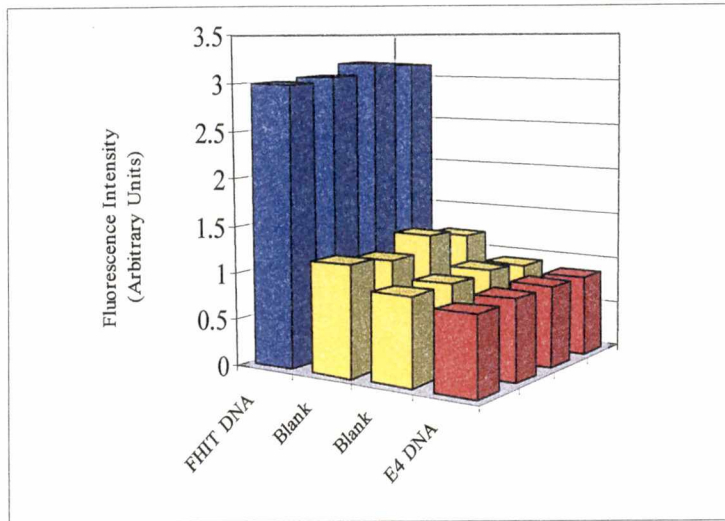


Figure 2.6 Fhit protein quantitative analysis. Biochip capability for quantitative analysis of different concentrations of the Fhit protein is demonstrated. The relative fluorescence signal detected by the biochip increased in response to increases in concentration of immobilized target MKN/FHIT lysate immobilized on the microarray in a curvilinear fashion.

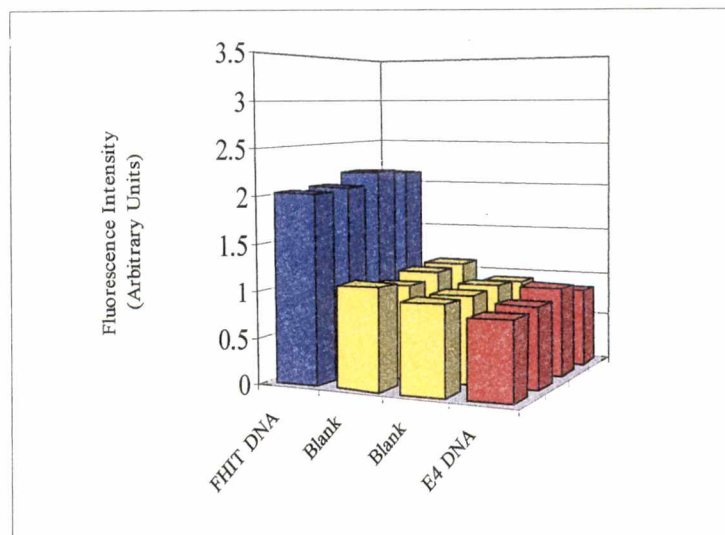
Figure 2.7 Genomic DNA was isolated from MKN/FHIT and MKN/E4 cell lysates using a guanidine- based lysing solution detected by gel electrophoresis (a). Extracted genomic DNAs were PCR amplified using sequence-specific primers for the FHIT gene and subjected to detection using fluorescently labeled FHIT DNA probes. As determined by the biochip, the MKN/FHIT cell line, PCR products, demonstrated significantly increased fluorescence signal over background as a result of retaining the FHIT gene. Presence of an intact FHIT gene did not present itself in the MKN/E4 cell line and the observed fluorescence signal was at the same level of the background fluorescence (b). Comparable biochip measurements were observed where targets were mixed with human serum (c).



(a)



(b)



(c)

Figure 2.7

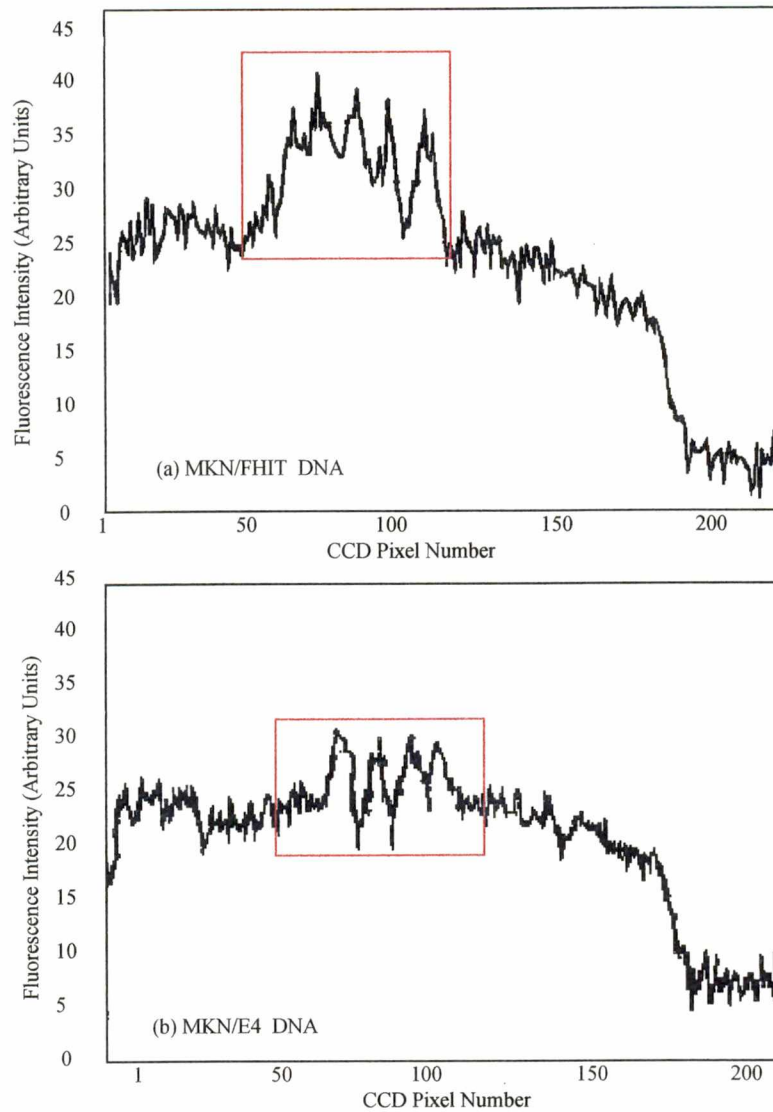


Figure 2.8 Application of CCD system for detection of FHIT DNA. The CCD captured histogram of the row corresponding to the immobilized MKN/FHIT DNA (a) displayed a higher fluorescence signal as compared to MKN/E4 DNA spots (b). The CCD imaging results correlated well with the results from the biochip study and reconfirmed the absence of the FHIT gene in MKN/E4 cell line genomic extracts.

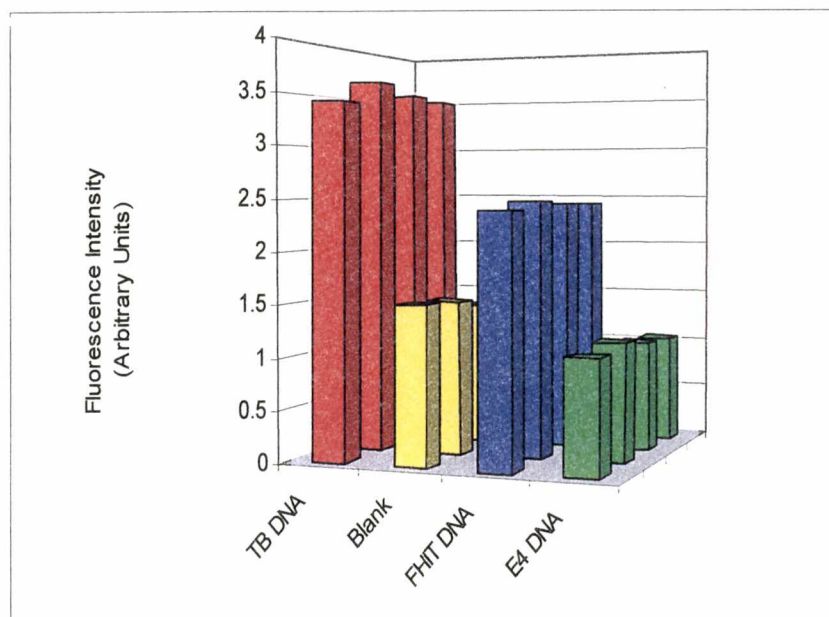
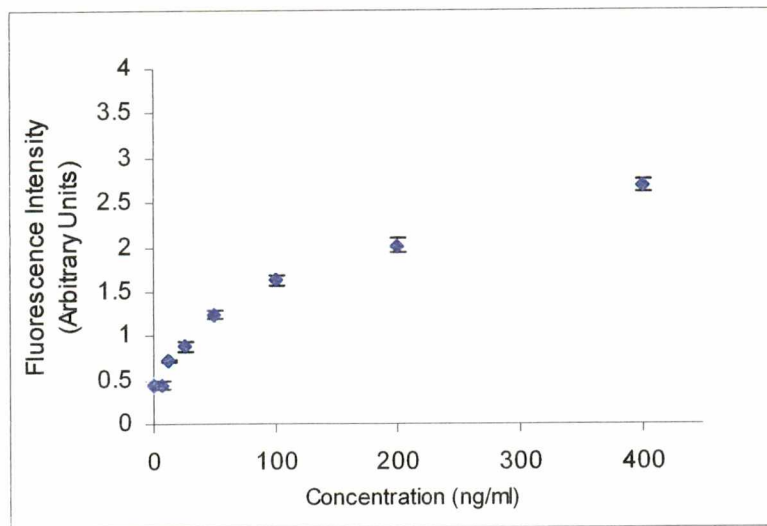
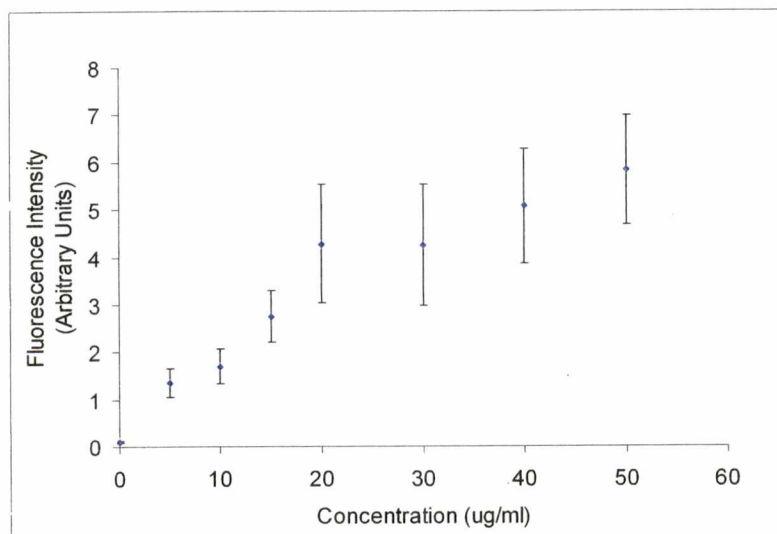


Figure 2.9 Application of the biochip for concurrent detection of various DNA molecules on the same microarray was accomplished. The biochip system simultaneously detected both immobilized target DNAs, the FHIT DNA and tuberculosis DNA (TB) on the same membrane using Cy5-labeled oligonucleotide probes for detection of both genes. Meanwhile, no fluorescence was detected from non-target MKN/E4 DNA row of spots. These results demonstrated the potential of the biochip for detection of a variety of distinct gene/ DNA probe molecules at one time.



(a)



(b)

Figure 2.10 FHIT DNA quantitative analysis. Biochip capability for quantitative analysis of FHIT DNA was illustrated by a relative increase in the signal output in response to increases in concentration of the membrane immobilized, FHIT DNA.

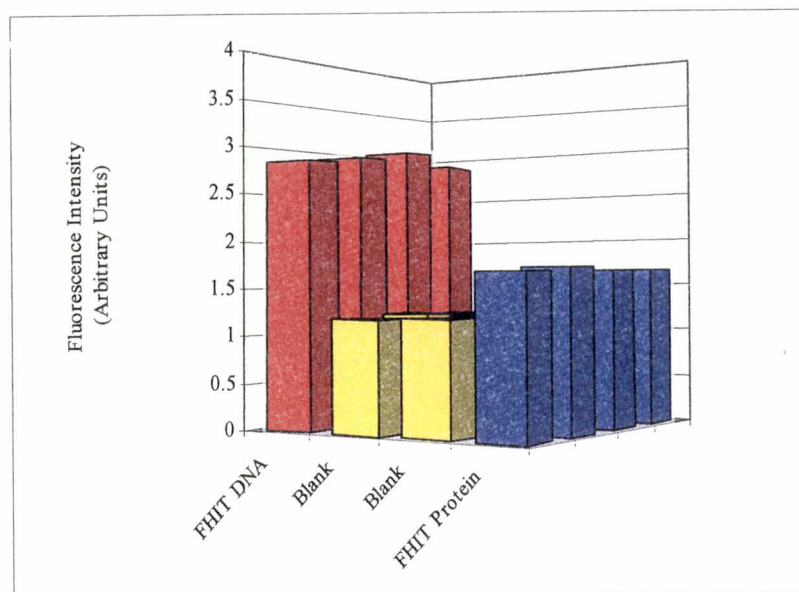


Figure 2.11 Study of multi-target detection. Biochip device permitted simultaneous detection of immobilized MKN/FHIT lysate protein and PCR amplified FHIT DNA target molecules spotted in the same microarray using Cy5 labeled polyclonal Fhit antibody, and fluorescently labeled FHIT DNA probe. Biochip measurements demonstrated significant fluorescent signals from MKN/FHIT lysate spots row and the row where PCR amplified MKN/FHIT DNA were dispensed.

PART THREE

**ANALYSIS OF HYDROLYSIS ACTIVITY OF THE FHIT PROTEIN;
APPLICATION OF SYNCHRONOUS LUMINESCENCE
SPECTROSCOPY**

3.1 ABSTRACT

Human Fhit tumor suppressor protein has been shown to have dinucleoside 5', 5'''- P₁, P_n - polyphosphates hydrolysis activity. The enzymatic activity of Fhit has been demonstrated on Ap_nA (n = 3-6) substrates with adenosine monophosphate (AMP) always being one of the reaction products. The use of Synchronous Luminescence (SL) Spectroscopy as a sensitive yet simple method for detection of the enzymatic activity of the Fhit protein was investigated. The SL methodology is based on synchronous excitation, in which both excitation (λ_{ex}) and emission (λ_{em}) wavelengths are scanned simultaneously, while a constant wavelength interval ($\Delta\lambda$) is maintained between the excitation and the emission monochromators. The results presented illustrate the ability of the SL technique to identify the constituents of the hydrolysis mixture (the Fhit protein and the Ap₄A substrate) and demonstrate production of the AMP. Using SL spectroscopy we detected increased fluorescence intensity of the AMP peak as a result of increased substrate concentration. Additionally, inhibition of hydrolysis activity by zinc chloride was demonstrated. These findings demonstrated the ability of the SL technique as a rapid detection method for identification of specific fluorescent compounds for analyzing enzymatic activity of proteins without the need for use of modified substrates.

3.2 INTRODUCTION

The recently cloned human tumor suppressor Fragile Histidine Triad (FHIT) gene encompasses the most fragile site in the human genome, the FRA3B region. The approximately 1-megabase FHIT gene includes 10 exons, encoding a 1.1 kb mRNA transcript and a 16.8 kDa, 147 amino acid protein. Human Fhit protein has recently assumed significant interest since studies have shown loss of heterozygosity and homozygous deletions within the FHIT gene, and absence of expression of Fhit protein occurring in several common cancers (6,7) (Fig. 3.1). Fhit protein is a member of the recently discovered Histidine Triad (HIT) family of nucleotide-binding proteins with high specific hydrolyzing activity for diadenosine 5', 5'''- P₁, P_n - polyphosphate (A_{p_n}A), where n = 3-6 (3). Catabolic activity of Fhit on the diadenosine tetraphosphate (A_{p₄}A) substrate has been observed repeatedly with adenosine monophosphate (AMP) always being one of the reaction products (2,3). Methods currently employed for determining the enzymatic activity of the Fhit protein and quantification of the byproducts of the hydrolysis reaction involve using either radioactively modified substrates in chromatographic assays, or fluorescently labeled substrates in conventional spectroscopic assays (1,4,5).

The goal of this study was to develop a simple, yet highly sensitive spectrometric technique without the need for use of modified substrates. Conventional luminescence spectrometry uses either a fixed excitation or a fixed emission wavelength to measure the luminescence intensity of different fluorescent compounds. In the synchronous

Luminescence (SL) methodology both excitation and emission wavelengths are scanned simultaneously while a constant wavelength interval ($\Delta\lambda$) is maintained between the two monochromators throughout the measurement (8). Excitation, emission and SL spectra of tryptophan are illustrated in Fig. 3.2. Resulting SL spectrum has more resolved structures and more readily identifiable peaks than the conventional luminescence spectrum. The ability of SL to offer better peak resolution makes it a highly selective analytical technique for detection of various compounds (9). SL has been extensively used to obtain spectral fingerprints of complex biological and chemical samples (8-11). We investigated the ability of the SL technique to analyze specific protein-substrate enzymatic activity, hydrolysis of the Ap₄A substrate by the Fhit protein through identification of the reaction byproducts.

3.3 MATERIALS AND METHODS

3.3.1 Fhit Hydrolysis Assay

A typical assay for Ap₄A hydrolase activity by the Fhit protein involved co-incubation of both the enzyme and the substrate in the hydrolysis solution (50 mM HEPES-NaOH, pH 6.8, and 0.5 mM MnCl₂ (Sigma Chemical Co, St. Louis, MO)). A complete reaction mixture was prepared by incubation of 20 μ M Ap₄A substrate (Sigma Chemical Co, St. Louis, MO) and 1 ng of the Fhit protein (a gift from Dr. Charles Brenner, Kimmel Cancer Center, Philadelphia, PA) in 100 μ l of hydrolysis solution at room temperature (4). A purification protocol for the active dimeric human Fhit protein has been described (3).

3.3.2 Synchronous Luminescence Spectroscopy

The SL technique is characterized by the simplicity of its instrumentation. All spectroscopic measurements were performed using a single integrated workstation spectrofluorimeter (Perkin Elmer, Model LS 50B, Norwalk, CT) with computer interfacing capabilities (Fig. 3.3). This commercial instrument has two monochromators that can be interlocked and scanned simultaneously and allows spectral correction for both excitation and emission spectra. Spectroscopic measurements of the reaction mixtures were performed in Starna quartz sub-micro cuvettes having 1-cm path lengths (Atascadero, CA). The FL WinLab software (Perkin Elmer, Norwalk, CT) was employed for instrumental control and fluorescent signal analysis.

3.4 RESULTS AND DISCUSSION

3.4.1 Selection of Wavelength Interval

The choice of $\Delta\lambda$ interval was critical for successful analysis. It was optimized through the following procedure. The SL spectra of the individual components of the hydrolysis reaction, the Fhit protein, and the A_p4A substrate and reaction byproduct were scanned with $\Delta\lambda$ intervals ranging from 5-100 nm, in 5-nm increments. From these measurements, it was determined that an interval of $\Delta\lambda = 50$ nm was the most suitable wavelength

interval. The obtained spectra using this wavelength interval provided the best spectral differentiation allowing for (i) identification of the individual reaction components, (ii) the byproducts of the reaction, and (iii) assessment of the hydrolysis activity of the Fhit protein. Additional data obtained from these preliminary assays indicated a rapid hydrolytic reaction. Total hydrolysis of 20 μM of Ap_4A by 1 ng of the Fhit protein was achieved in < five min. Enzymatic activities of the complete reaction mixtures were followed over an extended period of time to determine any changes in the hydrolysis reaction mixture. Samples were measured in 5-minute intervals for the first hr and then hourly for the next 5 hrs and finally at 19, 24 and 27 hrs. Except for some degradation of the Fhit protein, no change in fluorescence of the mixture was noticed (data not shown).

3.4.2 Fhit Hydrolysis Reaction

A representative SL spectrum ($\Delta\lambda = 50$ nm excitation wavelength) for individual components of the hydrolysis reaction (hydrolysis solution, Fhit, Ap_4A) (a-c), the complete reaction (d) and confirmation of byproduct formation (e) as a result of the breakdown of Ap_4A by Fhit protein (< 5 min) are presented in Figure 3.4. The fluorescence spectrum of the hydrolysis solution (a) demonstrated absence of any distinguishable peaks. The spectrum of Ap_4A substrate (b) however, exhibited low fluorescence intensity with two broad peaks at 320 nm and 360 nm. The spectrum of Fhit protein (c) had a higher fluorescence intensity than the Ap_4A substrate with two broad peaks at 285 nm and 370 nm. Addition of the Fhit protein to an Ap_4A containing solution

resulted in a spectrum profile different from the profiles of either the Fhit protein or the Ap₄A substrate. Synchronous detection of the enzymatic activity associated with the Fhit protein is illustrated in Fig. 3.4 d. There was a noticeable change in the ratio of the first peak at 285 nm to that of the second peak at 370 nm when compared to the fluorescence scan of Fhit protein alone (c).

This observation suggested the presence of other compounds in the reaction mixture since the simple summation of the fluorescence intensities of the Ap₄A and the Fhit in the sample cannot account for these changes in the fluorescence profile. Furthermore, we had previously determined that the synchronously measured SL peak for AMP ($\Delta\lambda = 50$ nm) occurred at about 285 nm (Fig. 3.5).

To correlate the 285-nm peak with the presence of reaction byproducts, a 10- μ M aliquot of AMP solution was added to the same reaction vial. The spectrum obtained (Figure 3.4 e) exhibited an increase only in fluorescence intensity of the peak at 285 nm, where the peak for the compound of interest, AMP, was located. The enhancement of the second peak at 370 nm, which was probably associated with the spectrum of Fhit protein, was not observed. Evaluation of fluorescence intensity distribution of SL profiles in Fig. 3.4 provided strong evidence for the presence of newly formed byproduct(s) in the reaction mixture as a result of enzymatic function of Fhit Ap₄A hydrolase activity.

A great advantage of the synchronous scanning technique is the ability to show small changes that come from variety of parameters including band narrowing effect, overlap of excitation and emission spectra, optical filter effect and solvent effect. These parameters are often difficult to observe in conventional fixed-excitation spectroscopy but are greatly enhanced in synchronous scanning.

3.4.3 Quantitative Analysis of the Hydrolysis Assay

The quantitative ability of the SL technique to measure the fluorescence intensity associated with AMP production, at a constant Fhit protein concentration and increasing concentrations of Ap₄A, ranging from 10-50 μM in 100 μl of the assay solution was investigated. The reactions were allowed to stand for 5 minutes at room temperature before carrying out the SL scans (140 s). Results of this quantitative analysis are illustrated in Figure 3.6. The increase in the fluorescence intensity of the 285-nm peak correlated well to the increasing concentrations of the Ap₄A ranging from 10-50 μM in the experimental samples.

The intensity of the SL fluorescence signal can be expressed in the following equation (9):

$$I_{SL}(\lambda_{ex}, \lambda_{em}) = KcbE_x(\lambda_{ex})E_m(\lambda_{em}) \quad (1)$$

with

$$\Delta\lambda = \lambda_{ex} - \lambda_{em} = const. \quad (2)$$

where c is the concentration of the analyte, b is the thickness of the sample, $E_x (\lambda_{ex})$ is the excitation spectrum, $E_m (\lambda_{em})$ is the emission spectrum, and K is a constant that includes the instrumental geometry factor and related parameters. Therefore, since the relative luminescence intensity of the synchronous peak is a direct function of the concentration of the compound in the assay mixture, this increase in fluorescent intensity of the 285-nm peak could prove useful for determining the concentration of the byproducts.

Using the following mathematical equations the specific activity (nmol of products formed per $\text{min}^{-1} \text{mg}^{-1}$) could be calculated.

$$\text{Specific Activity} = [P]_t / TM \quad (3)$$

Where $[P]_t$ is the concentration of the newly formed reaction byproducts (nmol) during T the time of reaction (min) at a given amount of protein mass M (mg). $[P]_t$ can be expressed as:

$$[P]_t / [Ap_4A]_0 = I_p / I_T \quad (4)$$

Where the total concentration of the substrate (nmol) at time 0, $[Ap_4A]_0$, is a function of the relative fluorescence intensity of the products formed, I_p , divided by the total fluorescence intensity of the reactant, I_T , during the reaction.

3.4.4 Inhibition of the Enzymatic Reaction in Presence of ZnCl₂

Data have been previously reported on the inhibitory effect of Zn²⁺ on the enzymatic activity of Fhit protein (1,4,5). To investigate this phenomenon, synchronous measurements of the hydrolysis solution containing (a) Fhit protein, (b) Fhit protein and Ap₄A substrate, and (c) Fhit, Ap₄A, and ZnCl₂ (100 μM) were obtained. The data are presented in Figure 3.7 as the ratio of the fluorescent intensity of 285 nm peak to the fluorescence intensity of the second peak. The intensity of the first peak does not increase relative to that of the second peak in the presence of ZnCl₂. This change in the fluorescence profile was expected if the Fhit protein had maintained its activity in the presence of Zn²⁺. The absence of activity of the Fhit protein in the presence of Zn²⁺ supports the previously reported data.

3.5 CONCLUSION

In conclusion, SL offered a simple, sensitive and rapid analytical technique with inexpensive instrumentation that allowed the study of hydrolysis activity of the Fhit protein. The results established the SL technique as a rapid detection technology (140 s/scan) with the ability to detect the hydrolysis function of the Fhit, human tumor suppressor protein on break down of the Ap₄A substrate by indicating presence of the reaction byproducts. This versatile technique eliminated the need for the use of relatively undesirable and expensive radioisotopes or fluorescently modified reaction compounds

and does not require further identification of the products through other analytical techniques such as various forms of chromatography.

3.6 ACKNOWLEDGEMENTS

This research was jointly sponsored by the Office of Biological and Environmental Research, U.S. Department of Energy under contract DE-AC05-00OR22725 with UT-Battelle, LLC., and by the ORNL Laboratory Directed Research and Development Program (Advanced Nanosystems). The authors would also like to thank Dr. Charles Brenner for the gift of FHIT protein (Kimmel Cancer Institute, Thomas Jefferson University).

REFERENCES

1. Asensio, A.C., Oaknin, S. & Rotllan, P. Fluorimetric detection of enzymatic activity associated with the human tumor suppressor Fhit protein. (1999) *Biochim. Biophys. Acta.*, 1432(2), 396-400
2. Barnes, L. D., Robinson, A. K., Mumford, C. H. & Garrison, P. N. Assay of diadenosine tetraphosphate hydrolytic enzymes by boronate chromatography. (1985) *Anal. Biochem.*, 144, 296-304
3. Brenner, C., Pace, H. C., Garrison, P. N., Robinson, A. K., Rosler, A., Liu, X., Blackburn, G. M., Croce, C. M., Huebner, K., and Barnes, L.D. Purification and crystallization of complexes modeling the active state of the fragile histidine triad protein. (1997) *Protein Eng.*, 10(12), 1461-1463
4. Draganescu, A., Hodawadekar, S., Gee, K., and Brenner, C. (2000) Fhit-nucleotide specificity probed with novel fluorescent and fluorogenic substrates. *Biol. Chem.*, 18,275(7), 4555-60
5. Ji, L., Fang, B., and Roth, J. A. A rapid, sensitive, and nonradioactive method for assay of FHIT Ap3A hydrolase activity by fluorescence thin-layer chromatographic image analysis. (1999) *Anal. Biochem.*, 271(1), 114-6
6. Ohta, M., Inoue, H., Cotticelli, M. G., Kastury, K., Baffa, R., Palazzo, J., Siprashvili, Z., Mori, M., McCue, P., Druck, T., Croce, C. M. & Huebner, K. The FHIT gene, spanning the chromosome 3p14.2 fragile site and renal carcinoma-associated t(3;8) breakpoint, is abnormal in digestive tract cancers. (1996) *Cell*, 84(4), 587-597

7. Sard, L., Accornero, P., Torielli, S., Delia, D., Bunone, G., Campiglio, M., Colombo, M. P., Gramegna, M., Croce C.M., Pierotti M. A. & Sozzi G. C. The tumor-suppressor gene FHIT is involved in the regulation of apoptosis and in cell cycle control. (1999) *Proc. Natl. Acad. Sci.*, 20,96(15), 8489-8492
8. Vo-Dinh, T. Synchronous luminescence for multi-component analysis. (1978) *Anal. Chem.*, 50, 396
9. Vo-Dinh, T. Analytical measurements and instrumentation for process and pollution control. Edited by Cheremisinoff, P., Perlis, H. Luminescence spectrometry, (1981) 47-80, Ann Arbor Science Publishers.
10. Vo-Dinh. T., Gammage, R. B. & Martinez, P. R. Analysis of a workplace air particulate sample by synchronous luminescence and room-temperature phosphorescence. (1981) *Anal. Chem.*, 53(2), 253-8
11. Watts, W. E., Isola, N. R., Frazier, D., and Vo-Dinh, T. Differentiation of normal and neoplastic cells by synchronous fluorescence: Rat liver epithelial and rat hepatoma cell models. (1999) *Analytical Letters*, 13, 2583-2594

APPENDIX

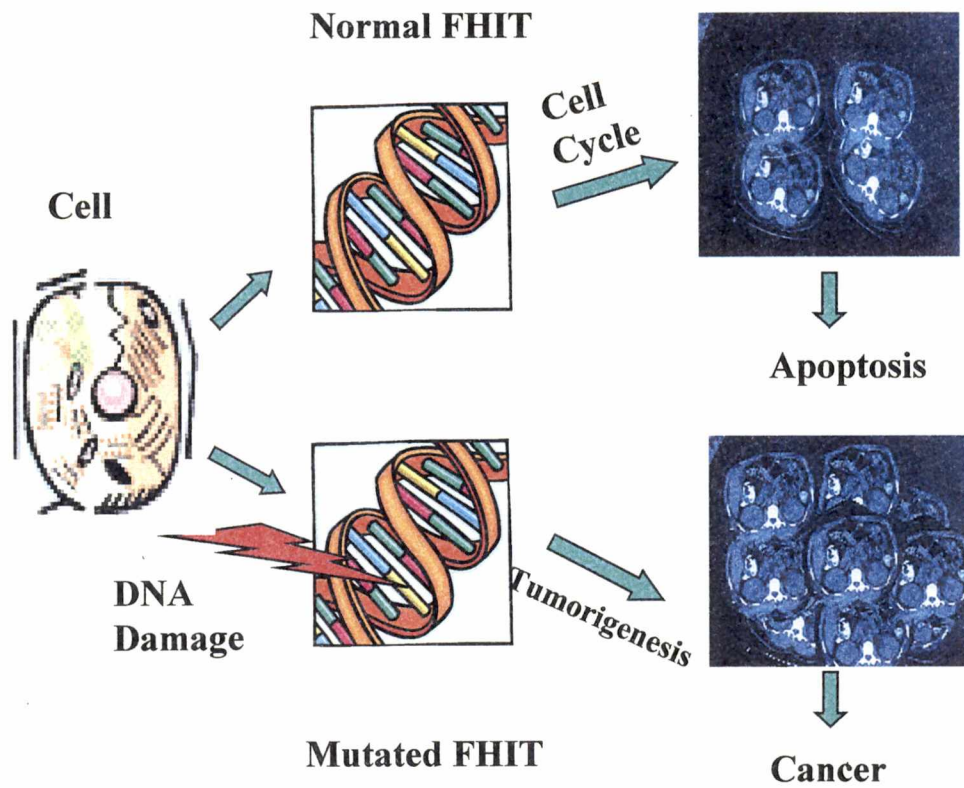


Figure 3.1 Deletions within the FHIT gene and absence of expression of Fhit protein occur in several common cancers.

Source: <http://dgl.microsoft.com/mgo1en/eula.asp>

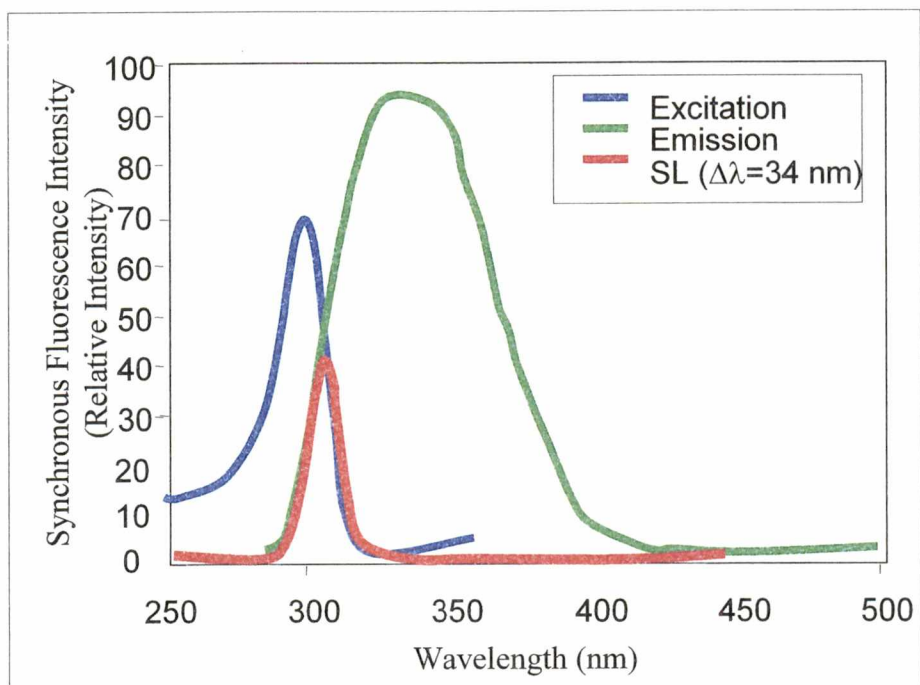
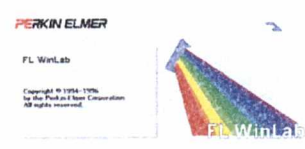
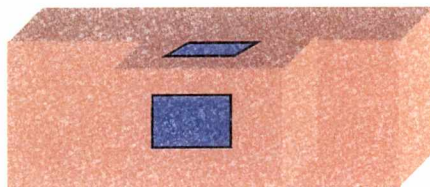
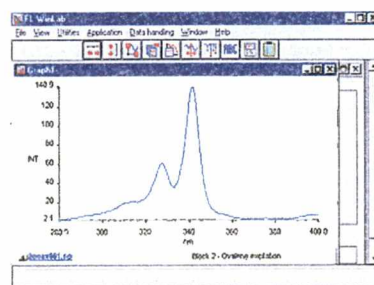
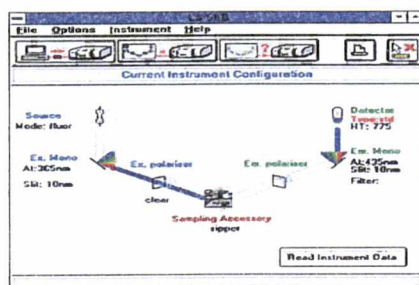


Figure 3.2 The excitation, emission and SL spectra of tryptophan.

LS-50B Spectrophotometer



↕ Computer Interface



FL Winlab Software

Computer Scanning and Analysis

Figure 3.3 Instrumentation. All spectroscopic measurements were performed using a single integrated workstation spectrofluorimeter with computer interfacing capabilities.

Source: <http://instruments.perkinelmer.com>

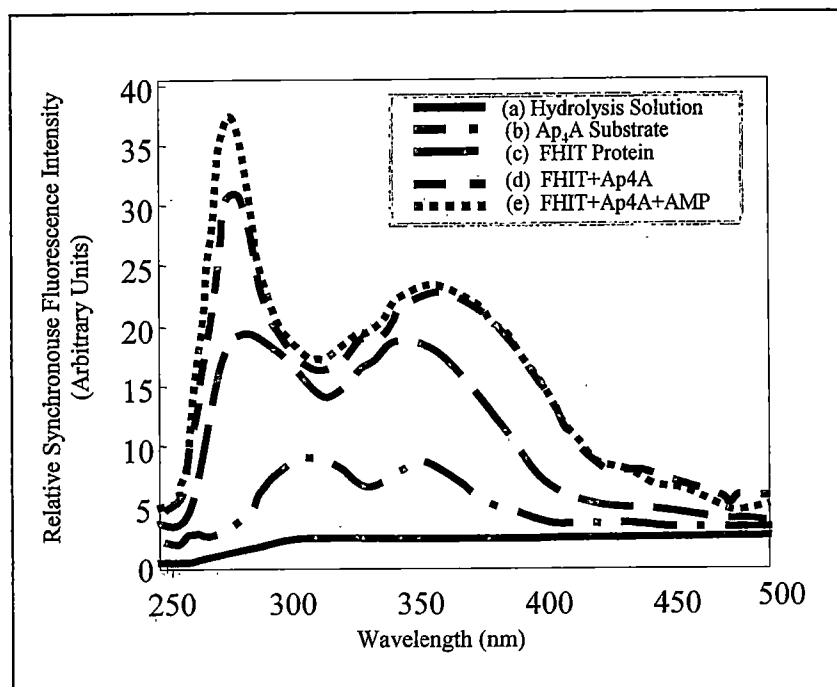


Figure 3.4 A representative SL spectrum ($\Delta\lambda = 50$ nm) for individual components of the hydrolysis reaction (a-c), the complete reaction (d) and confirmation of AMP formation (e) as a result of Ap₄A hydrolysis by Fhit protein are presented. The fluorescence spectrum of the hydrolysis solution (a) demonstrated absence of any distinguishable peaks. The spectrum of Ap₄A substrate (b) exhibited low fluorescence intensity with two broad peaks at 320 nm and 360 nm. The spectrum of Fhit protein (c) had higher fluorescence intensity than the Ap₄A substrate and two broad peaks at 285 nm and 370 nm. Addition of Fhit protein to an Ap₄A containing solution resulted in (d) a spectrum profile where there was a noticeable increase in the ratio of 285 nm to 370 nm, when compared to the fluorescence scan of Fhit alone. Addition of AMP to the same reaction vial (e) exhibited an increase only in the fluorescence intensity of the by-product peak at 285 nm.

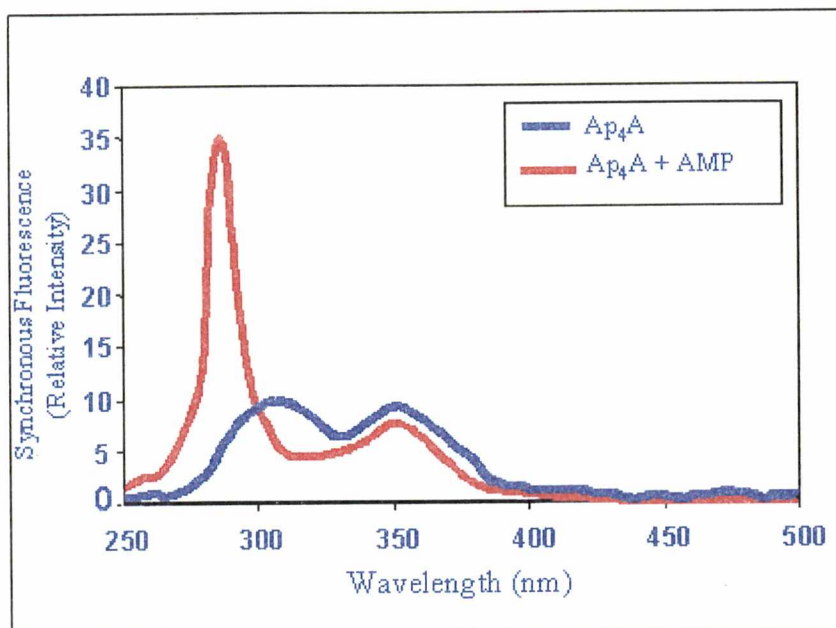


Figure 3.5 Synchronous Luminescence peak for AMP in the hydrolysis solution occurred at 285 nm ($\Delta\lambda = 50$ nm)

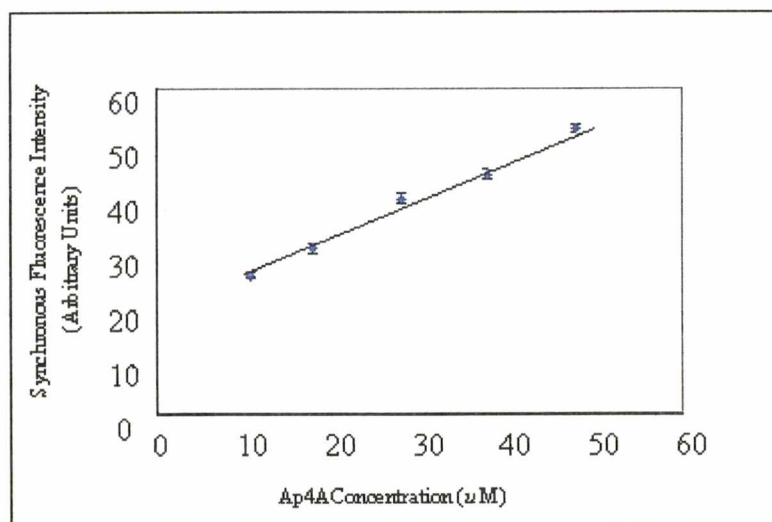
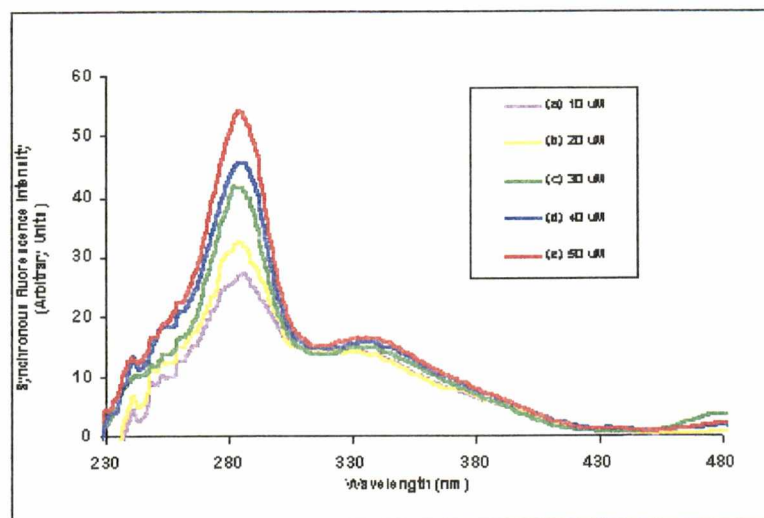


Figure 3.6 The quantitative ability of the SL technique to measure fluorescence intensity associated with increased AMP production at constant Fhit protein concentration and increasing concentrations of Ap₄A (10-50 μM) are illustrated.

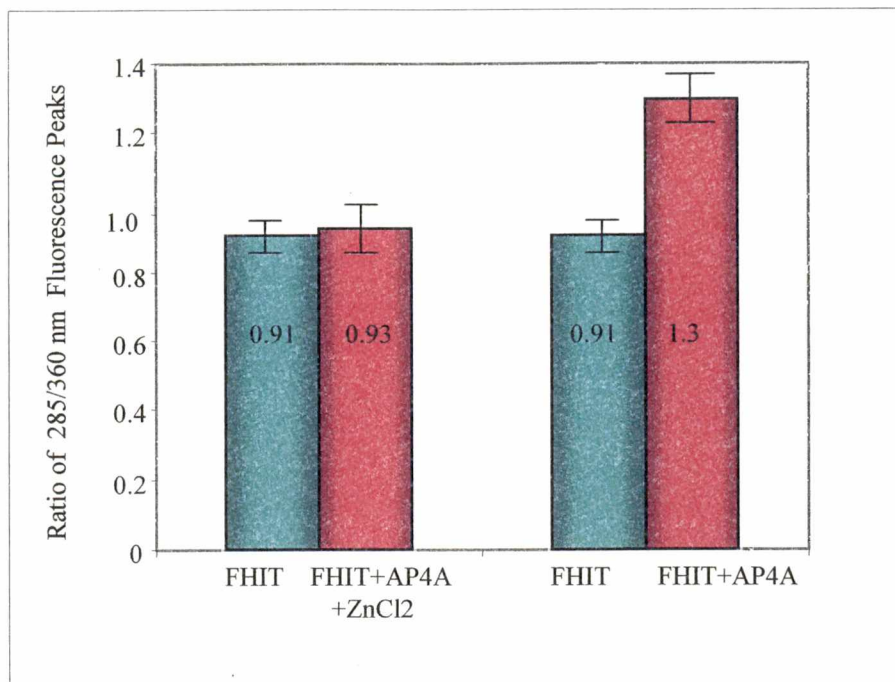


Figure 3.7 Inhibitory effects of ZnCl₂ (100 μl) on hydrolysis activity of Fhit protein is demonstrated. Fluorescence intensity of the 285 nm peak did not increase relative to the intensity of the second peak in presence of ZnCl₂. This alteration in the fluorescence profile was expected if Fhit protein had maintained its hydrolysis activity in the presence of Zn²⁺.

PART FOUR

**INVESTIGATION OF TUMOR SUPPRESSOR ACTIVITY
AND APOPTOSIS-RELATED PROCESSES
IN FHIT TRANSFECTED CELLS**

4.1 ABSTRACT

The candidate tumor suppressor gene, FHIT, includes both the common human chromosomal fragile site at 3p14.2 and the hereditary renal cancer translocation breakpoint. The structure and expression of the FHIT gene are altered frequently in tumors, and primary or cultured tumor cell lines. DNA structure alterations, due to loss of heterozygosity within the FHIT alleles, lead to aberrant exons and concomitant absence of full-length FHIT transcript and Fhit protein. Inference from such observations has been that an abnormality in the FHIT gene provides a selective advantage for the tumor cell, pointing to a tumor suppressor function for the FHIT gene. However, it has been argued that alterations in the FHIT gene may simply be a reflection of its inclusion in a fragile region, rendering it highly susceptible to breakage. In the present study, the tumor suppressor activity of the FHIT gene was investigated in cell lines that have been transfected with exogenous FHIT gene. First, the extent of cellular proliferation of these cells was determined by using the trypan blue, dead cell exclusion assay. The process of apoptosis in the cells was assessed by detection of annexin-V protein using flow cytometry, and the terminal deoxynucleotidyl transferase labeling of DNA fragments and identification by UV fluorescence microscopy. Morphology of the apoptotic cells was studied using electron microscopy. In apoptotic cells, alterations in the mitochondrial transmembrane potential ($\Delta\Psi_m$) was detected by rhodamine 123 staining using confocal microscopy and the degree of rhodamine 123 incorporation was measured by means of synchronous fluorescence spectroscopy. Data from these observations demonstrated reduced cell growth where Fhit protein was expressed. The tumor suppressor activity

of the FHIT gene was demonstrated in an animal model by reduced size of induced tumors, and observation of altered cell cycle kinetics of the tumor-derived cells *in tissue cultures* in the presence of Fhit protein expression. These data also provided direct evidence for involvement of the FHIT gene in induction of a mitochondria-dependent apoptotic pathway.

4.2 INTRODUCTION

The FHIT gene at chromosome 3p14 was identified initially by positional cloning in 1996 (1,2). The discovery of the FHIT gene, frequently exhibiting exon deletions or intron sequence insertions (1,3-5), drew great attention in the cancer research community. This interest was due to recognition of the loss of DNA sequences from chromosome 3p (6) as being one of the most frequent genetic and cytogenetic abnormalities in a broad range of solid tumors. Abnormalities with the FHIT transcripts have been observed in a variety of solid tumors, including cancers of the lung, stomach, breast, cervix, and the head and neck (6-8). These aberrant transcripts have been concordant with deletions of DNA within the FHIT gene and the lack of detectable Fhit protein in tumors or cell lines analyzed (6-9). Stable FHIT-transduced cells expressing exogenous wild-type FHIT, isolated after transfection of various cell lines with inactivated endogenous FHIT, show reduced colony-formation efficiency *in vitro* and inhibition of tumor development in nude mice (20). Observations such as these prompted some investigators to suggest that the FHIT gene might function as a tumor suppressor gene (6-15).

However, soon after the gene was reported as a candidate tumor suppressor, evidence began to accumulate against the hypothesis. Genomic deletions did not always affect exons of the gene and were not always associated with a lack of detectable full-length FHIT messenger RNA. Inactivating mutations were not commonly observed in the remaining FHIT allele in tumors and in cell lines. In some studies, genomic alterations were present in only a small fraction of the cells (7). In two reports, altered transcripts could not be consistently observed using polymerase chain reaction (PCR) analysis instead of the nested PCR (multiple rounds of amplification using different sets of primers spanning two introns), arguing that aberrant transcripts observed by nested PCR in some studies might represent an artifact of the PCR process (10,11). Some investigators have noted that aberrant FHIT transcripts could be observed in many non-tumor tissues (12,13) and that they also became more obvious in aging cells (14). These observations suggest that FHIT abnormalities are not tumor specific, but represent the result of randomly occurring deletion events at a fragile site. In addition, overexpression of FHIT did not suppress anchorage-independent growth or tumorigenicity of cervical carcinoma cell lines (15). Finally, overexpression of the sense or antisense FHIT DNA constructs have not affected cell proliferation, cell cycle distribution or apoptosis in human kidney cells carrying the FHIT gene (16).

However, observations of aberrant transcripts in nontumor tissues and in aging cells may indicate that loss of FHIT is a very early genetic event in tumorigenesis or reduced RNA-splicing fidelity in aging cells. In fact, frequent loss of heterozygosity (LOH) at 3p14 was observed in oral premalignant lesions (17) and in normal-appearing bronchial

epithelia of smokers (18). These findings support the notion that loss of the 3p14 region occurs early and frequently in tissues exposed to carcinogens. It is also possible that FHIT inactivation may be important in early tumor progression since stable overexpression of FHIT had no obvious effect on the tumorigenic properties of cervical carcinoma cell lines or on a lung carcinoma cell line reported previously by others to be suppressed by FHIT (15,16). The fact also remains that most tumor cell lines and primary tumors with FHIT abnormalities do not express or express only low levels of Fhit protein (6,8). The reasons for decreased expression remain to be elucidated, but one could hypothesize that aberrant transcripts might inhibit protein translation (post-translational modifications, *i.e.* methylation) or trigger protein degradation (post-translational signal-sequence *i.e.* ubiquitin-dependent proteolysis). To this end, frequent abnormalities have been observed with the FHIT gene (6,9), suggesting that at least some of these abnormalities are functionally important.

Because of these puzzling findings, the direct role of the FHIT gene and the consequences of Fhit protein loss-of-function in tumorigenesis needed further exploration. To investigate possible mechanisms for a selective growth advantage of FHIT-negative cells and tumors, we have examined the phenotypes of the FHIT-expressing cells relative to the FHIT negative parental cells both in *in vitro* and *in vivo* systems. Cell proliferation rates and cell cycle kinetics *in vitro* and tumor suppressor activity of the FHIT gene in a mouse model were analyzed. The possible role of FHIT gene in apoptosis was studied through evaluations of an early apoptotic event (externalization of phosphatidylserine), a late apoptotic event (DNA fragmentation),

and identification of ultrastructural alterations (formation of apoptotic bodies). Functional changes that occurred in apoptotic cells were assessed by studying alterations in the inner mitochondrial transmembrane potential *in vitro*. Our data indicates that Fhit expression is correlated with functions, which regulate cell growth *in vitro* and *in vivo*.

4.3 MATERIALS AND METHODS

4.3.1 Cell Culture

The FHIT-negative gastric carcinoma-derived MKN74 cells (19) that had been transfected with 15 µg of either pRcFHIT (MKN74/FHIT cell line) or control plasmid (pRcCMV) DNA (MKN74/E4 cell line) were kindly provided by Dr. Kay Huebner (Thomas Jefferson University, Kimmel Cancer Institute, Philadelphia, PA). Briefly, for construction of these cells, plasmids comprised of wild-type FHIT cDNA (excluded for construction of the MKN74/E4 control plasmid) ligated in-frame to a fusion protein tag, FLAG octapeptide coding sequence, and under the control of the immediate early human cytomegalovirus (CMV) promoter (Eastman Kodak, Rochester, NY), had been cloned into the HindIII and XbaI sites of the pRcCMV vector by using the calcium phosphate method (GIBCO/BRL, Grand Island, NY). Clones had then been selected in the presence of 200-400 µg/ml G418 (geneticin; GIBCO/BRL, Grand Island, NY) (20). Human cell lines, AGS (human stomach carcinoma) and the 293 (transformed human embryonic kidney cells), were obtained from the American Type Culture Collection (ATCC, Rockville, MD). These two cell lines have also been characterized previously for

structure and expression of endogenous FHIT alleles (7). The 293 cells express Fhit protein, whereas AGS stomach cancer cells exhibit homozygous deletions within the FHIT gene and do not express Fhit protein. The AGS culture was maintained in F-12K medium and the 293 cell line was maintained in DMEM medium. All of the above mentioned culture media were supplemented with 10% fetal bovine serum (FBS) (Sigma, St. Louis, MO), 1 ml of a 50 mg gentamicin/ml of water solution (GIBCO/BRL, Grand Island, NY), 1 % each of non essential amino acids (Sigma, St. Louis, MO), hepes buffer (Sigma, St. Louis, MO), L- glutamine (Sigma, St. Louis, MO) and sodium pyruvate (Sigma, St. Louis, MO) and maintained at 37°C and 5% CO₂.

4.3.2 Western Blot Analysis

Preparation of cell lysates and their subsequent analysis by Western blotting have been described previously (21). Briefly, tissue culture cells or the tumors were harvested, suspended in 10 parts (v/v) lysis buffer (0.5 % NP40 in phosphate-buffered saline (PBS) supplemented with 10 µg/ml leupeptin and 10 µg/mL PMSF (Sigma, St. Louis, MO)), and sonicated for 30 sec (Branson sonifier, Danbury, CT). Cellular debris was removed by a 10-min centrifugation at 8,500 x g at 4°C and the protein concentrations were determined using the Pierce BCA Protein assay (Rockford, IL) per manufacturer's instructions. Equal quantities of proteins were resolved on 14 % sodium dodecyl sulfate (SDS)-PAGE gels (Novax, San Diego, CA), transferred onto nitrocellulose membranes (Schleicher & Schuell, Keene, NH) and blocked with Blotto (5% nonfat dry milk (Kroger Co, Cincinnati, OH) and 0.1% Tween-20 (Sigma, St. Louis, MO) in PBS) for 1hr.

The membranes were then treated with a solution of 1 $\mu\text{g/ml}$ FHIT polyclonal antibody (Santa Cruz Biotechnologies, Santa Cruz, CA) in blocking buffer, for 2 hrs at room temperature. Protein bands were visualized using a horseradish peroxidase-conjugated secondary antibody (BioRad Laboratories, Richmond, CA) and a chemiluminescent substrate (Pierce DAB super signal system, Rockford, IL) as described by the manufacturer.

4.3.3 Biochip DNA Analysis

The genomic DNA of the two cell lines, MKN/FHIT and MKN/E4, were extracted using DNAzol reagent (GIBCO/BRL, Rochester, NY) following the manufacturer-suggested protocol. Using 100 ng of extracted genomic DNA and 50 pM of primers corresponding to the FHIT exon 5 (Oligos etc., Wilsonville, OR), the FHIT gene was PCR amplified (5 Units/ ml polymerase and 25mM MgCl_2 (GeneAmp, Perkin Elmer, Branchburg, NJ)). Thirty cycles of amplifications were performed in a Perkin Elmer Cetus thermal cycler at 94°C for 60 sec, 55°C for 60 sec, and 72°C for 45 sec after an initial 5-minute 95°C denaturation step (2). Biochip technology was employed to detect the FHIT DNA sequences in these PCR products. The procedure has been described previously in detail (21-23). In short, PCR products were immobilized on the Zeta probe membranes (BioRad Laboratories, Hercules, CA) by 1 min of UV dimerization. Membranes were then blocked in 5 ml of prehybridization solution (5X SSC, 0.02% sodium dodecyl sulfate (SDS) and 1% Carnation non-fat dry milk) for 1 hr at 37°C. This step was followed by 16 hrs of incubation in hybridization solution (prehybridization solution plus 100 ng/ml

Cy5-labeled DNA probes (Oligos etc. Wilsonville, OR) at 37°C. Membranes were then washed in 5 ml of wash solution (5X SSC, and 0.1% SDS) for 15 min at room temperature, followed by two 1-minute water rinses and analyzed using the biochip detection device.

4.3.4 Growth Kinetics Analysis

For determination of growth rate, the cells were seeded and maintained in 6-well plates in the growth medium. Every 24 hrs, the cells from three wells were trypsinized and counted using the trypan blue exclusion assay. The number of cells in each of the three wells was then averaged and used for analysis. To study the population doubling in apoptotic cells, the cells were seeded in the growth medium containing 60 μ M of mitomycin c (MMC) (Sigma, St. Louis, MO) for 20 hrs before harvest as described previously. Growth kinetic analysis was also performed on cells treated with a known mutagen, ethyl methanesulfonate (EMS, Eastman Kodak, Rochester, NY), at 50 μ g/ml of growth media.

Statistical analysis using general linear model (within subject factors), multivariate tests (tests within subject effects and within subject contrasts) and univariate analysis of variance (tests between-subjects factors and between-subjects effects) for significant at the .05 level was performed using SPSS for windows computer package.

4.3.5 Murine Model for Tumorigenicity Assay

The MKN/FHIT and the MKN/E4 cells were each grown in tissue culture flasks, harvested, and counted. Cells from each group were resuspended at 10^7 cells/ml in PBS solution. A volume of 0.2 ml of each cell suspension was injected subcutaneously into the right flank of 6-week-old female nude Balb/c mice (n=5) (Taconic, Germantown, NY). Control group of mice (n=5) was mock treated with 0.2 ml of PBS. All groups were monitored twice a week for tumor formation for 10 wk after inoculation. Using a linear caliper, tumor dimensions were measured and tumor growth rates were calculated from tumor volume data. On termination of experiment, tumors were excised and assessed for presence of the FHIT gene and expression of the Fhit protein. Histological evaluations were performed also on formalin-fixed paraffin-embedded tissues by hematoxylin/eosin (Sigma, St. Louis, MO) staining.

4.3.6 Analysis of DNA Content for Cell Cycle Progression

The MKN/FHIT and the MKN/E4 cells were harvested and 1×10^5 cells were fixed overnight in ice-cold 70% ethanol. Before flow cytometry analysis, cells were washed with PBS to remove the ethanol and treated with 100 μ g/ml RNase A (Sigma, St. Louis, MO) and 50 mg/ml propidium iodide (PI) (Sigma, St. Louis, MO) for 30 min. The stained cells were analyzed using a FACStarPlus flowcytometer (Becton-Dickinson, San Jose, CA) with Becton-Dickinson CellQuest3 software to determine percentage of cells in the G0/G1, S, and G2/M phases of the cell cycle as a function of their DNA content.

4.3.7 Analysis of Early Apoptotic Events

Apoptotic changes in plasma membrane phospholipids and transport function were probed by a combination of fluoresceinated annexin-V and DNA fluorochrome 7-aminoactinomycin D. To induce apoptosis, flasks of MKN/FHIT and MKN/E4 50% confluent cells were treated with MMC for 20 hrs as previously described. The cells were then harvested and suspended at 1×10^6 cells/ml in binding buffer (10 mM HEPES, pH 7.4, 140 mM NaCl, 2.5 mM CaCl₂), with 5 μ l of phycoerythrin (PE)-conjugated annexin-V (Pharmingen, San Diego, CA) as recommended by the manufacturer and 0.125 μ g/ml of 7-amino actinomycin D (7-AAD) (Sigma, St. Louis, MO) for 15 min at room temperature. These cells were analyzed by flow cytometry with a FACStarPlus flowcytometer (Becton Dickinson, San Jose, CA) where flurochromes, PE-annexin-V and 7-AAD, were excited by a laser tuned to 488 nm and emissions were detected at 575 and 650 nm, respectively. Data for 20,000 cells from each sample were next analyzed with the CellQuest3 software (Becton Dickinson, Franklin Lakes, NJ).

4.3.8 Analysis of DNA Fragmentation for Late Apoptotic Events Evaluation

Percentages of apoptotic MKN/FHIT and MKN/E4 cells were determined after MMC treatment, using the terminal deoxynucleotidyl transferase-mediated dUTP-biotin nicked-end labeling (TUNEL) technique per manufacturer's instructions. *In situ* detection of apoptotic cells was performed on adherent cells, cultured on chamber slides by using the

Fluorescein FragEL DNA fragmentation detection kit (Oncogene, Boston, MA). Image acquisition was performed with a Nikon Diaphot 300 fluorescence microscope (Japan) equipped with a 485-nm, B-1E, filter cube.

4.3.9 Analysis of Production of Apoptotic Bodies

MKN/FHIT and MKN/E4 cells were seeded and grown for 48 hrs on 0.45 μ m filter membranes housed at the bottom of 6 well tissue culture plates (Falcon, Lincoln Park, NJ). The adherent cells were treated with MMC to induce apoptosis as described previously. These cells, along with untreated MKN/FHIT and MKN/E4 cells, also grown on the membranes, were fixed in the fixative culture medium composed of cacodylate buffered 3% glutaraldehyde (Sigma, St. Louis, MO) for 1h at room temperature. The fixative was then drawn off the membranes and the cells were post-fixed in cacodylate buffered 2% osmium tetroxide (Sigma, St. Louis, MO) for 1h at room temperature. Samples were then dehydrated in an ethanol step gradient, followed by a final propylene oxide (Sigma, St. Louis, MO) dehydration step. These samples were then embedded in Epon resin (Sigma, St. Louis, MO), cut into 100 nm cross-section pieces and post-stained with uranyl acetate (Sigma, St. Louis, MO) and lead citrate (Sigma, St. Louis, MO). Sections were viewed with a Hitachi H-600 transmission electron microscope (TEM, Tokyo, Japan).

4.3.10 Alterations in the Mitochondrial Transmembrane Potential

Alterations in the mitochondrial membrane potential ($\Delta\Psi_m$) of the apoptotic cells were determined by mitochondrial uptake of rhodamine 123 (R123) using confocal microscopy. MMC-treated and untreated MKN/FHIT and MKN/E4 cells (as described previously) were washed twice with PBS and incubated in growth media containing 10 mg/ml R123 at 37 °C for 30 minutes. A Leica TCS SP2 spectral confocal and multiphoton system (Deerfield, IL) was used for visualization of mitochondrial fluorescence in apoptotically treated and untreated cells.

4.4 RESULTS AND DISCUSSION

Two criteria need to be met for a gene to be considered a tumor suppressor gene. First genetically, both alleles of a gene need to be inactivated directly through mutations, deletion, or epigenetic modifications such as methylation, in neoplastic counterparts of otherwise normal cells. Second, functionally, a tumor suppressor gene is a gene whose product can restrict tumorigenic and metastatic processes (1,2,7,11, 20). In 1996, the FHIT gene was cloned and shown to encompass the FRA3B common fragile site, numerous cancer cell-specific homozygous and hemizygous deletions, and a familial renal cancer chromosome translocation break (1,20). Early studies of a number of important human tumor types showed that altered FHIT RNA expression (13,5,24) correlated frequently with deletions within the FHIT gene plus the lack of detectable Fhit protein in tumor-derived cell lines (6). Homozygous deletions in a gene in cancer

cells and lack of expression of the protein product are hallmarks of tumor suppressor genes (1,20), so from many perspectives the FHIT gene was a strong candidate for a tumor suppressor gene. However, (a) occurrence of small homozygous deletions within large FHIT introns, apparently not affecting FHIT exons, (b) occurrence of apparent full-length FHIT transcripts accompanied by aberrant transcripts in cancer-derived cell lines and tumors, and (c) lack of point mutations in remaining FHIT alleles in cancer-derived cell lines, argue against a tumor suppressor role for the FHIT gene. A gene can be positively categorized as a tumor suppressor when its pattern of inactivation, or loss-of-function, meet the classical genetic and functional parameters set for tumor suppressor genes. To enhance our understanding of the role of FHIT gene in carcinogenesis, using our *in vitro* and *in vivo* models, we further analyzed its possible tumor suppressor function.

4.4.1 Status of the FHIT Gene and Fhit Protein Expression in Cells

As a required step for these experiments, presence of the transfected FHIT gene and expression of Fhit protein in the MKN/FHIT and their absence in the null transfected, MKN/E4 cell lines was determined. First, the extracted genomic DNAs from both cell lines were employed to attempt to amplify the FHIT DNA using primers flanking FHIT exon 5. Fluorescent DNA products were analyzed by specific hybridization on the biochip. Results showed fluorescence signal from the MKN/FHIT samples to be significantly higher than background fluorescence, indicating presence of FHIT exon 5 DNA product (Fig. 4.1). On the other hand, signals from the MKN/E4 samples were

about the same level as the background fluorescence, and significantly lower than that obtained from the MKN/FHIT samples. Results indicated that exon 5 was not present in the template DNA of the MKN/E4 cells.

Next, we evaluated these cell lines for expression of Fhit protein. We also included the AGS cell line, which inherently lacks FHIT gene (24,25), and therefore Fhit protein and the 293 cell line (24,25), with demonstrated endogenous Fhit expression, as controls for this study. Immunoblot analysis of cellular lysates using anti-Fhit antibody, are illustrated in Fig. 4.2. As expected, the observed protein bands at about 17 kDa demonstrated that the MKN/FHIT and the 293 cell lines expressed a protein the size of the Fhit protein. Conversely, absence of a similar size protein band in the MKN/E4 and the AGS cell lines was indicative of the absence of the Fhit protein expression in these cell lines. These results reconfirmed the status of the FHIT gene and the Fhit protein expression in the cell lines used in the present study.

4.4.2 Phenotypic Effects of FHIT Expression on Cell Proliferation *In vitro*

To determine if expression of exogenous or endogenous wild-type FHIT effects the ability of the cells to grow, cell proliferation assays were conducted. The MKN/FHIT and the MKN/E4 cell lines along with the AGS and the 293 cells were seeded and grown continuously in their appropriate growth media. To investigate the consequences of expression of FHIT on cell proliferation in unfavorable, mutation inducing, growth conditions, the same cell lines were grown in media supplemented with mitomycin C

(MMC) or Ethyl methane sulfonyl (EMS). We found no statistically significant differences in the growth rate of the MKN/FHIT and the 293 cells (+Fhit protein expression) when compared to the growth rate of the MKN/E4 and AGS cell lines (-Fhit expression) cultured under similar conditions (Fig. 4.3 a,b) (considering the lower plating efficiency of MKN/FHIT compared to MKN/E4 cell line). However, when the MKN/FHIT and the 293 cells, were grown in media supplemented with MMC or EMS, they demonstrated a significant decrease ($p < 0.05$) in their doubling time as compared to the growth rate of the MKN/E4 and the AGS cells maintained under similar conditions (Fig. 4.3 a,b). In addition, no significant ($p < 0.05$) difference in the growth rate of the MKN/E4 and AGS with their MMC treated counterparts was observed in this study. From the information gathered here we concluded that in these cell lines, the *in vitro* cell proliferation rates changed significantly ($p < 0.05$) as a result of FHIT DNA presence and Fhit protein expression.

4.4.3 Cell Cycle Kinetics

Using flow cytometry technique, we constructed DNA histograms of MKN/FHIT and MKN/E4 cell populations, which measures the proportion of cells in each phase of the cell cycle as a function of DNA content of cells. The position of a cell along the mitotic cell cycle is strictly related to its DNA content. A cell in G₀/G₁ phase has 2N DNA content, a cell in the G₂/M phase has 4N DNA content and a cell in the S phase has a DNA content between 2N and 4N. The percentage of propidium iodide stained MKN/FHIT and MKN/E4 cells in the G₀/G₁, S, and G₂/M phases of the cell cycle

was determined (Fig. 4.4 a,b). Using Becton-Dickinson CellQuest3 software the DNA profiles showed that approximately 41.3% +/- 2.4 of the MKN/FHIT cells were in the G0/G1 phase, 55.7% +/- 3.3 in the S phase and 3.2% +/- 1.2 in the G2/M phase. Histogram of the MKN/E4 cell varied distinctly from the MKN/FHIT histogram, having only 27.3% +/- 2.9 of the cells in the G0/G1 phase, which represents a decrease of about 14%. The population of MKN/E4 cells in the S phase was about 69.3% +/- 3.9, 13.6% increase over the MKN/FHIT, S phase population. Despite alterations in the number of cells in the G0/G1, and the S phases of the cell cycle profiles, the subpopulation of the cells in the G2/M phase in both cell lines was approximately 3-4% +/- 1.2 (Table 4.1). Overall analysis of the cell cycle-phase distribution indicated specific G0/G1 arrest of FHIT positive cells suggesting a possible role for FHIT expression which could be related to regulation of cell cycle.

4.4.4 Tumor Suppressor Activity of the FHIT Expression *In vivo*

We tested FHIT positive and FHIT negative cell lines for growth in balb/c nude mice. We inoculated flanks of 6-wk-old female nude mice with 5×10^6 MKN/ FHIT or MKN/E4 cells. Four of the five mice injected with the MKN/E4 cells developed tumors within 1 wk after injection, with the average size of tumors reached approximately 1.25 cm³ after 8 wk and 2.25 cm³ by 10 wk. In contrast, only 2 of the 5 mice injected with MKN/FHIT cells developed any tumors. These tumors were smaller and grew more slowly than the MKN/E4 tumors (Fig. 4.5 a). By wk 5, the average size of the FHIT expressing tumors (0.1 cm³) was about 75% smaller than the, the average size of MKN/E4 tumors (0.4

cm³) at the same time. Tumor size differences were larger at termination of the study; the MKN/FHIT tumors were about 20% of the size of MKN/E4 tumors. Histologically all tumors were similar, having undifferentiated phenotypes (Fig. 4.5 b). Presence of the FHIT gene and expression of the Fhit protein were assessed in the excised MKN74/FHIT and MKN/E4 tumors as described previously. The results, presented in Fig. 4.6 (a,b) indicated the presence of the FHIT DNA and expression of the Fhit protein only in the MKN/FHIT tumors as compared with the MKN/E4 tumors.

The nude mice tumorigenicity results corroborated with cell growth rate obtained from the *in vitro* analysis. The FHIT DNA positive MKN74 gastric carcinoma cell line produced fewer and smaller tumors than did the FHIT DNA negative MKN/E4 cells. These results suggest that FHIT inactivation provides a selective advantage for growth expansion *in vivo*. In light of these results, it was crucial to improve our understanding of the mechanisms underlying activity of the FHIT gene.

4.4.5 Potential Role of FHIT Gene in Apoptosis

The biological mechanism of FHIT activity and the cellular pathways associated with its tumor suppressor function are yet unknown. Recently, Sard *et al.* (25) and Ji *et al.* (24) have suggested the possible involvement of the FHIT gene in induction of apoptosis. Apoptosis is a highly regulated form of physiological cell death. Morphological changes associated with apoptosis include cell shrinkage, condensation of the nuclear chromatin, fragmentation of the nucleus, cleavage of chromosomal DNA and, formation of

apoptotic bodies that are engulfed by phagocytosis (26). Sard *et al.* (25) showed altered phase distribution in cell cycle profiles and a significantly higher rate of apoptosis induction, in cells carrying the Fhit DNA, as compared to cells with negative Fhit expression *in vitro*. Studying the effects of FHIT overexpression on cell proliferation, cell cycle kinetics, apoptosis and tumorigenicity, Ji *et al.* (24) proposed that the FHIT gene functions as a tumor suppressor, both *in vitro* and *in vivo*, with a possible role in induction of apoptosis (24). In contrast, the results obtained by Guo *et al.* (16) indicated that expression of FHIT is not involved in cell cycle regulation and that the tumor suppressor activity of the FHIT gene may be independent of an effect on the cell cycle and apoptosis mechanisms. Also, Wu *et al.* (15) reported that stable overexpression of Fhit had no effect on the anchorage-independent growth and tumorigenicity in nude mice, using two cervical carcinoma cell lines and a lung carcinoma cell line, previously reported to be suppressed by Fhit expression.

We investigated the possible involvement of FHIT in induction of apoptosis *in vitro* by focusing on different stages of programmed cell death. One of the earliest events in programmed cell death is the externalization of phosphatidylserine, a membrane phospholipid, normally restricted to the inner leaflet of the lipid bilayer, providing a recognition signal for engulfment of the apoptotic cells by phagocytes (27,28). Annexin-V, an endogenous human protein with a high affinity for membrane bound phosphatidylserine, has been used to detect apoptosis *in vitro* before other well described morphologic or nuclear changes occur (29,30). Detection of externalized phosphatidylserine by annexin-V was used in flow cytometry assays for

identification of apoptotic, MKN74/FHIT and MKN/E4, cells. Initially, MKN/FHIT and MKN/E4 cells were treated with MMC for 20 hrs to induce apoptosis. These cells were then comparatively analyzed, using staining profiles of PE-conjugated annexin-V, which identified early apoptotic cells, and the 7-AAD staining profiles which identified the dead cells. Flow cytometry data showed a much higher percentage of apoptosis-positive MKN/FHIT cells (number of annexin-V positive cells located in the upper right quadrant) as compared to the FHIT minus MKN/E4 cells (Fig. 4.7).

Flow cytometry data were confirmed by the results of TUNEL assay that detects DNA strand breaks in cells and tissue sections and allows quantification of apoptotic cells by fluorescence light microscopy (25). Results of fluorescence microscopy analysis revealed that a higher number of condensed and fragmented nuclei from the MKN/FHIT cell populations incorporated the fluorescein-labeled dUTPs, thus indicating a higher ratio of apoptosis-induced DNA strand breaks, whereas MKN/E4 cells showed a considerably lower level of apoptotic nuclei (Fig. 4.8 a,b). Percentage of apoptotic MKN/FHIT cells was 31% +/- 3.6 (percentage of fluorescently labeled cells in total cell population) as compared to 16% +/- 2.5 for the MKN/E4 cells and 9% +/- 2.4 and 7% +/- 2.5 for the PBS treated MKN/FHIT and MKN/E4 cells, respectively (Table 4.2).

4.4.6 Morphologic Analysis of Apoptosis

Morphologic hallmarks of apoptosis include chromatic margination, nuclear condensation and fragmentation, and condensation of the cell with preservation of

organelles (26-31). The process is followed by fragmentation of the cell into membrane-bound apoptotic bodies, which undergo phagocytosis by nearby cells without associated inflammation (31). Since apoptosis was defined originally by morphologic criteria, the biomolecular-defined (flow cytometry) data gathered here, were confirmed by further morphologic examination. This quality assurance measurement of the ultrastructural features of the apoptotic cell morphology was provided by electron microscopy to specifically identify the presence of apoptotic bodies as a typical late occurrence in the apoptotic pathway. After 20 hrs of culture in the presence of MMC, a substantial number of MKN/FHIT cells underwent programmed cell death. Typical apoptotic bodies, composed of plasma membranes containing cell fragments such as broken pieces of chromatin together with small portions of the cytoplasm, were visualized in the MKN/FHIT cell line using transmission electron microscopy (TEM, Fig. 4.9). Quantitative evaluations (800 total cells) revealed approximately 30% +/- 3.4 of MMC induced MKN/FHIT cells showing ultrastructural signs of programmed cell death. Treatment of the MKN/E4 cells with MMC, apoptotically modified the morphology of about 16% +/- 2.3 of the cells (Table 4.3). Therefore, observation of the enhanced cellular degradation in the MKN/FHIT cells over the MKN/E4 cells implicated the FHIT gene as possibly having a specific role in the programmed cell death pathway.

4.4.7 Alterations in the Inner Mitochondrial Transmembrane Potential

Previous research has implicated mitochondrial physiology in the initiation and progression of apoptosis of cells in culture and in tissue environments (32,33). Early

apoptosis is invariably accompanied by a disruption of inner mitochondrial transmembrane potential ($\Delta\Psi_m$). The sensitivity and specificity of rhodamine 123 (R123) dye to monitor the $\Delta\Psi_m$ in apoptotic cells has been established (16,35). This indicator dye is a lipophilic cation, which is accumulated by the mitochondria in proportion to $\Delta\Psi_m$ (36). For functional characterization of involvement of the FHIT gene in programmed cell death, Fhit-induced modulations of mitochondrial $\Delta\Psi_m$ in apoptotic MKN/FHIT and MKN/E4 cells, using R123 indicator dye were evaluated. Populations of the two cell lines, both MMC treated and untreated, and incubated in R123 containing media were subsequently imaged using confocal laser scanning microscopy (CLSM).

CLSM captured fluorescence images illustrated a clear overall tendency of the MMC-treated MKN/FHIT and the MKN/E4 cells, over the untreated cells, for increased mitochondrial incorporation of R123, where they displayed a significant loss of $\Delta\Psi_m$ (Fig. 4.10 a,b,c,d). However, the fluorometric analysis of the MMC-treated MKN/FHIT cells showed a noticeably higher mitochondrial accumulation of R123 over that observed in the mitochondria of the similarly treated, MKN/E4 cells (Fig. 4.10 b,d). These observations could possibly be explained by the MKN/E4 cells having a higher threshold than the MKN/FHIT cells for apoptotic induction due to the absence of Fhit protein expression. The outcome lends further support to the previously stated view that, the expression of the Fhit protein might have a possible role in the activation of the death program.

4.5 CONCLUSION

FHIT molecule has been shown to play an important role in carcinogenesis.

Apoptotic signals are activated by various stimuli and converge toward a common death pathway. These data indicate that the observed tumor suppressor activity in cells with FHIT expression could be related to a regulatory effect of the Fhit protein to facilitate apoptosis.

In this study, we demonstrated that the FHIT gene transfer into gastric cancer cell line lacking endogenous Fhit protein expression resulted in reversion of tumorigenicity *in vivo*, and caused modifications of cell cycle kinetics *in vitro*. Analysis of early and late events of apoptosis using a variety of techniques revealed a high rate of apoptotically-induced cells in the presence of Fhit protein expression. These *in situ* results were confirmed by functional analysis showing alterations of mitochondrial transmembrane potential in the Fhit-expressing apoptotically-induced cells. In light of these observations, and since the therapeutic interest in FHIT as a molecular target of anticancer intervention could benefit greatly from a better understanding of its apoptotic capability, elucidating FHIT-mediated apoptosis is all the more pressing.

4.6 ACKNOWLEDGEMENTS

This research was jointly sponsored by the Office of Biological and Environmental Research, U.S. Department of Energy under contract DE-AC05-00OR22725 with

UT-Battelle, LLC., and by the ORNL Laboratory Directed Research and Development Program (Advanced Nanosystems).

REFERENCES

1. Ohta, M., Inoue, H., Cotticelli, M. G., Kastury, K., Baffa, R., Palazzo, J., Siprashvili, Z., Mori, M., McCue, P., Druck, T., Croce, C. M. & Huebner, K. The FHIT gene, spanning the chromosome 3p14.2 fragile site and renal carcinoma-associated t(3;8) breakpoint, is abnormal in digestive tract cancers. (1996) *Cell*, 84, 587-597
2. Barnes, L. D., Garrison, P. N., Siprashvili, Z., Guranowski, A., Robinson, A. K., Ingram, S. W., Croce, C. M., Ohta, M. & Huebner, K. Fhit, a putative tumor suppressor in humans, is a dinucleoside 5',5'''-P1,P3-triphosphate hydrolase. (1996) *Biochemistry*, 35, 11529-11535
3. Sozzi, G., Veronese, M. L., Negrini, M., Baffa, R., Cotticelli, M. G., Inoue, H., Tornielli, S., Pilotti, S., DeGregorio, L., Pastorino, V., Pierotti, M. A., Ohta, M., Huebner, K. & Croce, C.M. The FHIT gene 3p14.2 is abnormal in lung cancer. (1996) *Cell*, 85, 1726
4. Virgilio, L., Shuster, M., Gollin, S. M., Veronese, M. L., Ohta, M., Huebner, K. & Croce, C. M. FHIT gene alterations in head and neck squamous cell carcinomas. (1996) *Proc. Natl. Acad. Sci. USA*, 93, 9770-9775
5. Greenspan, D.L., Connolly, D.C., Wu, R., Lei, R.Y., Vogelstein, J. T., Kim, Y. T., Mok, J. E., Munoz, N., Bosch, F. X., Shah, K., Cho, K. R. Loss of FHIT expression in cervical carcinoma cell lines and primary tumors. (1997) *Cancer Res.*, 57, 4692-4698
6. Linehan, W. M., Lerman, M. I., & Zbar, B. Identification of the von Hippel-Lindau (VHL) gene. Its role in renal cancer. (1995) *JAMA*, 273, 564-570

7. Druck, T., Hadaczek, P., Fu, T.-B., Ohta, M., Siprashvili, Z., Baffa, R., Negrini, M., Kastury, K., Veronese, M. L., Rosen, D., Rothstein, J., McCue, P., Cotticelli, M. G., Inoue, H., Croce, C. M. & Huebner, K. Structure and expression of the human FHIT gene in normal and tumor cells. (1997) *Cancer Res.*, 57, 504-512
8. Sozzi, G., Tornielli, S., Tagliabue, E., Sard, L., Pezzella, F., Pastorino, U., Minoletti, F., Pilotti, S., Ratcliffe, C., Veronese, M. L., Goldstraw, P., Huebner, K., Croce, C. M., & Pierotti, M. A. Absence of Fhit protein in primary lung tumors and cell lines with FHIT gene abnormalities. (1997) *Cancer Res.*, 57, 5207-12
9. Mao, L., Fan, Y. H., Lotan, R. & Hong, W. K. Frequent abnormalities of FHIT, a candidate tumor suppressor gene, in head and neck cancer cell lines. (1996) *Cancer Res.* 56, 5128-5131
10. Thiagalingam, S., Lisitsyn, N.A., Hamaguchi, M., Wigler, M. H., Willson, J. K., Markowitz, S. D., Leach, F. S., Kinzler, K. W., & Vogelstein, B. Evaluation of the FHIT gene in colorectal cancers. (1996) *Cancer Res.*, 56, 2936-9
11. Fong, K. M., Biesterveld, E. J., Virmani, A., Wistuba, I., Sekido, Y., Bader, S. A., Ahmadian, M., Ong, S. T., Rassool, F. V., Zimmerman, P. V., Ciaccone, G., Gazdar, A. F. & Minna, J. A. FHIT and FRA3B 3p14.2 allele loss are common in lung cancer and preneoplastic bronchial lesions and are associated with cancer-related FHIT cDNA splicing aberrations. (1997) *Cancer Res.*, 57, 2256-2267
12. Panagopoulos, I., Thelin, S., Mertens, F., Mitelman, F., & Aman P. Variable FHIT transcripts in non-neoplastic tissues. (1997) *Genes Chromosomes Cancer*, 19, 215-19

13. van den Berg, A., Draaijers, T. G., Kok, K., Timmer, T., Van der Veen, A.Y., Veldhuis, P. M., de Leij, L., Gerhartz, C. D., Naylor, S. L., Smith, D. I., & Buys, C. H. Normal FHIT transcripts in renal cell cancer- and lung cancer-derived cell lines, including a cell line with a homozygous deletion in the FRA3B region. (1997) *Genes Chromosomes Cancer*, 19, 220-227.
14. Gayther, S.A., Barski, P., Batley, S.J., Li, L., de Foy, K.A., Cohen, S.N., Ponder, B.A., & Caldas, C. Aberrant splicing of the TSG101 and FHIT genes occurs frequently in multiple malignancies and in normal tissues and mimics alterations previously described in tumours. (1997) *Oncogene*, 15,2119-2126.
15. Wu, R., Connolly, D. C., Dunn, R. L. & Cho, K. R. Restored expression of fragile histidine triad protein and tumorigenicity of cervical carcinoma cells. (2000) *J. Natl. Cancer Inst.*, 92(4), 338-44
16. Guo, Z. & Vishwanatha, J. K. Effect of regulated expression of the fragile histidine triad gene on cell cycle and proliferation. (2000) *Mol. Cell Biochem.*, 204(1-2), 83-8
17. Mao, L., Lee, J. S., Kurie, J. M., Fan, Y. H., Lippman, S. M., Lee, J. J., Ro, J. Y., Broxson, A., Yu, R., Morice, R. C., Kemp, B. L., Khuri, F. R., Walsh, G. L., Hittelman, W. N. & Hong, W. K. Clonal genetic alterations in the lungs of current and former smokers. (1997) *J. Natl. Cancer Inst.*, 89, 857-862
18. Mao, L., Lee, J.S., Fan, Y.H., Ro, J.Y., Batsakis, J.G., Lippman, S., Hittelman, W. & Hong, W. K. Frequent microsatellite alterations at chromosomes 9p21 and 3p14 in oral malignant lesions and their value in cancer risk assessment. (1996) *Nat. Med.*, 2, 682-685

19. Matoyama, T., Hojo, M. & Watanabe, H. Comparison of seven cell lines derived from human gastric carcinomas. (1986) *Acta. Pathol. Japonica*, 36, 65-83
20. Siprashvili, Z., Sozzi, G., Barnes, L. D., McCue, P., Robinson, A. K., Eryomin, V., Sard, L., Tagliabue, E., Greco, A., Fusetti, L., Schwartz, G., Pierotti, M. A., Croce, C. M., & Huebner, K. Replacement of Fhit in cancer cells suppresses tumorigenicity. (1997) *Proc. Natl. Acad. Sci. U S A*, 94(25),13771-13776
21. Askari, M., Alarie, J. P., Moreno-Bondi, M., & Vo-Dinh, T. Application of an antibody biochip for p53 detection and cancer diagnosis. (2001) *Biotechnology Progress*, 17(3):543-552
22. Allain, L. R., Askari, M., Stokes, D. L. & Vo-Dinh, T. Microarray sampling platform fabrication using bubble-Jet technology for a biochip System. (2001) *Fresenius J. Anal. Chem.*, (In press)
23. Askari, M., Miller, G. & Vo-Dinh, T. Simultaneous detection of the FHIT gene and protein using Microarray-based biochip. *Cancer* (2001) (submitted)
24. Ji, L., Fang, B., Yen, N., Fong, K., Minna, J. D. & Roth, J. A. Induction of apoptosis and inhibition of tumorigenicity and tumor growth by adenovirus vector-mediated fragile histidine triad gene overexpression. (1999) *Cancer Res.*, 59(14), 3333-9
25. Sard, L., Accornero, P., Tornielli, S., Delia, D., Bunone, G., Campiglio, M., Colombo, M. P., Gramegna, M., Croce, C. M., Pierotti, M. A. & Sozzi, G. The tumor-suppressor gene FHIT is involved in the regulation of apoptosis and in cell cycle control. (1999) *Proc. Natl. Acad. Sci. U S A*, 96(15), 8489-92

26. Kerr, J. F. R., Winterford, C. M. & Harmon, B. V. Apoptosis: Its significance in cancer and cancer therapy. (1994) *Cancer*, 73, 2013
27. Fadok, V. A., Voelker, D. R., Campbell, P. A., Cohen, J. J., Bratton, D. L. & Henson, P. M. Exposure of phosphatidylserine on the surface of apoptotic lymphocytes triggers specific recognition and removal by macrophages. (1992) *J. Immunol.*, 148, 2207
28. Martin, S. J., Reuterlingsperger, C. P., McGahon, A. J., Rader, J. A., van Schie, R. C., LaFace, D. M. & Green, D. R. Early redistribution of plasma membrane phosphatidylserine is a general feature of apoptosis. (1995) *J. Exp. Med.* 182, 1545
29. Yang, D. J., Azhdarinia, A., Wu, P., Yu, D. F., Tansey, W., Kalimi, S. K., Kim, E. E. & Podoloff, D. A. In vivo and in vitro measurement of apoptosis in breast cancer cells using 99mTc-EC-annexin V. (2001) *Cancer Biother. Radiopharm.*, 16(1), 73-83
30. Kravtsov, V. D., Daniel, T. O. & Koury, M. J. Comparative analysis of different methodological approaches to the in vitro study of drug-induced apoptosis. (1999) *Am. J. Pathol.*, 155(4), 1327-39
31. Wride, M. A. Minireview: apoptosis as seen through a lens. (2000) *Apoptosis*, 5(3), 203-9
32. Thomas, W. D., Zhang, X. D., Franco, A.V., Nguyen, T. & Hersey, P. TNF-related apoptosis-inducing ligand-induced apoptosis of melanoma is associated with changes in mitochondrial membrane potential and perinuclear clustering of mitochondria. (2000) *J. Immunol.*, 165(10), 5612-20

33. Hail, N. Jr. & Lotan, R. Mitochondrial permeability transition is a central coordinating event in N-(4-hydroxyphenyl) retinamide-induced apoptosis. (2000) *Cancer Epidemiol. Biomarkers. Prev.*, (12),1293-301
34. Rocchi, E., Vigo, J., Viallet, P., Bonnard, I., Banaigs, B. & Salmon, J. M. Multiwavelength videomicrofluorometric study of cytotoxic properties of a marine peptide, didemnin B, using adriamycin as reference compound. (1999) *Anticancer Res.*, 19(4C), 3559-68
35. Aisaki, K., Kanno, H., Oyaizu, N., Hara, Y., Miwa, S. & Ikawa, Y. Apoptotic changes precede mitochondrial dysfunction in red cell-type pyruvate kinase mutant mouse erythroleukemia cell lines. (1999) *Jpn. J. Cancer Res.*, 90(2), 171-9
36. Scaduto, R. C. & Grotyohann, L. Measurement of mitochondrial membrane potential using fluorescent rhodamine derivatives. (1999) *Biophys. J.*, 76(1 Pt 1), 469-77

APPENDIX

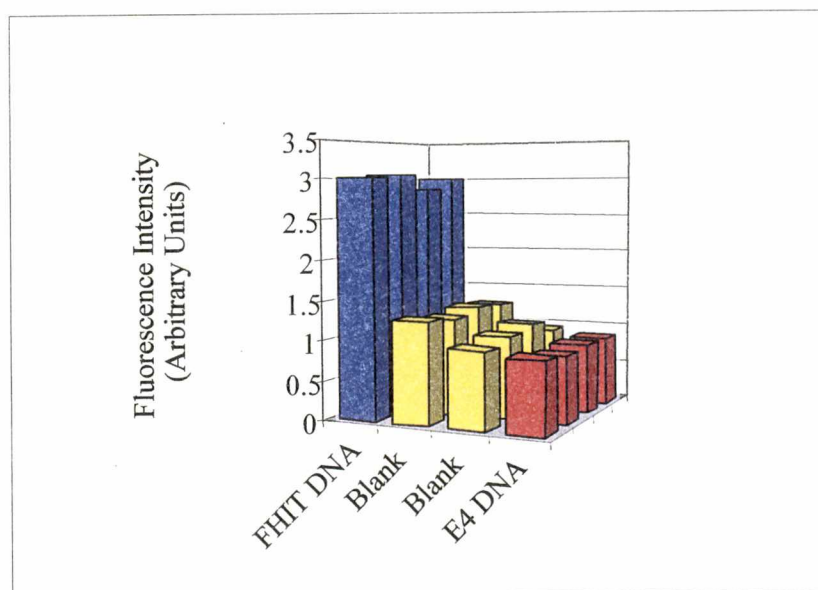


Figure 4.1 Stable transfection of FHIT gene. Genomic DNAs isolated from MKN/FHIT and MKN/E4 cell lysates were PCR amplified using sequence-specific primers for the FHIT gene and subjected to detection using fluorescently labeled FHIT DNA probes. As determined by the biochip the MKN/FHIT cell line demonstrated significantly increased fluorescence signal over the background as a result of retaining the FHIT gene. Presence of an intact FHIT gene did not present itself in the MKN/E4 cell line and the observed fluorescence signal was at about same level as background fluorescence in the MKN/FHIT cell line.

AGS 293 E4 FHIT Markers

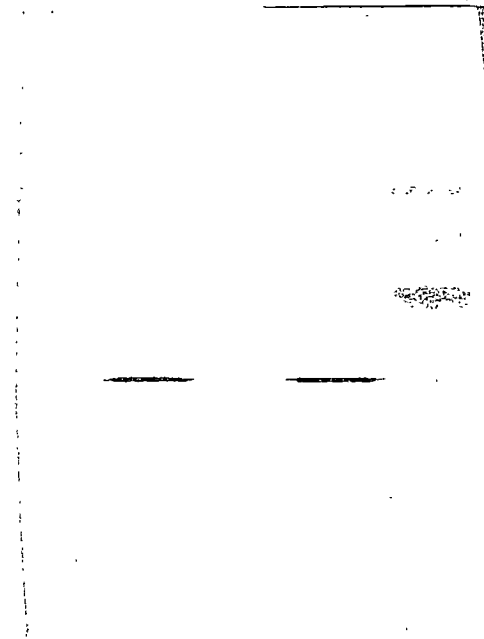
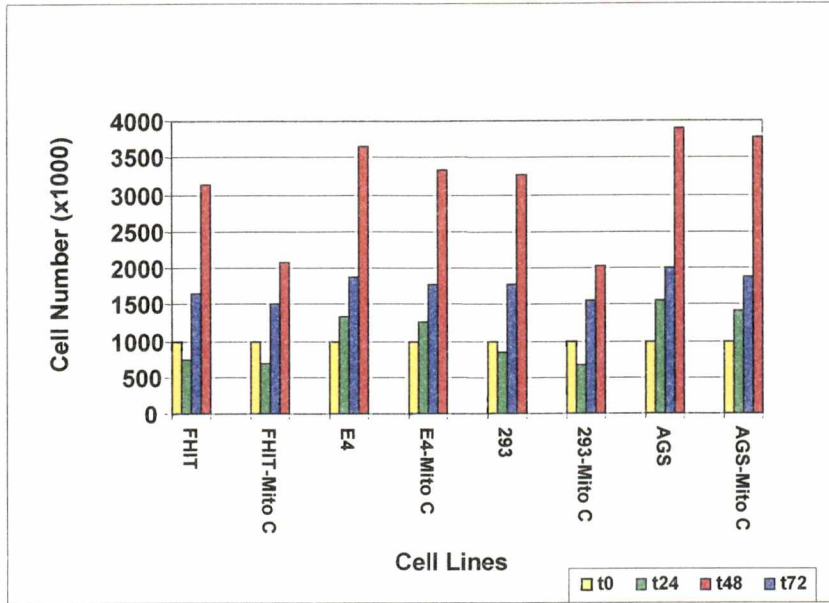
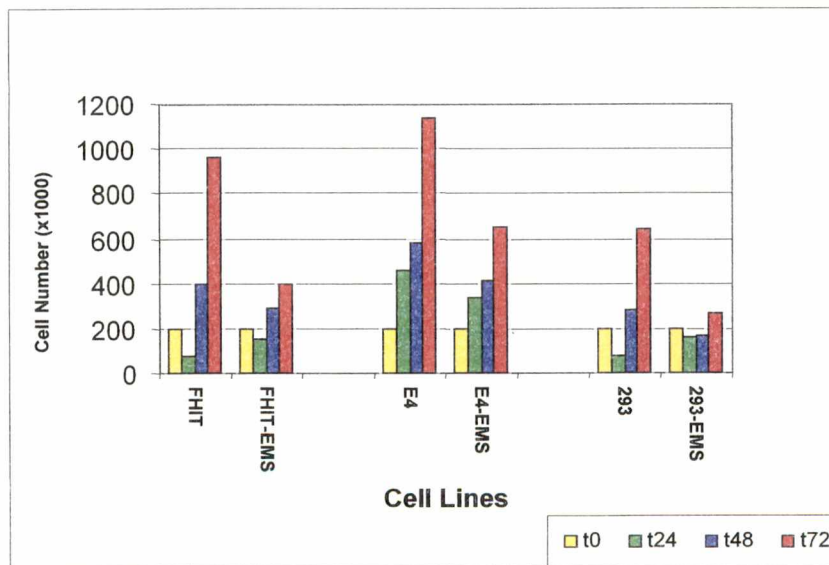


Figure 4.2 Fhit protein expression in cell lines. The MKN/FHIT, MKN/E4, 293 and AGS cell lines were tested for expression of the Fhit protein. Western immunoblot analysis of cell lysates using anti-Fhit polyclonal antibody showed expression of detectable Fhit protein only in MKN/FHIT and 293 cell lines. Conversely, no exogenous Fhit expression was detected in MKN/E4 or AGS cell lines.

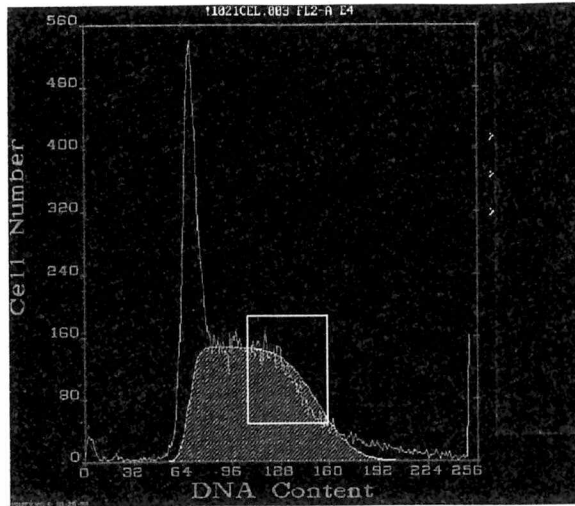
Figure 4.3 Effects of Fhit expression on the ability of cells to proliferate. MKN/FHIT transfected cell line and FHIT-positive 293 cell line along with Fhit-minus MKN/E4 and AGS cell lines were maintained continuously in their growth media. Significant difference in growth rates of each of the four cell lines were found. The MMC-treated (a) and EMS-treated (b) cells with stable Fhit expression demonstrated decreased proliferation rates as evidenced by their increased doubling time compared with FHIT-minus cells grown under the same conditions.



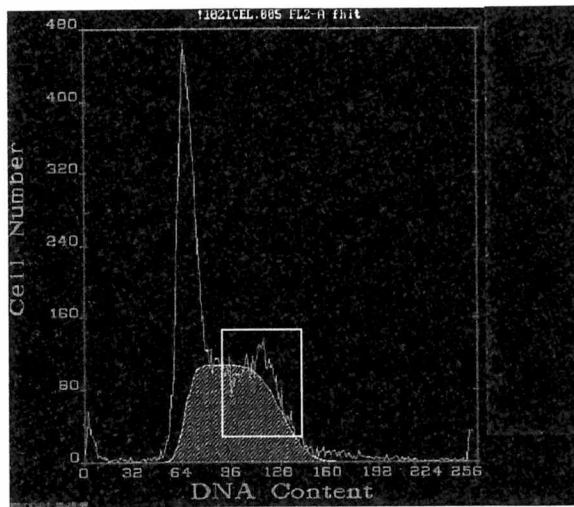
(a)



(b)



MKN/E4



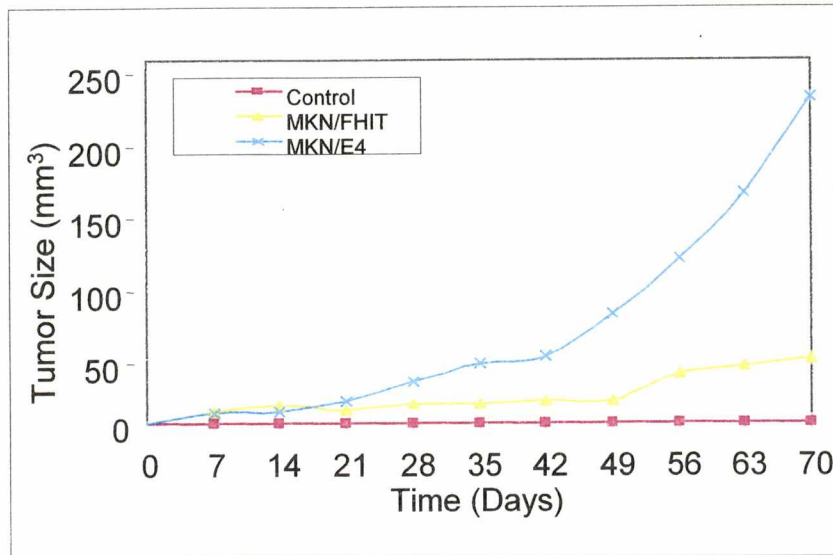
MKN/FHIT

Figure 4.4 Distribution of nuclear DNA content measured by flowcytometry. Distribution of nuclear DNA content in MKN/FHIT cells (a) and MKN/E4 cells (b) grown under normal tissue culture conditions harvested 3 days after seeding. Different DNA contents and variation in percentages of cells in each stage of the cell cycle were observed.

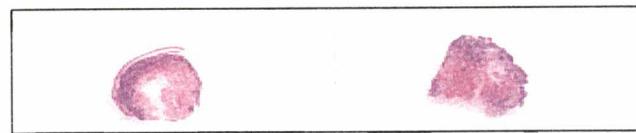
Table 4.1

Percentages of cells in different stages of the cell cycle

<i>Cell Cycle Phase</i>	<i>G1</i>	<i>G2</i>	<i>S</i>
<i>MKN/FHIT</i>	41.3 \pm 2.4	3.2 \pm 1.2	55.5 \pm 3.3
<i>MKN/E4</i>	27.3 \pm 2.9	3.5 \pm 1.2	69.2 \pm 3.9



(a)

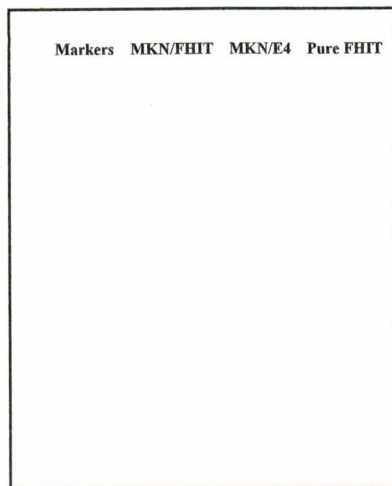


MKN/E4

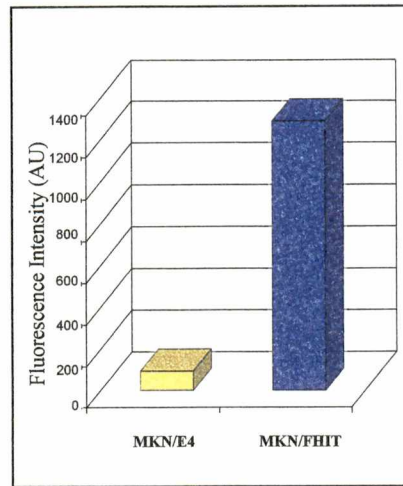
MKN/FHIT

(b)

Figure 4.5 (a) Demonstration of *in vivo* tumor suppressor activity of the FHIT gene. Transfected cells from MKN/FHIT and MKN/E4 cultures were harvested by trypsinization and resuspended in PBS at 2.5×10^7 /ml. A population of 5×10^6 cells in 0.2 ml of PBS were injected subcutaneously into the right flank of 6-week-old female nude mice, five mice per cell line. A group of 5 control mice were injected only with 0.2 ml of PBS. Inoculated animals were monitored twice weekly for tumor formation. Stable Fhit wild-type expression in transfected cancer cell clones suppressed tumor growth in nude mice. (b) The H&E stained tumors excised from mice.



(a) *Fhit* Protein Detection



(b) *FHIT* Gene Identification

Figure 4.6 Representative MKN/FHIT and MKN/E4 tumors were excised from mice. Western immunoblot analysis of MKN/FHIT and MKN/E4 tumor lysates demonstrated presence of Fhit protein only in MKN/FHIT tumors (a). Genomic DNA was isolated from these tumors and PCR amplified for the *FHIT* gene. Using the biochip, presence of the *FHIT* gene in the MKN/FHIT tumors and its absence in the MKN/E4 tumors was demonstrated (b).

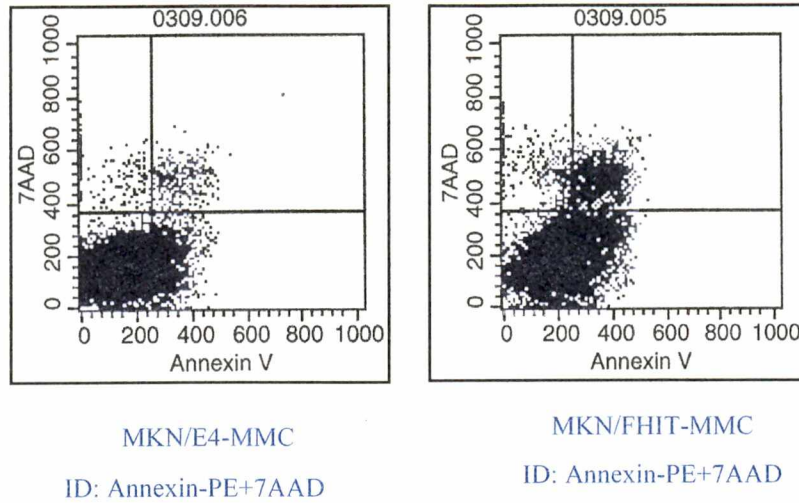
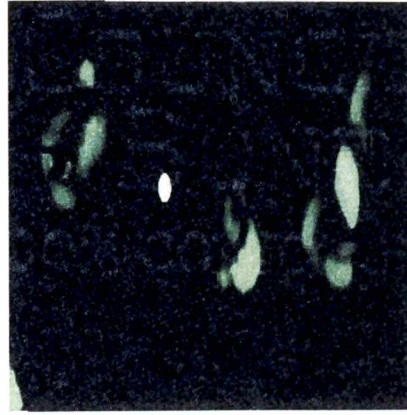


Figure 4.7 Apoptosis among transfected MKN cells were analyzed by staining profiles of PE-conjugated Annexin-V for identification of early apoptotic cells and 7-AAD for identifying dead cells. Flow cytometric comparisons among the MKN/E4 cells (a) and MKN/FHIT cells (b) indicated a significantly higher number of apoptotic cells in MKN/FHIT cells.



MKN/FHIT-MMC



MKN/E4-MMC

Figure 4.8 In situ TUNEL staining of MKN/FHIT and MKN/E4 cells. Higher percentage of MKN/FHIT cells than MKN/E4 cells showed condensed and fragmented nuclei illustrated by higher number of MKN/FHIT cells incorporating the fluorescein-labeled dUTP. This indicates a higher ratio of apoptosis-induced DNA strand breaks in these cells.

Table 4.2

Percentage of the MMC induced MKN/FHIT and MKN/E4 apoptotic cells analyzed by TUNEL assay.

<i>Cell Lines</i>	<i>MMC</i>	<i>PBS</i>
<i>MKN/FHIT</i>	31 +/- 3.6	9 +/- 2.4
<i>MKN/E4</i>	16 +/- 2.5	7 +/- 2.5

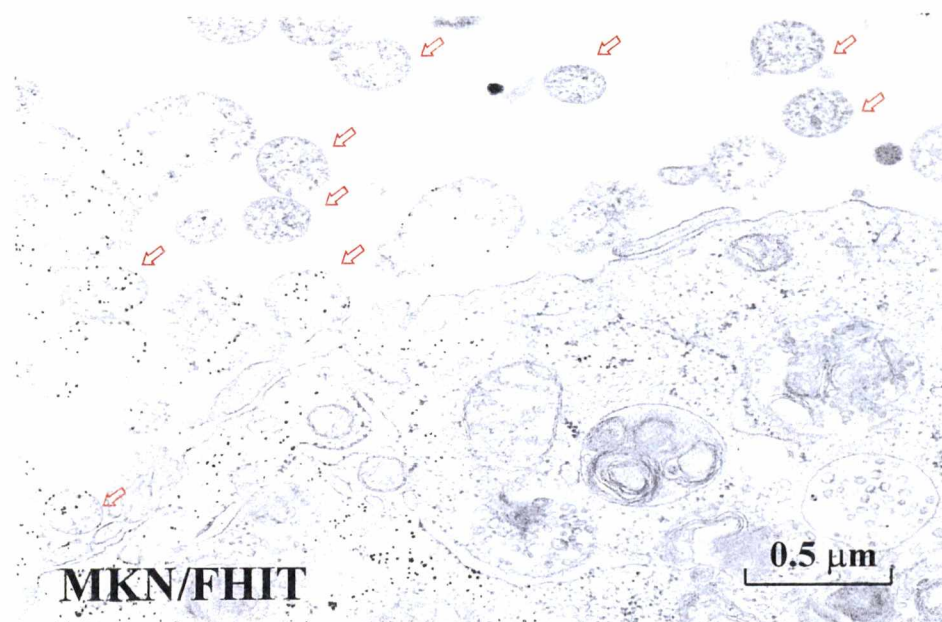


Figure 4.9 Transmission electron micrograph of MMC-treated MKN/FHIT cells. Formation of typical apoptotic bodies that contain intact intracellular organelles is demonstrated (x 5000).

Table 4.3

Observed percentage of apoptotic cells in MMC-induced MKN/FHIT and MKN/E4 cell lines determined by transmission electron microscopy.

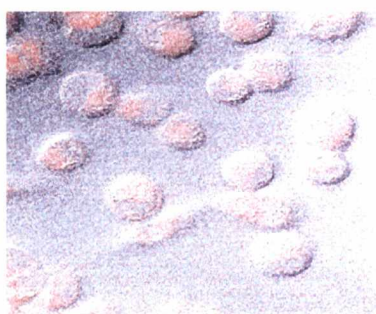
<i>Cell Lines</i>	<i>MMC</i>
<i>MKN/FHIT</i>	30 +/- 3.4
<i>MKN/E4</i>	16 +/- 2.3



(a) MKN/FHIT + R 123



(b) MKN/FHIT + MMC + R 123



(c) MKN/ E4 + R 123



(d) MKN/ E4 +MMC + R 123

Figure 4.10 Confocal microscopy of MKN/FHIT and MKN/E4 cells incubated in media containing rhodamine 123. Increased in the mitochondrial uptake of rhodamine 123 by MMC-treated MKN/FHIT is observed.

PART FIVE

**IMPLICATION OF MITOCHONDRIAL INVOLVEMENT IN APOPTOTIC
ACTIVITY OF THE FHIT GENE**

5.1 ABSTRACT

The fragile histidine triad (FHIT) putative tumor suppressor gene includes the common human chromosomal fragile site at 3p14.2, and the hereditary renal cancer translocation breakpoint. The structure and expression of the FHIT gene are frequently altered in many cancers. We and others have demonstrated that FHIT has properties of tumor suppressor activity, potentially involving induction of cellular apoptosis. Data here in, implicates the involvement of mitochondria in the apoptotic activity of the FHIT gene. A number of morphological and biochemical events are recognized as characteristic features of the apoptotic progress. Among these, the disruption of the inner mitochondrial transmembrane potential ($\Delta\Psi_m$) and the release of apoptogenic cytochrome c protein into the cytoplasm appear to be early events in many systems. In this investigation, we studied the proapoptotic activity of the FHIT gene by investigating the loss of $\Delta\Psi_m$ in mitochondria and translocation of the cytochrome c as consequences of the presence of active Fhit protein. Synchronous luminescence spectroscopy was applied to measure mitochondrial incorporation of rhodamine 123 for direct analysis of alterations in the mitochondrial transmembrane potential. Immunoblotting was used to determine cytosolic translocation of cytochrome c. These findings suggested an enhanced loss of $\Delta\Psi_m$ in apoptotically induced FHIT expressing cells, relative to the FHIT negative cells treated in the same manner. Translocation of cytochrome c from the mitochondria into the cytoplasmic compartment in the FHIT expressing cells as an early event during induction of the apoptotic pathway was also demonstrated. This loss of $\Delta\Psi_m$ was restricted in the presence of the apoptotic inhibitor; cyclosporin A. Expression of the Fhit protein may

maintain apoptotic function by altering the mitochondrial transmembrane potential and enhancing cytochrome c efflux from the mitochondria to the cytoplasm.

5.2 INTRODUCTION

The tumor suppressor FHIT (fragile histidine triad) gene at chromosome 3p14 was identified by positional cloning in 1996 (1,2). The discovery of the FHIT gene, which frequently displays a variety of DNA and RNA level alterations (1,3-8), captivated the attention of the cancer research community. This interest was due to recognizing the loss of DNA sequences from this region as one of the most frequent genetic abnormalities in a broad range of cancers (9,10). The biological mechanism of the tumor suppressor activity of the FHIT gene and the cellular pathways associated with its function are not completely understood. However, analysis of the data obtained from *in vitro* and *in vivo* studies, investigating the tumor suppressor activity of the Fhit expression have suggested a strong link to apoptosis (11-13).

Apoptosis is a tightly regulated form of physiological cell death, which is dependent on the expression of cell-intrinsic suicide machinery. Prominent morphological changes include cell shrinkage, condensation of the nuclear chromatin, fragmentation of the nucleus, cleavage of chromosomal DNA and formation and release of membrane-bound apoptotic bodies (14). Recent developments in the area of apoptosis research have demonstrated mitochondria and death receptors as two key regulators of critical signaling events in programmed cell death (15-18) (Fig. 5.1).

Mitochondria may induce apoptosis by releasing cytochrome c from its intermembrane space to the cytosol (19-21). In the presence of adenosine triphosphate (ATP), cytosolic cytochrome c interacts directly with apoptotic protease activating factor 1 (APAF-1) and procaspase 9 to form the apoptosome. An apoptosome is a macromolecular complex that cleaves procaspase 9 to active caspase 9, which, in turn, cleaves procaspase 3 to active caspase 3 (19). Mitochondria also release other proteins during apoptosis, e.g., apoptosis-inducing factor (AIF), which does not activate caspases but translocates directly into the nucleus and induces DNA fragmentation (20), and the second mitochondria-derived activator of caspase protein (Smac), which blocks the inhibitors of apoptosis proteins that inhibit caspases (21) (Fig. 5.2).

Apoptosis can also be induced by activation of death receptors (22,23). Binding of extracellular ligands, such as Fas ligand or tumor necrosis factor (TNF), to their respective receptors induces receptor trimerization, which, in turn, recruits adaptor molecules such as Fas receptor-associated death domain protein, TNF receptor-associated death domain protein, and procaspase 8. This signaling complex activates procaspase 8, and the downstream events including activation of procaspase 3 and the release of cytochrome c, which is mediated by cleavage of the Bid protein. Both the mitochondrial and the death receptor pathways thus converge on cleavage of procaspase 3. Activation of caspase 3 results in DNA fragmentation after activation of caspase-activated deoxyribonuclease or the DNA fragmentation factor (24-26) (Fig. 5.1).

In this study, we investigated whether FHIT associated apoptosis involves changes in the mitochondrial activity. Since apoptotic events could involve a mitochondrial permeability transition and release of cytochrome c (27-29). Effects of Fhit protein expression on: (i) the $\Delta\Psi_m$ loss in the mitochondria of apoptotically induced cells, (ii) the translocation of cytochrome c from the mitochondria into the cytosolic compartment, and (iii) Impedance of the $\Delta\Psi_m$ loss in mitochondria due to presence of apoptotic inhibitors were studied. These criteria were examined using conventional biological approaches and a unique spectroscopic method, the synchronous luminescence (SL) spectroscopy.

5.3 MATERIALS AND METHODS

5.3.1 Cell Culture

FHIT-negative gastric carcinoma (MKN74) cells (30), that had been previously transfected with vectors containing either the pRcFHIT gene (MKN/FHIT cell line) and the neomycin resistance gene, or only the neomycin resistance gene (MKN/E4 cell line) were employed in this study. Whereas the MKN/FHIT cell line expresses the Fhit protein, the MKN/E4 cells lack Fhit protein expression (2). These two cell lines were kindly provided by Dr. Kay Huebner (Thomas Jefferson University, Kimmel Cancer Institute, Philadelphia, PA). Construction of these cells has been described previously in detail (31). In short, using the calcium phosphate method (GIBCO/BRL, Grand Island, NY), plasmids comprised of *wt*-FHIT cDNA ligated in-frame to a FLAG octapeptide coding sequence, and under control of the immediate early human cytomegalovirus

(CMV) promoter (Eastman Kodak, Rochester, NY), had been cloned into the HindIII and XbaI sites of the pRcCMV vector. Selection of the clones was performed in the presence of 200-400 $\mu\text{g/ml}$ G418 (geneticin; GIBCO/BRL, Grand Island, NY). The cells were cultured in Dulbecco's modified eagle's medium (DMEM), supplemented with 10% fetal calf serum (Life Technologies, Inc., Gaithersburg, MD), 1 ml of a 50 mg gentamicin/ml water solution (GIBCO/BRL, Grand Island, NY), and 1 % each of non essential amino acids, hepes buffer, L- glutamine and sodium pyruvate (Sigma, St. Louis, MO). These cultures were maintained in a humidified atmosphere of 95% air and 5% CO_2 at 37 $^\circ\text{C}$.

5.3.2 Apoptosis Assay

As an essential preliminary step, the status of the presence of the FHIT gene and expression of Fhit protein were determined in the MKN/FHIT and MKN/E4 cell lines (32-34). To induce apoptosis, 50% confluent MKN/FHIT and MKN/E4 cells, grown on chamber slides, were incubated in a medium containing 60 μM of mitomycin c (MMC) (Sigma, St. Louis, MO) (35) for 20 hrs. In order to detect apoptotic cells, the MMC treated cells were analyzed by an *in situ* terminal deoxynucleotidyl transferase labeling (TUNEL) assay according to the protocol recommended by the Fluorescein FragEL DNA fragmentation detection kit (Oncogene, Boston, MA). Percentage of apoptotic MKN/FHIT and MKN/E4 cells was determined by fluorescence imaging using a Nikon Diaphot 300 microscope (Japan) equipped with a 485 nm, B-1E filter cube.

5.3.3 Visualization of Altered Mitochondrial Activity

Confocal and fluorescence light microscopy were used to visually demonstrate alterations in the mitochondrial activity of the cells. MMC-treated (60 μM) and untreated MKN/FHIT and MKN/E4 cells were washed twice with phosphate buffered saline (PBS) and incubated in medium containing 5 μM R123 at 37 $^{\circ}\text{C}$ for 30 min. A Leica TCS SP2 spectral confocal and multiphoton system (Deerfield, IL) and a Nikon Diaphot 300 fluorescent microscope (Japan) were used for image acquisitions.

5.3.4 Evaluation of the Alterations in the Mitochondrial Membrane Potential

For assessment of $\Delta\Psi_m$ alterations in the mitochondria, MKN/FHIT cells were MMC-treated (60 μM), rinsed twice with PBS and subsequently incubated in a medium containing 5 μM R123 for 30 min at 37 $^{\circ}\text{C}$. The cells were then washed 3 times with PBS, harvested and counted. These cells (1×10^6) were placed in a plastic disposable cuvette (Starna, Essex, England) with a 1-cm path length, and the inner $\Delta\Psi_m$ was determined using Synchronous Luminescence spectroscopy (SL) (57-59). The synchronous spectra were collected in a 400-600 nm range with a 5 nm interval maintained between the 2 monochromators. Additionally, the excitation spectra were collected with the emission wavelength set to 510 nm and the emission spectra were taken with the excitation wavelength set at 535 nm. All spectroscopic measurements were recorded at 25 $^{\circ}\text{C}$ using a single integrated workstation, JobinYvon Spex spectrofluorimeter (Edison, NJ), with computer interfacing capabilities. This

commercial instrument has two monochromators that can be interlocked and scanned simultaneously. Bandwidths for excitation and emission were set at 1 nm each. Manufacturers software was employed for instrumental control and fluorescent signal analysis.

5.3.5 Evaluation of the Effects of Cyclosporin A

The MKN/FHIT cells were seeded and maintained in 6-well plates (Falcon, Oxnard, CA). Cell proliferation rates were analyzed in 3 groups of: untreated, MMC treated and simultaneously MMC and cyclosporin A (CsA) treated groups of cells. A group of untreated cells were used as control. To prepare apoptotic cells, the MKN/FHIT cells were treated with MMC (60 μ M) for 20 hrs before harvest as described previously. In the third group, the inhibitory effects of CsA on apoptosis were investigated on cells simultaneously treated with MMC (60 μ M) and 200 nM CsA. Every 24 hrs for 48 hrs from the time of treatments, the cells from three wells in each group were trypsinized and counted using trypan blue to exclude dead cells.

5.3.6 Inhibitory Effects of Cyclosporin A on Loss of Transmembrane Potential

A population of the MKN/FHIT cells was treated for 20 hrs with MMC before harvesting as previously described. Another population of the same cells was treated simultaneously with both MMC and 200 nM of CsA, while the third group of cells was maintained under normal tissue culture conditions. Effects of CsA treatment on mitochondrial

permeability were assessed using SL by measuring the $\Delta\Psi_m$ -dependent uptake of R123 as the previously described.

5.3.7 Cytochrome c Translocation, and Western Blot Analysis

Preparations of cell lysates and Western blot analysis have been described previously in detail (11,33,34). Briefly, 4×10^7 cells were harvested and suspended in 10 parts (v/v) lysis buffer (0.5 % NP40 in PBS supplemented with 10 $\mu\text{g}/\text{mL}$ leupeptin and 10 $\mu\text{g}/\text{mL}$ PMSF (Sigma, St. Louis, MO) and sonicated for 30 sec (Branson sonifier, Danbury, CT). Cellular debris was removed by a 10-min centrifugation at 8,500 x g at 4°C.

In order to obtain mitochondria-free cytosol, 3×10^6 cells were harvested via scraping into 500 μl of CLB/5mM EDTA/PI (10 mM HEPES, 10 mM NaCl, 1 mM KH_2PO_4 , 5 mM NaHCO_3 , 1 mM CaCl_2 , 0.5 mM MgCl_2 , 1 mM PMSF, 10 $\mu\text{g}/\text{ml}$ aprotinin, 10 $\mu\text{g}/\text{ml}$ leupeptin, 1 $\mu\text{g}/\text{ml}$ pepstatin (Sigma, St. Louis, MO)) solution. The cells were allowed to swell for 5 to 10 min. The swollen cells were then homogenized using a tight-fitting glass-teflon Dounce-type pestle (clearance: 0.0005-0.0025 in, Bellco Glass, Vineland, NJ). The suspension was centrifuged at 5500 x g for 5 min. The supernatant, consisting of cytosol plus plasma membranes, was removed and further centrifuged in a SW41 rotor at 25,000 rpm for 30 min to obtain the cytosolic fraction. Protein concentrations were determined using the Pierce BCA Protein assay by following the manufacturer's instructions. Equal quantities of protein (20 μg) were loaded onto 14% polyacrylamide gels (Novax, San Diego, CA) containing sodium dodecyl sulfate (SDS), subjected to

electrophoresis and transferred to nitrocellulose membranes (Schleicher & Schuell, Keene, NH). The blots were blocked with Blotto (5% nonfat dry milk (Kroger Co, Cincinnati, OH) and 0.1% Tween-20 (Sigma, St. Louis, MO) in PBS) for 60 min. Blots were incubated for 2 hrs at room temperature in the primary antibody solution containing 1 µg/ml cytochrome c polyclonal antibody (Santa Cruz Biotechnologies, Santa Cruz, CA) in the blocking buffer. Immunocomplexes were visualized by chemiluminescence using horseradish peroxidase-conjugated secondary antibody (1:500) (BioRad Laboratories, Richmond, CA) and chemiluminescent substrate (Pierce DAB super signal system, Rockford, IL) as described by the manufacturer.

5.4 RESULTS AND DISCUSSION

Recent investigations have demonstrated the tumor suppressor function of the FHIT gene. Studies on a number of important human tumors (1,22,39,40) and cancer-derived cell lines (10,41) have frequently shown altered FHIT RNA (5,17,30,36-38), that correlated with deletions within the FHIT gene and lack of detectable Fhit protein. Genetic changes, such as these, involving oncogenes and tumor suppressor genes, may contribute to the deregulated expansion of malignant cells. While some of these changes result in increased proliferation, others contribute to increased cell numbers by inhibiting apoptosis (programmed cell death) (42,43). Impairment of apoptosis function, due to lack of Fhit expression, has been implicated by us and by others (11-13) as a possible mechanism of action for the tumor suppressor activity of FHIT gene.

Induction of apoptosis can be divided into three stages: (1) interaction of the inducing signal with the cell, (2) biochemical transduction of the death signal, and (3) execution of apoptosis (44). During the biochemical transduction phase of apoptosis, two major changes in the mitochondrial membrane permeability have been observed. On the one hand, the electrochemical gradient built up on the mitochondrial inner membrane dissipates early during apoptosis (45). On the other hand, apoptogenic proteins that normally are sequestered in mitochondria are released via the outer mitochondrial membrane. Such proteins include cytochrome c (46) and AIF (47,48) leading to activation of caspase 3 and execution of apoptosis (49,50).

5.4.1 Characterization of the *In vitro* Model System

To enhance our understanding of the apoptotic mechanism of action of the FHIT gene an *in vitro* model consisting of the FHIT positive MKN/FHIT and the FHIT negative MKN/E4 cell lines was used. These cell lines have previously been analyzed and the presence of the FHIT gene and expression of the Fhit protein in the MKN/FHIT and their absence in the MKN/E4 cell lines have been confirmed (32-34). The apoptotic activity of the FHIT gene has been assessed using the TUNEL assay, which detects DNA strand breaks in apoptotic cells (11-12). Initially, the MKN/FHIT and MKN/E4 cells were MMC treated. Twenty hours later the cells were harvested and analyzed by TUNEL (n=900 cells). A higher number of condensed and fragmented nuclei from the MKN/FHIT cells incorporated the fluorescein-labeled dUTPs, thus indicating apoptosis-induced DNA strand breaks, whereas MKN/E4 cells displayed a significantly lower

level of labeled, condensed nuclei (Fig. 5.3). The staining profiles of the apoptotic-positive cells, obtained from this study, indicated about 30% +/- 3.5% apoptotic MKN/FHIT cells as compared to 15% +/- 2.6% apoptotic MKN/E4 cells and 9% +/- 2.3% and 6% +/- 2.5% for the PBS-treated MKN/FHIT and MKN/E4 cells, respectively.

5.4.2 Alterations in the Inner Mitochondrial Transmembrane Potential

Previous research has implicated mitochondrial physiology in the initiation and progress of apoptosis of cells in culture and in tissue environments (51-52). Early apoptosis is invariably accompanied by a disruption and collapse of the inner mitochondrial transmembrane potential ($\Delta\Psi_m$) (53). To further elucidate whether expression of the Fhit protein had a direct effect on enabling the cells to initiate programmed cell death upon exposure to an apoptotic stimulus, we looked into MMC-induced modulations of mitochondrial $\Delta\Psi_m$ in MKN/FHIT and MKN/E4 cells by staining with rhodamine 123. Subpopulations of MKN/FHIT and MKN/E4 cells were treated with MMC. These cells along with cells grown under normal tissue culture conditions were incubated in media containing rhodamine 123. R123 fluorescent dye is a lipophilic cation that is taken up by mitochondria in proportion to the $\Delta\Psi_m$ (54). R123 uptake was confirmed visually by fluorescent light microscopy (Fig. 5.4) and laser scan confocal microscopy (CLSM) (Fig. 5.5) (55). Untreated cells in both MKN/FHIT and MKN/E4 groups showed comparable mitochondrial membrane potential by a similarly small R123 uptake, indicating a low $\Delta\Psi_m$ in both groups (Fig. 5.4 a,b). However, in the MMC-treated groups, the MKN/FHIT cells were stained in a much stronger fashion than the FHIT negative

MKN/E4 cells that showed little change in the mitochondrial membrane potential (Fig. 5.4 c,d) when compared to the untreated MKN/E4 group. This observation confirmed our previous finding that Fhit expression correlates with higher apoptotic induction, propelling the cells to lose their mitochondrial membrane potential. Similar results were obtained with the CLSM where the fluorescence images also showed a clear tendency for higher incorporation of R123 in the MKN/FHIT cells after induction of programmed cell death, where they displayed an increase in R123 uptake indicating loss of $\Delta\Psi_m$ (Fig. 5.5 a). Fluorometric analysis of the MMC-treated MKN/E4 cells, showing less incorporation of R123 in their mitochondria (Fig. 5.5 b), led to the conclusion that these cells might have higher resistance to apoptotic induction than the MKN/FHIT cells due to the absence of the Fhit protein expression. The outcome lends further support to the view that the expression of the Fhit protein in these cells potentially has a role in activation of a mitochondrial-dependent death program pathway.

We further analyzed apoptosis-induced alterations in the $\Delta\Psi_m$ of the MKN/FHIT cell lines using SL. This unique methodology provides a simple, yet sensitive, alternative approach for fluorescence detection. In recent years, SL has been used extensively to obtain spectral fingerprints of complex biological and chemical samples (56-59).

Application of SL to analyze mitochondrial R123 uptake provided a means for a more detailed investigation of the changes occurring in the mitochondria of apoptotic cells. Conventional luminescence spectrometry uses either a fixed excitation or a fixed emission wavelength to measure the luminescence intensity of different fluorescent compounds. Excitation and emission spectra of the R123 taken up by mitochondria of

the cells are presented (Fig. 5.6 a,b). In the SL methodology, both excitation and emission wavelengths are scanned simultaneously while a constant wavelength interval ($\Delta\lambda$) is maintained between the two monochromators throughout the measurement (56). The SL ability to offer better peak resolution makes it a highly selective analytical technique for detection of various compounds (57). The SL spectrum of a PBS solution containing R123, demonstrating a SL peak at 510 nm, is presented (Fig. 5.7 a). The resulting SL spectra of R123 uptake by the mitochondria of the MMC-treated and the untreated MKN/FHIT as the consequence of alterations in the mitochondrial membrane potential are illustrated (Fig. 5.7 b). The spectrum of the MMC treated cells has a readily identifiable peak at 510 nm corresponding to the expected peak for R123. This R123 uptake suggests occurrence of a change in the mitochondrial $\Delta\Psi_m$ of MKN/FHIT due to their induction for apoptosis. The relationship between loss of $\Delta\Psi_m$ in mitochondria of MMC treated cells as a function of time was also investigated (Fig. 5.8 a). A steady increase in the concentration of R123 in the MMC treated cells was noticed for the first 30 min of the assay after which it remained steady (Fig. 5.8 b).

5.4.3 Possible Involvement of Mitochondrial Pores and Channels

Mitochondrial transmembrane potential is an electrical potential across the inner membrane, which is created by H^+ pumping during electron transfer and plays a key role in mitochondrial bioenergetics (60,61). The $\Delta\Psi_m$ collapse is an important event in MMC-induced apoptosis (45,51). Pharmacologic and functional studies have suggested that $\Delta\Psi_m$ collapse can be attributed to the opening of mitochondrial permeability

transition pores or mitochondrial megachannels, which are formed by multiprotein complexes at the contact sites between the mitochondrial inner and outer membranes (62). Opening of a high conductance permeability transition (PT) pore in mitochondrial inner membrane abruptly increases permeability of the mitochondrial inner membrane to allow solutes of molecular mass up to 1500 Da to equilibrate across the inner membrane (63-64). It has been proposed that mitochondrial apoptogenic factors might be released through pores during apoptosis (47). In fact, a mitochondrial protein, apoptosis-inducing factor, which has the ability to induce apoptotic changes of the nucleus *in vitro* and the activation of caspases, has been shown to be released through pores (65).

Cyclosporin A (CsA), a transition pore blocker and thereby an inhibitor of mitochondrial $\Delta\Psi_m$, locks this mitochondrial permeability transition (66-69). To investigate the details of the apoptotic mechanism of Fhit expression, effects of CsA treatment on induction of apoptosis and loss of mitochondria $\Delta\Psi_m$ of the MKN/FHIT cells were examined. Effects of expression of exogenous Fhit protein on the ability of the cells to proliferate under apoptotic conditions were investigated. The MKN/FHIT cells were maintained in (a) growth media, (b) growth media supplemented with MMC and (c) growth media containing both MMC and CsA. A significant decrease in the growth rate of the MMC-treated MKN/FHIT cells as compared to the cells grown in regular media was found (Fig. 5.9). However, the doubling time of the MKN/FHIT cells grown in the media containing both, MMC and CsA, was comparable to the rate of proliferation of the untreated cells (Fig. 5.9). Results demonstrated that in this cell line, the subsequent apoptosis induction of MMC treatment was blocked by the effects of the megachannel antagonist CsA.

Using SL, the $\Delta\Psi_m$ -dependent uptake of R123 was assessed in MMC treated MKN/FHIT cells, treated or untreated with CsA. CsA treatment abolished the MMC-induced $\Delta\Psi_m$ as it had been previously shown to decrease the MMC-evoked, apoptotic cell death in these cells (Fig. 5.10). Results were also confirmed visually using fluorescence microscopy (Fig. 5.11). As demonstrated, the observed increase in R123 uptake by the mitochondria of the MMC treated MKN/FHIT cells (Fig. 5.11 a,b) was abolished in the presence of CsA (Fig. 5.11 c). These results suggest that the MMC-induced apoptotic process, in the FHIT expressing cells, was mediated by a CsA-sensitive pathway promoting the idea of involvement of both mitochondria and mitochondrial pores in this cell death program.

5.4.4 Cytochrome C Translocation

Cytochrome c protein is encoded by a nuclear gene and translated by cytosolic ribosomes as apocytochrome c (58). Apocytochrome c is subsequently translocated into the mitochondria where a heme group is attached covalently to form holocytochrome c. Cells undergoing apoptosis were found to have an elevation of cytochrome c in the cytosol and a corresponding cytochrome c decrease in the mitochondria (70). Here, we confirmed the translocation of the cytochrome c from the mitochondria into the cytosolic compartment by protein immunoblot analysis (Fig. 5.12). The FHIT-positive MKN/FHIT and the FHIT-negative MKN/E4 cell lines were treated with 60 μ M mitomycin c for 20 hrs. Whole cell lysates and mitochondria free cell lysates were subjected to gel electrophoresis and western blot analysis for the presence of cytochrome c.

As expected, cytochrome c was detected in the whole cell lysates of both MKN/FHIT and MKN/E4 cells (Fig. 5.12 lanes 1 and 3). These results demonstrated similar total cellular expression of the cytochrome c in both cell lines. However, detection of the cytochrome c in sonication prepared cellular lysates does not indicate translocation of the protein from the mitochondria into the cytoplasm since during the course of lysate preparation, the mitochondria could have ruptured and released their internal cytochrome c protein into the cytosolic pool. This is only a measure of total cytochrome c expression. To assess the true concentration of the translocated cytochrome c from the mitochondria into the cytosol, we removed whole mitochondria from the cellular lysates after MMC treatment and before western analysis. As demonstrated in Fig. 5.12 lane 2, treatment of the MKN/FHIT cells with MMC resulted in the detection of the cytochrome c into the cytosol. This was indicated by the similarly comparable concentrations of the cytochrome c in the cytosol, where mitochondria was present (lane 2), or where it was removed from the cytosolic compartment (lane 1). However, in the case of the MKN/E4 cells, the highest amount of the detectable cytochrome c was retained in the mitochondria. This was indicated by the diminished protein band in the mitochondria-free cytosolic compartment (Fig. 5.12 lane 4) as compared with the lane, containing total expressed cytochrome c (Fig. 5.12, lane 3), which showed a significantly stronger cytochrome c band. Cytosolic fractions, prepared at various time points after MMC treatment, were used for immunoblot analysis of cytochrome c presence.

5.5 CONCLUSION

Knowledge of the complex biochemical pathways, involved in the regulation of apoptosis in FHIT expressing cells, is expanding. This study has focused on demonstrating different aspects of cellular alterations in the FHIT expressing cells with particular relevance to changes occurring in the mitochondrial inner transmembrane potential, the release of mitochondrial cytochrome c, and its subsequent translocation into the cytoplasmic compartment after treatment with MMC. Obtained data indicate that in the presence of apoptotic stimuli, Fhit protein expression alters the mitochondrial flux and efflux of molecules, causing alterations in the transmembrane potential. It was found that cyclosporin A treatment inhibited the MMC-induced cell death and abolished alterations of mitochondrial permeability transition, thereby preventing disruption of transmembrane potential. Cytoplasmic migration of cytochrome c, which is one of the key events in the molecular apoptotic pathway involving mitochondria was also demonstrated. However, apoptosis is a complex physiological process, which is dependent on the integrated functioning of a large number of gene products. Elucidation of the precise mechanisms involving FHIT in apoptotic killing of cells is a major topic for future research.

New strategies designed for detection of apoptotic signals is of great value in cancer research. In this study, a unique application of SL spectroscopy for use in biological laboratories was also investigated. This methodology proved effective for selective and sensitive detection of hodamine123, which is a widely used fluorescence marker in apoptosis studies.

5.6 ACKNOWLEDGEMENTS

This research was jointly sponsored by the Office of Biological and Environmental Research, U.S. Department of Energy under contract DE-AC05-00OR22725 with UT-Battelle, LLC., and by the ORNL Laboratory Directed Research and Development Program (Advanced Nanosystems).

REFERENCES

1. Ohta, M., Inoue, H., Cotticelli, M. G., Kastury, K., Baffa, R., Palazzo, J., Siprashvili, Z., Mori, M., McCue, P., Druck, T., Croce, C. M. & Huebner, K. The FHIT gene, spanning the chromosome 3p14.2 fragile site and renal carcinoma-associated t(3;8) breakpoint, is abnormal in digestive tract cancers. (1996) *Cell*, 84, 587-597
2. Barnes, L. D., Garrison, P. N., Siprashvili, Z., Guranowski, A., Robinson, A. K., Ingram, S. W., Croce, C. M., Ohta, M. & Huebner, K. Fhit, a putative tumor suppressor in humans, is a dinucleoside 5',5''-P1,P3-triphosphate hydrolase. (1996) *Biochemistry*, 35, 11529-11535
3. Sozzi, G., Veronese, M. L., Negrini, M., Baffa, R., Cotticelli, M. G., Inoue, H., Tornielli, S., Pilotti, S., DeGregorio, L., Pastorino, V., Pierotti, M. A., Ohta, M., Huebner, K. & Croce, C. M. The FHIT gene 3p14.2 is abnormal in lung cancer. (1996) *Cell*, 85, 1726.
4. Virgilio, L., Shuster, M., Gollin, S. M., Veronese, M. L., Ohta, M., Huebner, K. & Croce, C. M. FHIT gene alterations in head and neck squamous cell carcinomas. (1996) *Proc. Natl. Acad. Sci. USA*, 93, 9770-9775
5. Panagopoulos, I., Thelin, S., Mertens, F., Mitelman, F. & Aman P. Variable FHIT transcripts in non-neoplastic tissues. (1997) *Genes Chromosomes Cancer*, 19, 215-219
6. Segawa, T., Sasagawa, T., Saijoh, K. & Inoue, M. Clinicopathological significance of fragile histidine triad transcription protein expression in endometrial carcinomas. (2000) *Clin. Cancer Res.*, 6(6), 2341-8

7. Gayther, S. A., Barski, P., Batley, S. J., Li, L., de Foy, K. A., Cohen, S.N., Ponder, B.A., & Caldas, C. Aberrant splicing of the TSG101 and FHIT genes occurs frequently in multiple malignancies and in normal tissues and mimics alterations previously described in tumours. (1997) *Oncogene*, 15, 2119-2126
8. Mao, L., Lee, J.S., Fan, Y.H., Ro, J.Y., Batsakis, J.G., Lippman, S., Hittelman, W. & Hong, W. K. Frequent microsatellite alterations at chromosomes 9p21 and 3p14 in oral malignant lesions and their value in cancer risk assessment. (1996) *Nat. Med.*, 2, 682-685
9. Greenspan, D. L., Connolly, D. C., Wu, R., Lei, R.Y., Vogelstein, J. T. & Kim, Y. T., et al. Loss of FHIT expression in cervical carcinoma cell lines and primary tumors. (1997) *Cancer Res.*, 57, 4692-4698
10. Mao, L., Lee, J. S., Kurie, J. M., Fan, Y. H., Lippman, S. M., Lee, J. J., Ro, J. Y., Broxson, A., Yu, R., Morice, R. C., Kemp, B. L., Khuri, F. R., Walsh, G. L., Hittelman, W. N. & Hong, W. K. Clonal genetic alterations in the lungs of current and former smokers. (1997) *J. Natl. Cancer Inst.*, 89, 857-862
11. Askari, M. & Vo-Dinh, T. Investigation of tumor suppressor activity and apoptosis-related processes in FHIT transfected cell lines. (2001) (in preparation)
12. Sard, L., Accornero, P., Tornielli, S., Delia, D., Bunone, G., Campiglio, M., Colombo, M. P., Gramegna, M., Croce, C. M., Pierotti, M. A. & Sozzi, G. The tumor-suppressor gene FHIT is involved in the regulation of apoptosis and in cell cycle control. (1999) *Proc. Natl. Acad. Sci. USA*, 96(15), 8489-92

13. Ji, L., Fang, B., Yen, N., Fong, K., Minna, J. D. & Roth, J. A. Induction of apoptosis and inhibition of tumorigenicity and tumor growth by adenovirus vector-mediated fragile histidine triad gene overexpression. (1999) *Cancer Res.*, 59(14), 3333-9
14. Gastman, B.R. Apoptosis and its clinical impact. (2001) *Head Neck*, 23(5), 409-25
15. Pucci, B., Kasten, M. & Giordano, A. Cell cycle and apoptosis. (2000) *Neoplasia*, 2(4), 291-9
16. Tang, D.G. & Porter, A.T. Apoptosis: A Current Molecular Analysis. (1996) *Pathol. Oncol. Res.*, 2(3), 117-131
17. Narula, J., Pandey, P., Arbustini, E., Haider, N., Narula, N., Kolodgie, F. D., DalBello, B., Semigran, M. J., Bielsa-Masdeu, A., Dec, G. W., Israels, S., Ballester, M., Virmani, R., Saxena, S. & Kharbanda, S. Apoptosis in heart failure: release of cytochrome c from mitochondria and activation of caspase-3 in human cardiomyopathy. (1999) *Proc. Natl. Acad. Sci. U S A.*, 96(14),8144-9
18. Fesus, L. Biochemical events in naturally occurring forms of cell death. (1993) *FEBS Lett.*, 328(1-2), 1-5
19. Li, P., Nijhawan, D. , Budihardjo, I. , Srinivasula, S. M. , Ahmad, M. , Alnemri, E. S. & Wang, X. Cytochrome c and dATP-dependent formation of Apaf-1/caspase-9 complex initiates an apoptotic protease cascade. (1997) *Cell*, 91, 479-489
20. Susin, S. A. , Lorenzo, H. K. , Zamzami, N. , Marzo, I. , Snow, B. E. , Brothers, G. M. , Mangion, J. , Jacotot, E. , Costantini, P. , Loeffler, M. , Larochette, N., Goodlett, D. R., Aebersold, R., Siderovski, D. P., Penninger, J. M. & Kroemer, G. Molecular characterization of mitochondrial apoptosis-inducing factor. (1999) *Nature*, 397, 441-446

21. Du, C., Fang, M., Li, Y., Li, L. & Wang, X. Smac, a mitochondrial protein that promotes cytochrome c-dependent caspase activation by eliminating IAP inhibition. (2000) *Cell*, 102, 33-42
22. Nagata, S. Apoptosis mediated by Fas and its related diseases. (1997) *Nippon Ika Daigaku Zasshi.*, 64(5), 459-62
23. Luo, X. , Budihardjo, I. , Zou, H. , Slaughter, C. & Wang, X. Bid, a Bcl2 interacting protein, mediates cytochrome c release from mitochondria in response to activation of cell surface death receptors (1998) *Cell*, 94, 481-490
24. Sakahira, H., Enari, M. & Nagata, S. Cleavage of CAD inhibitor in CAD activation and DNA degradation during apoptosis. (1998) *Nature*, 391, 96-99
25. Enari, M., Sakahira, H., Yokoyama, H., Okawa, K., Iwamatsu, A. & Nagata, S. A. Caspase-activated DNase that degrades DNA during apoptosis, and its inhibitor ICAD. (1998) *Nature*, 391,43-50
26. Gastman, B. R., Yin, X. M., Johnson, D.E., Wieckowski, E., Wang, G. Q., Watkins, S. C. & Rabinowich, H. Tumor-induced apoptosis of T cells: amplification by a mitochondrial cascade. (2000) *Cancer Res.*, 60(24), 6811-7.
27. Wride, M.A. Minireview: apoptosis as seen through a lens. (2000) *Apoptosis*, 5(3), 203-9
28. Thomas, W.D., Zhang, X.D., Franco, A.V., Nguyen, T. & Hersey, P. TNF-related apoptosis-inducing ligand-induced apoptosis of melanoma is associated with changes in mitochondrial membrane potential and perinuclear clustering of mitochondria. (2000) *J. Immunol.*, 165(10), 5612-20

29. Hail, N. Jr. & Lotan, R. Mitochondrial permeability transition is a central coordinating event in N-(4-hydroxyphenyl) retinamide-induced apoptosis. (2000) *Cancer Epidemiol. Biomarkers Prev.*, 9(12),1293-301
30. Matoyama, T., Hojo, M. & Watanabe, H. Comparison of seven cell lines derived from human gastric carcinomas. (1986) *Acta. Pathol. Japonica*, 36, 6583
31. Siprashvili, Z., Sozzi, G., Barnes, L.D., McCue, P., Robinson, A.K., Eryomin, V., Sard, L., Tagliabue, E., Greco, A., Fusetti, L., Schwartz, G., Pierotti, M.A., Croce, C.M. & Huebner K. Replacement of Fhit in cancer cells suppresses tumorigenicity. (1997) *Proc. Natl. Acad. Sci. USA*, 94(25),13771-13776
32. Askari, M., Alarie, J. P., Moreno-Bondi, M. & Vo-Dinh, T. Application of an antibody biochip for p53 detection and cancer diagnosis. (2001) *Biotechnology Progress*, (In press)
33. Allain, L. R., Askari, M., Stokes, D. L., & Vo-Dinh, T. Microarray sampling platform fabrication using bubble-Jet technology for a biochip System. (2001) *Fresenius J. Anal. Chem.*, (In press)
34. Askari, M., Miller, G. & Vo-Dinh, T. Simultaneous detection of the FHIT gene and protein using Microarray-based biochip. (2001) (In preparation)
35. Kravtsov, V. D., Daniel, T.O. & Koury, M. J. Comparative analysis of different methodological approaches to the in vitro study of drug-induced apoptosis. (1999) *Am. J. Pathol.*, 155(4),1327-39

36. Druck, T., Hadaczek, P., Fu, T. B., Ohta, M., Siprashvili, Z., Baffa, R., Negrini, M., Kastury, K., Veronese, M. L., Rosen, D., Rothstein, J., McCue, P., Cotticelli, M. G., Inoue, H., Croce, C. M. & Huebner, K. Structure and expression of the human FHIT gene in normal and tumor cells. (1997) *Cancer Res.*, 57, 504-512
37. Sozzi, G., Tornielli, S., Tagliabue, E., Sard, L., Pezzella, F., Pastorino, U., Minoletti, F., Pilotti, S., Ratcliffe, C., Veronese, M. L., Goldstraw, P., Huebner, K., Croce, C. M., & Pierotti, M. A. Absence of Fhit protein in primary lung tumors and cell lines with FHIT gene abnormalities. (1997) *Cancer Res.*, 57, 5207-12
38. Thiagalingam, S., Lisitsyn, N.A., Hamaguchi, M., Wigler, M. H., Willson, J. K., Markowitz, S. D., Leach, F. S., Kinzler, K. W, & Vogelstein, B. Evaluation of the FHIT gene in colorectal cancers. (1996) *Cancer Res.*, 56, 2936-9
39. Fong, K. M., Biesterveld, E. J., Virmani, A., Wistuba, I., Sekido, Y., Bader, S. A., Ahmadian, M., Ong, S. T., Rassool, F. V., Zimmerman, P. V., Ciaccone, G., Gazdar, A. F. & Minna, J. A. FHIT and FRA3B 3p14.2 allele loss are common in lung cancer and preneoplastic bronchial lesions and are associated with cancer-related FHIT cDNA splicing aberrations. (1997) *Cancer Res.*, 57, 2256-2267
40. Mao, L., Fan, Y-H., Lotan, R. & Hong, W. K. Frequent abnormalities of FHIT, a candidate tumor suppressor gene, in head and neck cancer cell lines. (1996) *Cancer Res.* 56, 5128-5131
41. van den Berg, A., Draaijers, T.G., Kok, K., Timmer, T., Van der Veen, A.Y. Veldhuis, P.M., de Leij, L., Gerhartz, C.D., Naylor, S.L., Smith, D.I., & Buys, C.H. Normal FHIT transcripts in renal cell cancer- and lung cancer-derived cell lines, including a cell line with a homozygous deletion in the FRA3B region. (1997)

Genes Chromosomes Cancer, 19, 220-227

42. Fisher, D.E. Apoptosis in cancer therapy: Crossing the threshold. (1994) *Cell*, 78, 539
43. Kerr, J. F. R., Winterford, C. M. & Harmon, B. V. Apoptosis: Its significance in cancer and cancer therapy. (1994) *Cancer* 73, 2013
44. Wickremasinghe, R. G. & Hoffbrand, A.V. Biochemical and Genetic Control of Apoptosis:Relevance to Normal Hematopoiesis and Hematological Malignancies (1999) *Blood*, 93 (11), 3587-3600
45. Zamzami, N., Marchetti, P., Castedo, M., Zanin, C, Vayssière, J. L., Petit, P. X. & Kroemer, G. Reduction in mitochondrial potential constitutes an early irreversible step of programmed lymphocyte death in vivo. (1995) *J. Exp. Med.*, 181,1661-1672
46. Liu, X., Kim, C. N., Yang, J., Jemmerson, R. & Wang, X. Induction of apoptotic program in cell-free extracts: requirement for dATP and cytochrome c. (1996) *Cell*, 86, 147-157
47. Zamzami, N., Susin, S. A., Marchetti, P., Hirsch, T., Gómez-Monterrey, I., Castedo, M. & Kroemer, G. Mitochondrial control of nuclear apoptosis. (1996) *J. Exp. Med.*, 183,1533-1544
48. Susin, S.A., Zamzami, N., Castedo, M., Hirsch, T., Marchetti, P., Macho, A., Daugas, E., Geuskens, M. & G. Kroemer. Bcl-2 inhibits the mitochondrial release of an apoptogenic protease. (1996) *J. Exp. Med.*, 184, 1331-1342
49. Yang, J., Liu, X., Bhalla, K., Kim, C. N., Ibrado, A. M., Cai, J., Peng, T.I., Jones, D. P. & Wang, X. Prevention of apoptosis by Bcl-2: release of cytochrome c from mitochondria blocked. (1997) *Science*, 275, 1129-1132

50. Kluck, R. M., Bossy-Wetzell, E., Green, D. R. & Newmeyer, D. D. The release of cytochrome c from mitochondria: a primary site for Bcl-2 regulation of apoptosis. (1997) *Science*, 275, 1132-1136
51. Shimizu, S., Eguchi, Y., Kamiike, W., Waguri, S., Uchiyama, Y., Matsuda, H. & Tsujimoto, Y. Bcl-2 blocks loss of mitochondrial membrane potential while ICE inhibitors act at a different step during inhibition of death induced by respiratory chain inhibitors. (1996) *Oncogene*, 13, 21-29
52. Zamzami, N., Susin, S. A., Marchetti, P., Hirsch, T., Gomez-Monterrey, I., Castedo, M. & Kroemer, G. Mitochondrial control of nuclear apoptosis. (1996) *J. Exp. Med.*, 183, 1533-1544.
53. Marchetti, P., Castedo, M., Susin, S. A., Zamzami, N., Hirsch, T., Macho, A., Haeffner, A., Hirsch, F., Geuskens, M. & Kroemer, G. Mitochondrial permeability transition is a central coordinating event of apoptosis. (1996) *J. Exp. Med.*, 184, 1155
54. Kroemer, G., Zamzami, N. & Susin, S. A. Mitochondrial control of apoptosis. (1997) *Immunol. Today*, 18, 44-51
55. Susin, S. A. Zamzami, N., Castedo, M., Hirsch, T., Marchetti, P., Macho, A., Daugas, E., Geuskens, M. & Kroemer, G. Bcl-2 inhibits the mitochondrial release of an apoptogenic protease. (1996) *J. Exp. Med.* 184, 1331-41
56. Vo-Dinh, T. (1978) Synchronous luminescence for multi-component analysis. *Anal. Chem.* 50, 396
57. Vo-Dinh, T. Analytical measurements and instrumentation for process and pollution control. Edited by Cheremisinoff, P., Perlis, H. Luminescence spectrometry, 47-80, Ann Arbor Science publishers.

58. Vo-Dinh, T., Gammage, R. B. & Martinez, P. R. Analysis of a workplace air particulate sample by synchronous luminescence and room-temperature phosphorescence. (1981) *Anal. Chem.*, 53(2), 253-8
59. Watts, W.E., Isola, N.R., Frazier, D. & Vo-Dinh, T. Differentiation of normal and neoplastic cells by synchronious fluorescence: Rat liver epithelial and rat hepatoma cell models. (1999) *Analytical letters*, 13, 2583-2594
60. Walker, J. E. The regulation of catalysis in ATP synthase. (1994) *Curr. Biol.* 4, 912-918
61. Marzo, I., Brenner, C., Zamzami, N., Susin, S. A., Beutner, G. Brdiczka, D., Remy, R., Xie, Z.H., Reed, J.C., & Kroemer, G. The permeability transition pore complex: a target for apoptosis regulation by caspases and bcl-2-related proteins. (1998) *J. Exp. Med.*, 187, 1261-71
62. Gunter, T. E. & Pfeiffer, D. R. Mechanisms by which mitochondria transport calcium. (1990) *Am. J. Physiol.*, 258, C755-C786.
63. Shimizu, S., Eguchi, Y., Kamiike, W., Funahashi, Y., Mignon, A., Lacronique, V., Matsuda, H., & Tsujimoto, Y. Bcl-2 prevents apoptotic mitochondrial dysfunction by regulating proton flux. (1998) *Proc. Natl. Acad. Sci. USA*, 95, 1455
64. Pfeiffer, D. R., Gudz, T. I., Novgorodov, S. A. & Erdahl, W. L. (1995) *J. Biol. Chem.*, 270, 4923-2932
65. Susin, S. A., Zamzami, N., Castedo, M., Daugas, E., Wang, H.G., Geley, S., Fassy, F., Reed, J. C. & Kroemer, G. (1997) *J. Exp. Med.*, 186, 25-37

66. Yang, J. H., Gross, R.L., Basinger, S. F. & Wu, S. M. Apoptotic cell death of cultured salamander photoreceptors induced by cccp: CsA-insensitive mitochondrial permeability transition. (2001) *J. Cell Sci.*, 114(Pt 9), 1655-1664
67. Kristian, T., Gertsch, J., Bates, T. E. & Siesjo, B. K. Characteristics of the calcium-triggered mitochondrial permeability transition in nonsynaptic brain mitochondria: effect of cyclosporin A and ubiquinone O. (2000) *J. Neurochem.*, 74(5), 1999-2009
68. Khaspekov, L., Friberg, H., Halestrap, A., Viktorov, I. & Wieloch, T. Cyclosporin A and its ionimmunosuppressive analogue N-Me-Val-4-cyclosporin A mitigate glucose/oxygen deprivation-induced damage to rat cultured hippocampal neurons. (1999) *Eur. J. Neurosci.*, 11(9), 3194-8
69. Siesjo, B.K., Elmer, E., Janelidze, S., Keep, M., Kristian, T., Ouyang, Y.B. & Uchino, H. Role and mechanisms of secondary mitochondrial failure. (1999) *Acta. Neurochir. Suppl. (Wien)*, 73,7-13
70. Gonzales, D. H. & Neupert, W. Biogenesis of mitochondrial c-type cytochromes. (1990) *Bioenerg. Biomembr.*, 22, 753

APPENDIX

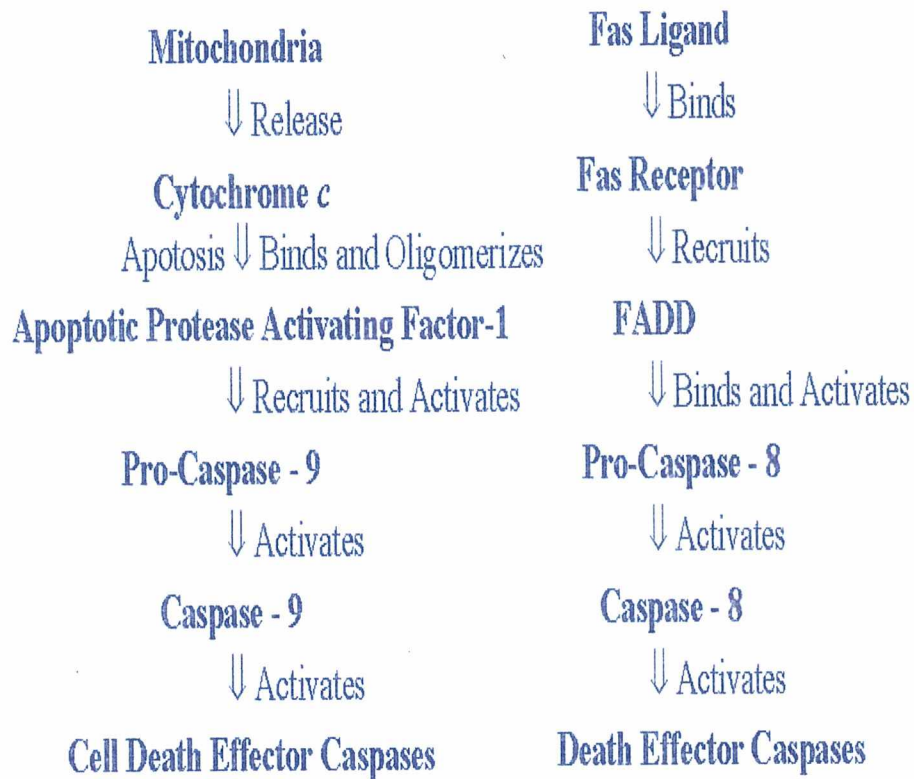


Figure 5.1 Mitochondrial and death receptor pathways are the two major apoptotic pathways that converge on cleavage of the cell death effector procaspases.

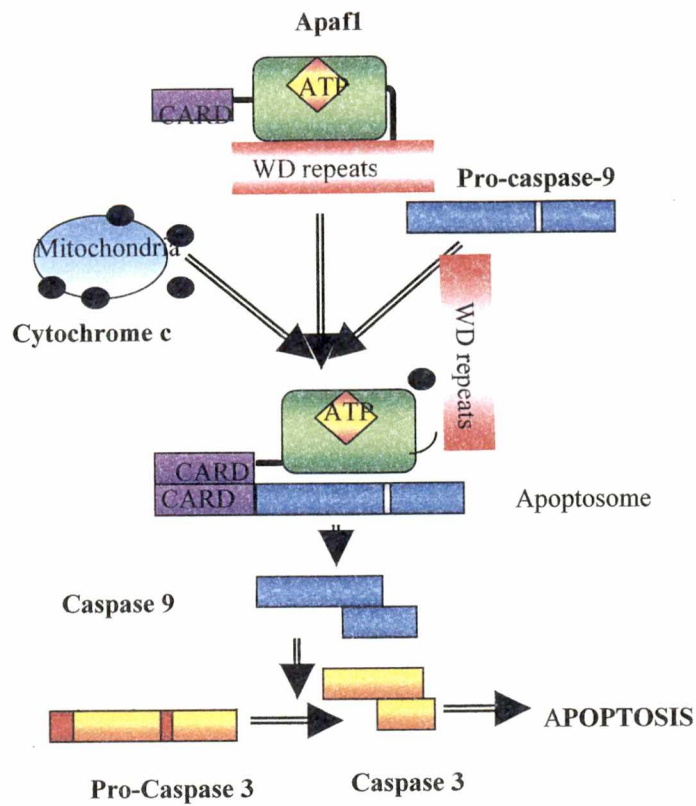
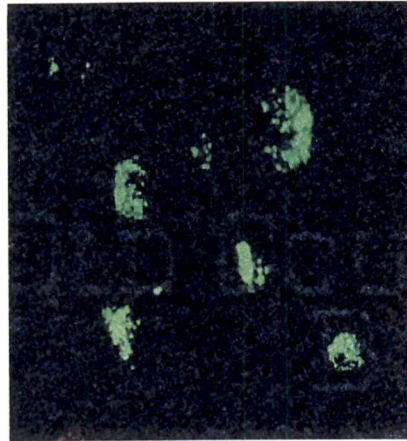


Figure 5.2 Mitochondria induce apoptosis by releasing cytochrome c from the intermembrane space to the cytosol. Cytosolic cytochrome c interacts with apoptotic protease activating factor 1 and procaspase 9 to form the apoptosome. In the presence of ATP, the apoptosome cleaves procaspase 9 to the active form caspase 9, which, in turn, cleaves procaspase 3 to active caspase 3.



(a) MMC-MKN/FHIT



(b) MMC-MKN/E4

Figure 5.3 Expression of FHIT significantly inhibited apoptosis induced by MMC treatment for 20 h and analyzed by in situ TUNEL staining. Comparison of staining profiles of the MKN/FHIT (a) expressing Fhit protein with that of FHIT-minus MKN/E4 cells indicated a higher percentage of apoptotic MKN/FHIT with condensed and fragmented nuclei incorporating fluorescein-labeled dUTP.

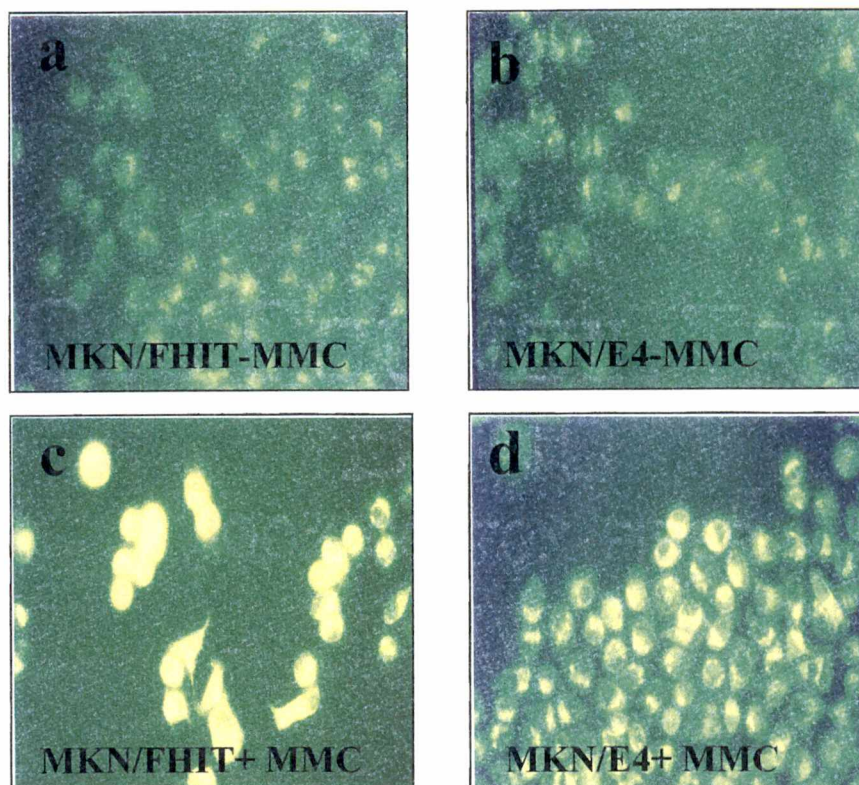
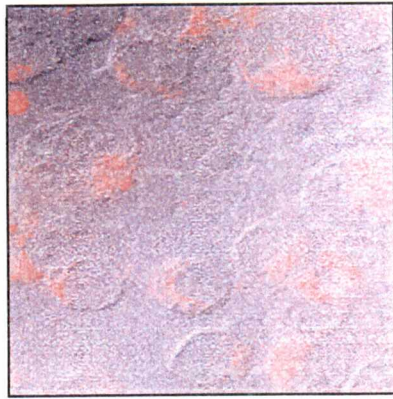
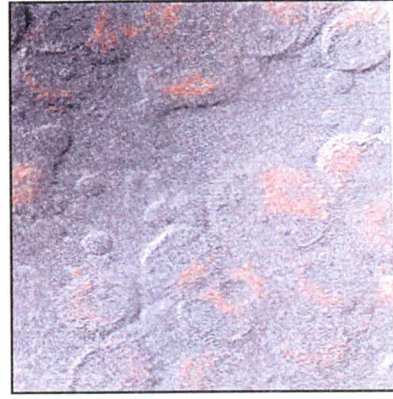


Figure 5.4 Apoptotically-induced and untreated MKN/FHIT and MKN/E4 cells were incubated in growth media containing rhodamine123 which is a mitochondria specific lipophilic cation fluorescent dye. The dye is taken up in proportion to $\Delta\Psi_m$. The increase in rhodamine 123 uptake by MMC-treated cells was visually confirmed by fluorescent light microscopy (c,d) over untreated cells (a,b). However, MMC-treated MKN/FHIT cell staining (c) was significantly enhanced as compared to staining of FHIT-negative MKN/E4 cells (d).

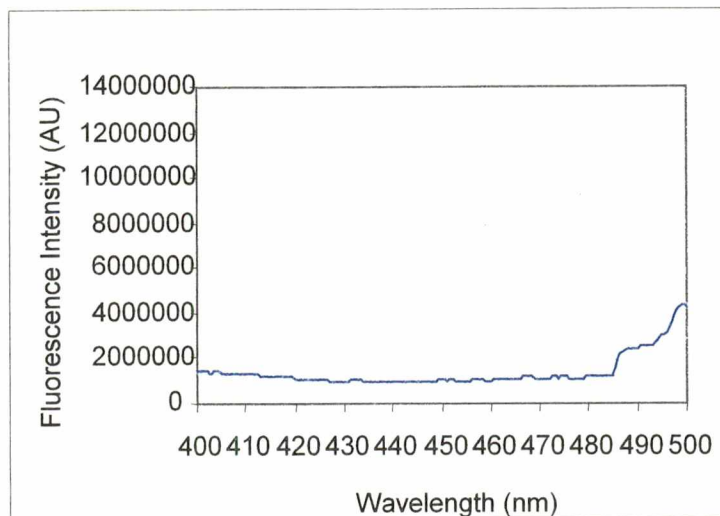


(a) MMC-MKN/FHIT

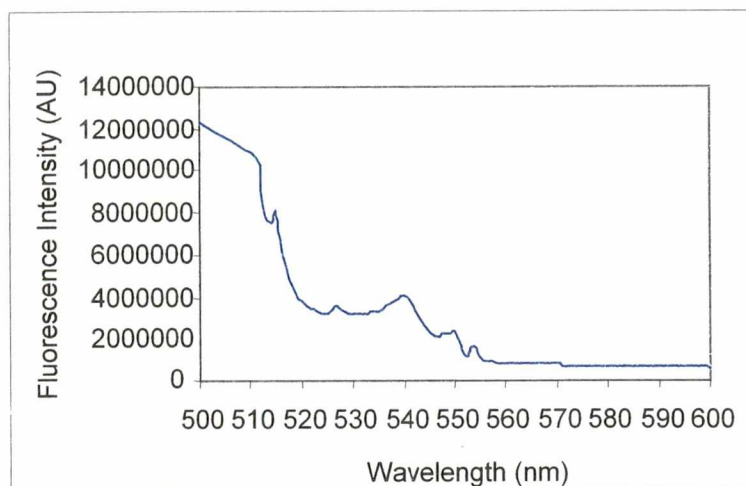


(b) MMC-MKN/E4

Figure 5.5 Confocal microscopy of MKN/FHIT and MKN/E4 cells incubated in media containing rhodamine 123 after induction of programmed cell death. Loss of mitochondrial membrane potential was demonstrated by increased uptake of rhodamine 123 by MKN/FHIT over MKN/E4 cells.

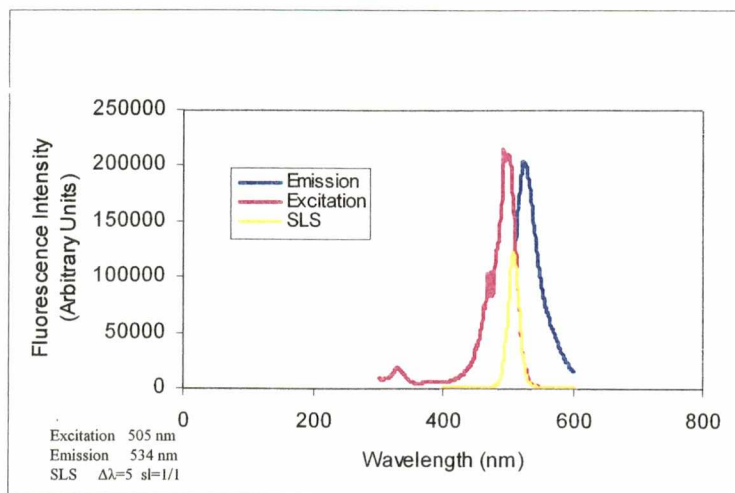


(a) MKN/FHIT Cells and R 123 Excitation spectrum

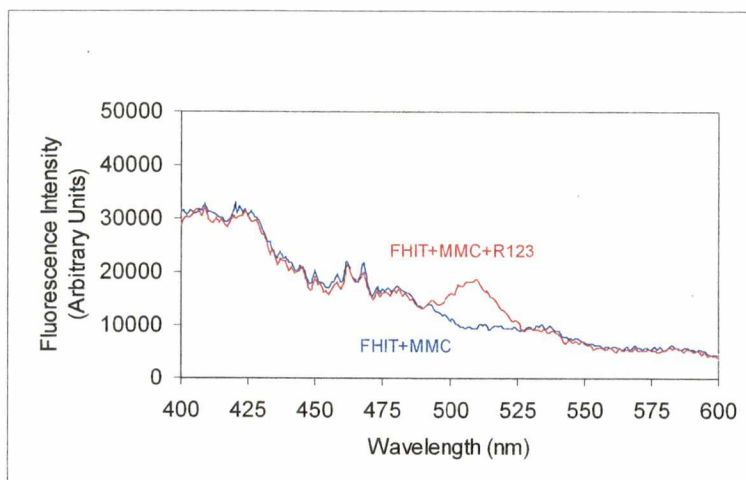


(b) MKN/FHIT Cells and R 123 Emission spectrum

Figure 5.6 Excitation (a) and emission (b) spectra of rhodamine 123 which was taken up by mitochondria of MKN/FHIT cells.

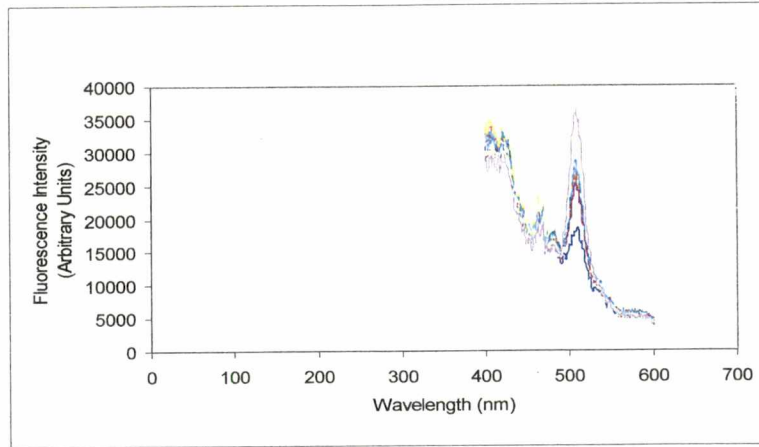


(a) Rhodamine 123 spectra

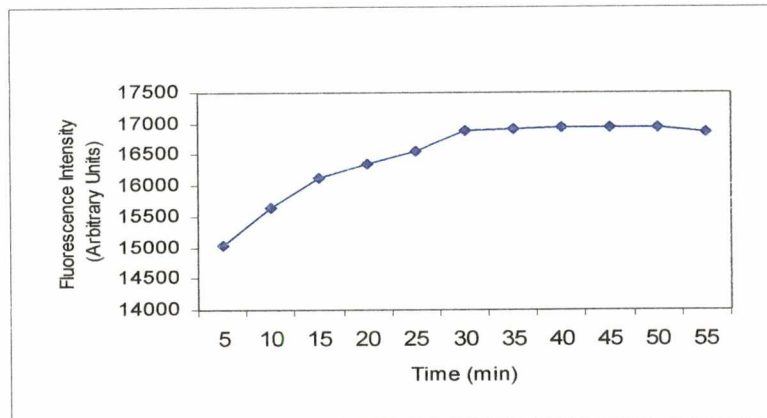


(b) Mitochondrial Rhodamine 123 uptake

Figure 5.7 Excitation, emission and eynchronous spectra of R123 in PBS with a peak at 510 nm (a), and Synchronous spectra of cellular R123 uptake as a result of alterations in mitochondrial membrane potential of the MMC-treated and untreated MKN/FHIT (b) are illustrated.



(a) R123 uptake in apoptotic MKN/FHIT cells



(b) R123 uptake in apoptotic MKN/FHIT cells/time

Figure 5.8 Loss of $\Delta\Psi_m$ in the mitochondrial transmembrane of apoptotically-induced cells as a function of time (a). A steady increase in the cellular uptake of R123 was observed for the first 30 min after which the cells reached a steady state of equilibrium (b).

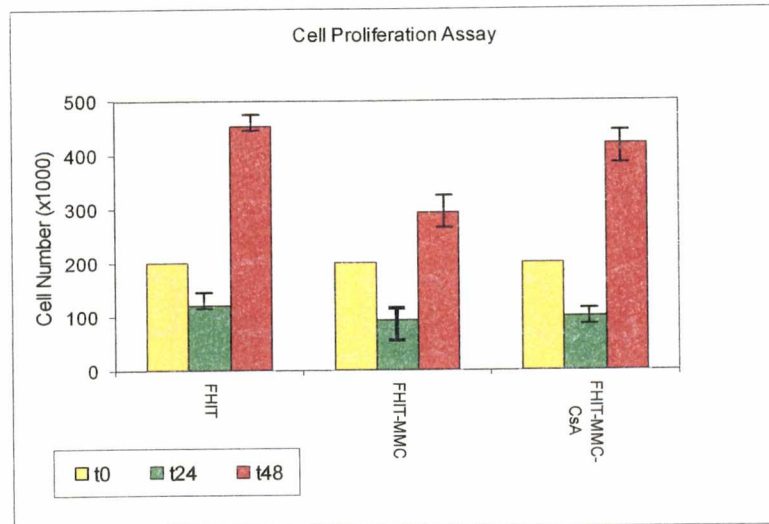


Figure 5.9 Effects of Fhit protein expression on cell proliferation in presence or absence of apoptotic inhibitor was investigated. The proliferation rate of MKN/FHIT cells maintained in growth media supplemented with MMC (second group of bar graphs) was significantly decreased ($p < 0.05$) in comparison with the growth rate of cells cultured in the unsupplemented growth media (first group of bar graphs). Effects of the megachannel antagonist CsA blocked decrease in the doubling time of cells (third group of bar graphs) (c).

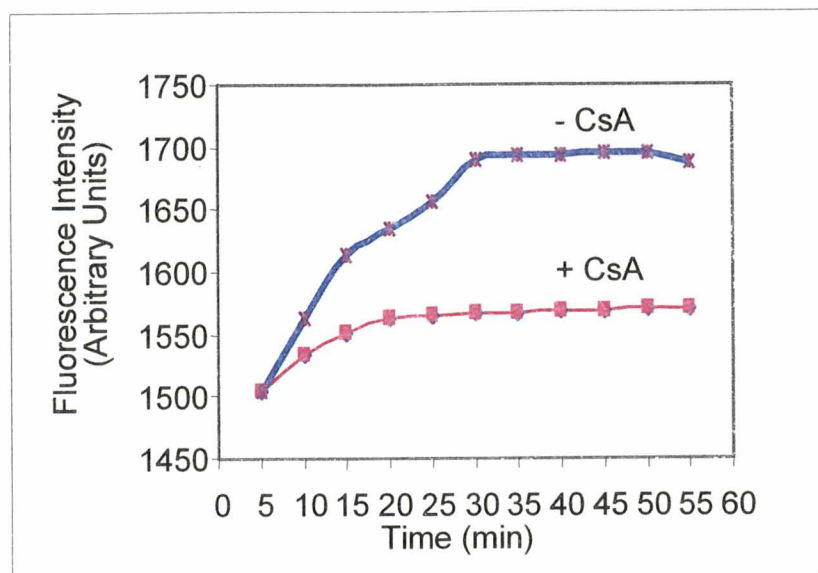
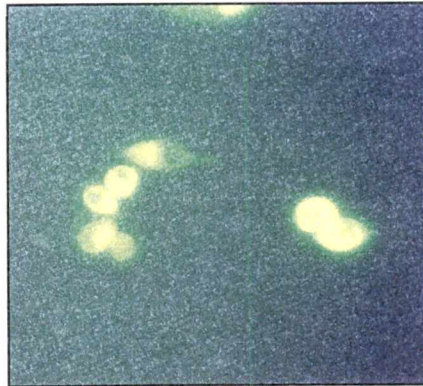


Figure 5.10 Synchronous luminescence spectroscopy revealed prevention of $\Delta\Psi_m$ -dependent uptake of R123 in apoptotically induced MKN/FHIT cells treated with CsA.

Figure 5.11 Ultraviolet fluorescence microscopy of MKN/FHIT cells after rhodamine 123 incubation. MMC treatment (b) induced loss of membrane potential in mitochondrial organelles and increased rhodamine 123 uptake over untreated cells (a). Cyclosporin A inhibited loss of membrane potential as indicated by a lower level of rhodamine 123 uptake by cells.



MKN/FHIT



MKN/FHIT

+MMC

- CsA



MKN/FHIT

+MMC

+ CsA

Figure 5.11

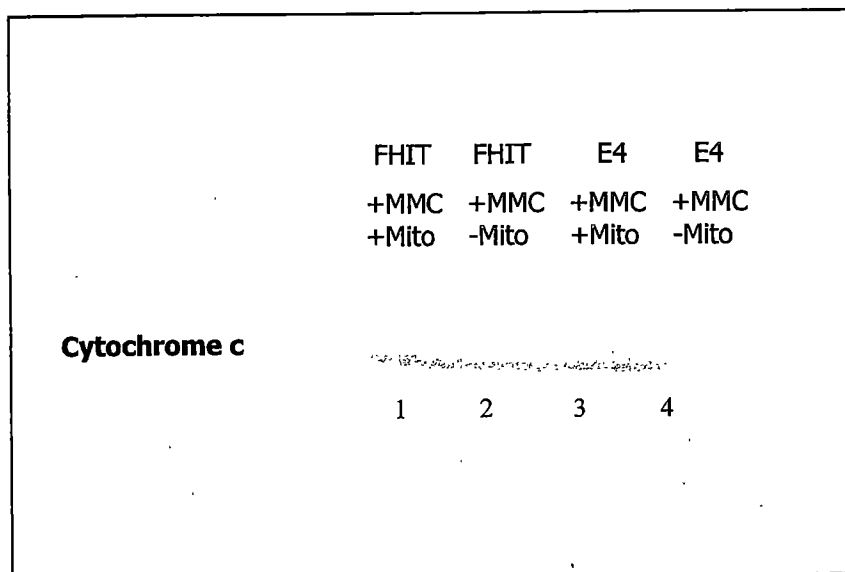


Figure 5.12 Protein immunoblot analysis of cytochrome c expression in lysates of apoptotically induced MKN/FHIT and MKN/E4 cells. Samples of whole cell lysates or mitochondria extracted lysates were subjected to PAGE electrophoresis, western blotting, cytochrome c antibody probing and chemiluminescence visualization. Cytochrome c was detected in whole cell lysates of both MKN/FHIT and MKN/E4 cells (lanes 1 and 3). However, treatment of the MKN/FHIT cells with MMC resulted in translocation of cytochrome c from the mitochondria into the cytosol (lane 2), indicated by equivalent concentration of cytochrome c in the sample where mitochondria was present in the cytosol (lane 1). Detectable cytochrome c in MKN/E4 cell lysate did not translocate into the cytoplasm as indicated by diminished protein band in the mitochondria removed lane (lane 4) as compared with the lane containing total expressed cytochrome c (lane 3).

PART SIX

SUMMARY AND CONCLUSION

6.1 SUMMARY

6.1.1 FHIT Gene

Human chromosomal fragile sites map to chromosome bands that are nonrandomly altered by translocations or deletions in human neoplasms (1). The recombinant nature of fragile sites, possibly enhanced by environmental carcinogens, has been linked to altered expression of oncogenes or tumor suppressor genes at these regions (2). This finding implies that alterations of expression of genes at fragile sites could trigger clonal expansion of preneoplastic and neoplastic cells. Fragile histidine triad, the FHIT gene, spanning the most inducible human common fragile site, FRA3B, at chromosome 3p14.2, is thus far the only example of a frequently altered gene at a constitutive fragile region and it shows hallmarks of a tumor suppressor gene (3).

The FHIT gene is altered by deletions in a large fraction of cancer, including lung, breast, head and necks, cervical, bladder, esophageal, stomach and pancreatic cancer (2, 4). FHIT is also interrupted by an inherited translocation in a family with predisposition to the development of renal carcinomas. Immunohistochemical studies and immunoblot analysis of human malignancies have demonstrated that tumors and cell lines expressing altered FHIT transcripts, with genomic rearrangements of the FHIT locus, either do not express the Fhit protein or express it at reduced levels (4-7). Given that both FHIT alleles are altered frequently in human tumors, and that the translocation associated with hereditary kidney cancer disrupts one FHIT allele, it is reasonable to consider FHIT

as a tumor suppressor gene (3).

Nonetheless, several lines of evidence garnered over the past few years have called into question the role of FHIT as a classical tumor suppressor gene, and have raised the question of whether its apparent cancer involvement simply reflects its location within an unstable region of the genome (Part one). The paradigm of FHIT emphasized that confirming its role as a tumor suppressor gene was essential.

Tumor suppressor genes are genes whose protein products are important for the normal regulation of the balance between cell growth and differentiation. Tumor suppressor genes are recessive, evolutionarily conserved genes that are defined by the impact of their absence. Mutation, inactivation or deletion of such genes, resulting in a loss of homozygosity through allele elimination, causes a loss in cell function and confer genetic predisposition to increased risk of tumor development. To verify the tumor suppressor activity of the FHIT gene it was necessary to evaluate effects of Fhit protein expression on i) cell proliferation *in vitro*, ii) tumor formation efficiency *in vivo*, and iii) cell cycle kinetics. To investigate mechanisms for a possible selective growth advantage of FHIT-negative cells, we obtained an *in vitro* model for expression of Fhit protein in cancer-derived cells. The experimental model consisted of a human stomach cancer cell line, which originally lacked Fhit expression. This cell line was transduced with FHIT cDNA and stable Fhit protein expressing clones were derived. Phenotypes of such exogenous Fhit-expressing cells relative to the parallel vector/neo transfected but Fhit-negative cells, both derived from the common gastric carcinoma parental cell line were examined.

As a prerequisite for these studies, the stability of the FHIT gene transfection and the status of expression of Fhit protein in these transfected gastric carcinoma cell lines were investigated by using the biochip detection technology and western blot analysis, respectively (Part two).

Fhit-related proteins have been found in mammals and yeasts (8,9) and constitute a branch of the histidine triad (HIT) superfamily of proteins (10). The Fhit branch includes the *Schizosaccharomyces pombe* diadenosine tetraphosphate hydrolase [dinucleoside 5,5-P₁,P₄-tetraphosphate (Ap₄A) hydrolase] (11,8) to which Fhit is functionally similar. Here, we have shown that *in vitro*, Fhit protein behaves as a typical dinucleoside 5,5-P₁,P₃-tetraphosphate (Ap₄A) hydrolase. We used synchronous luminescence spectroscopy for analyses of substrate breakdown by the Fhit enzyme and detection of the byproducts of the hydrolysis reaction (Part three).

To determine if expression of exogenous wild-type Fhit affected the ability of the stable transfectants to grow, the transfected cells were tested for growth in liquid medium supplemented with 10% FBS, in presence and absence of mutagens and apoptosis inducing stimuli. The results demonstrated a decrease in cell proliferation of the FHIT-positive cells over the rates observed in the FHIT-negative cells. The cellular kinetics and the cell cycle progression of the FHIT-positive cells were found to be different than in those cells not expressing the Fhit protein. The re-expression of Fhit, inhibited cell growth, induced apoptosis and resulted in accumulation of cells in the S phase of the cell cycle (Part four).

To demonstrate that FHIT is a bona fide tumor suppressor, the Fhit-expressing cells and cells with no detectable Fhit expression were implanted into nude mice and analyzed for their ability to form tumors. In these experiments, the size and frequency of tumor induction were reduced in mice inoculated with the FHIT expressing cells. Taken together, results of the *in vitro* and *in vivo* studies imply the tumor suppressor activity of FHIT gene in cancer development (Part four).

Although the precise mechanism of the FHIT activity remains unclear, the role of FHIT as a tumor suppressor gene has been experimentally verified in cultured human cancer cells and in animal models by us and by others (12-18). In this investigation, re-expression of Fhit protein in a human gastric cancer cell line was linked to apoptosis *in vitro*. We assessed an array of biomarkers using various techniques including transmission electron microscopy, confocal microscopy, flow cytometry and TUNEL for these apoptotic analyses (Part four).

In most examples of physiological or pathological cell death, loss of mitochondrial membrane integrity constitutes an early critical event of the apoptotic lethal process. One of the signs of alterations in the mitochondrial membrane permeability that precede nuclear apoptosis is the translocation of cytochrome c from mitochondria to another localization, as well as the dissipation of the mitochondrial transmembrane potential. We determined the loss of mitochondrial transmembrane potential and translocation of cytochrome c from the mitochondria into the cytoplasm using fluorescence microscopy, synchronous luminescence spectroscopy and western blotting. These observations

strongly suggested that a mitochondria-involved apoptotic signaling pathway may be playing an important role in the tumor suppressor activity of the Fhit protein (Part five).

6.1.2 Biotechnology

Revolutionary scientific advances are enabling understanding of our genes and proteins in ways that can enhance our daily lives. An additional aim of the present study was to take advantage of the available wealth of knowledge to develop rapid, simple and practical approaches for cancer detection in molecular biology research laboratories and in clinical settings.

6.1.2.1 *Biochip Technology*

In the previous segments, we described an approach based on the development and further application of a unique technology, the biochip, utilizing the excellent sensitivity of fluorescence detection in conjunction with the biological specificity of antibody for antigen and DNA sequence specific annealing and interactions. The biochip technology, described in this work, is a multiarray optical biosensor that is based on integrating the photosensing microchip systems and signal amplifiers with data treatment technologies. Our results indicated that complexes of membrane-immobilized antibodies or DNA molecules and their respective, fluorescently-labeled antigens and single stranded DNA probes could be reliably detected in both saline solution and in human serum. The biochip not only allowed quantitative analysis of immobilized target DNA and

protein and their combination thereof, but also provided the means for simultaneous detection of multiplexed DNA and protein arrays, immobilized on the sampling platform (Part 2).

6.1.2.2 *Synchronous Luminescence Spectroscopy*

Spectroscopy techniques, widely recognized as powerful and sensitive analytical tools, are based on the detection of electromagnetic radiation emitted from molecules transitioning between different electronic states (34). Here, we have described a simple, yet highly sensitive and selective spectrometric technique, Synchronous Luminescence spectroscopy, for analysis of enzymatic action of Fhit protein. The qualitative and quantitative analysis of cleavage of the Ap₄A substrate by the Fhit protein was performed without the use of radioactive material or fluorescently labeled molecules. The spectra obtained from the hydrolysis reaction cell indicated presence of newly formed byproduct of the enzymatic reaction. An increase in the intensity of the byproduct peak was observed after addition of adenosine mono phosphate (AMP) to this reaction vial and also as the consequence of the increase in the substrate concentration. The obtained information confirmed the ability of the SL technique quantitatively measure the reaction byproducts. These results indicated the utility of the SL for analysis of enzymatic reactions and identification of compounds of interest (Parts 3,5).

6.2 CONCLUSION

6.2.1 FHIT GENE

In solid tumors, specific chromosomal deletions cause inactivation of tumor suppressor genes. Their inactivations usually result in abnormal cell cycle control and/or increased cell survival, leading to malignant transformations (19). The identification and understanding of the earliest genetic changes that initiate transformation in solid tumors, and detection of these events in premalignant lesions may result in development of new therapeutic approaches or synthesis of novel drugs for destroying premalignant cells, providing new opportunities for cancer prevention. In addition, we could use the proteins, encoded by the genes involved in these early steps of tumor development (or their biochemical pathways), as targets for novel therapeutical agents.

Taken together, (i) the observations made in this study and (ii) the recognition that some tumors and tumor-derived cell lines contain homozygous deletions in the FHIT gene and (iii) that translocation breakpoints of t(3;8)(p14.2;q24) are associated with familial kidney cancer and LOH in most common human malignancies, we have concluded that FHIT gene is indeed a target of chromosomal abnormalities at 3p14.2 observed in human carcinogenesis. Such abnormalities could lead to the loss of tumor suppressor activity through a mitochondria mediated programmed cell death pathway.

6.2.2 Biotechnology

Development of new technologies is essential for researchers and clinicians to be able to identify molecular alterations and diagnose diseases with precision, predetermine a patient's response to therapy, and empower individuals to make preventive lifestyle changes based on their susceptibility to certain diseases. In addition to investigating the tumor suppressor role of the FHIT gene, another major goal of this project was to develop new tools and techniques for research and medical laboratory applications.

6.2.2.1 *Biochip Technology*

The fusion of microelectronics, CMOS technology and molecular biology has created the new biochip technology, a sensitive and cost-effective tool in molecular diagnostics.

Biochip is suited for integration into fully automated systems, thus providing the basis for automation of molecular diagnostics with potential for high-sample throughput. This compact system is a user-friendly, inexpensive device amenable to on-site use with future potential for cancer detection in clinical settings.

6.2.2.2 *Synchronous Luminescence Spectroscopy*

The complexity of real-life samples in biological applications is such that conventional luminescence spectra, despite their remarkable features, are of little analytical value because of their featureless appearance. Synchronous Luminescence is a unique

technique that offers improved selectivity over conventional luminescence spectroscopy. This versatile technique eliminates the need for use of relatively undesirable and expensive radioisotopes and fluorescently labeled probes, as identifying markers for compounds of interest. It also does not require further identification of these compounds through other analytical techniques such as various forms of chromatography. This technique offers a great deal of selectivity and sensitivity, without sacrificing simplicity, for characterization of complex biological samples.

6.3 FUTURE RESEARCH DIRECTIONS

Further research into the molecular biology of FHIT-associated carcinogenesis will enhance our understanding of the genetic events, critical for the initiation and progression of variety of cancers, leading to more effective surveillance and treatment methodologies. Future goals of the FHIT related studies need to focus on finding the biological functions of the FHIT gene that affect cell growth, differentiation and cell death.

The ongoing identification and characterization of factors influencing apoptosis will eventually make it possible to predict tumor. The involvement of FHIT gene in programmed cell death has been determined. However, the exact sequence of events, *i.e.* activation of different caspase cascade pathways, in the FHIT-induced apoptosis is yet unknown. It is possible that multiple interacting molecular pathways are involved in the progression of the premalignant cells to neoplastic cancer cells. Examining the role of FHIT as a predictive and prognostic factor in apoptosis could prove promising.

Despite involvement of the FHIT gene in most common human cancers, the underlying molecular mechanisms of the FHIT deletions remain unknown. Further examination of the molecular basis of chromosomal fragility at 3p14.2 of the FHIT/FRA3B locus is necessary. A better understanding of the mechanisms of these events could allow early identification and elimination of precancerous cells.

In lung cancer associated with smoking, inactivation of FHIT occurs very early in tumor development (22). In other tumors, such as clear cell renal carcinoma and breast carcinoma, FHIT inactivation occurs in later stages of tumor progression (7,22). Thus, evaluation of FHIT expression in premalignant lesions and tumors may be of importance.

The current delineation of the molecular basis of cancer provides a strong rationale to consider tumor suppressor-gene therapy approaches for cancer as a complement to other cancer therapies. Prospective trials focusing on delivery of wild-type, tumor inhibitory FHIT gene to compliment FHIT mutations could establish the use of gene therapy as a component of the multimodal treatment for certain cancers.

Exploration of these venues could provide for a better understanding of the FHIT mechanism of action, identification of molecular events that predispose an individual to carcinoma development and potential identification of early markers of malignant transformation. In future, the enhanced knowledge of the activities of the gene will allow for early identification more precise and earlier risk assessment for individual patients, therefore, enabling more effective therapy.

REFERENCES

1. Yunis, J. J. & Soreng, A. L. Constitutive fragile sites and cancer. (1984) *Science*, 226, 1199-1204
2. Huebner, K., Garrison, P. N., Barnes, L. D. & Croce, C. M. The role of the FHIT/FRA3B locus in cancer. (1998) *Annu. Rev. Genet.*, 32, 7-31
3. Ohta, M., Inoue, H., Cotticelli, M. G., Kastury, K., Baffa, R., Palazzo, J., Siprashvili, Z., Mori, M., McCue, P., Druck, T., Croce, C. M. & Huebner, K. The FHIT gene, spanning the chromosome 3p14.2 fragile site and renal carcinoma-associated t(3;8) breakpoint, is abnormal in digestive tract cancers. (1996) *Cell*, 84, 587-597
4. Huebner, K., Sozzi, G., Brenner, C., Pierotti, M. A. & Croce, C. M. Fhit Loss in Lung Cancer: Diagnostic and Therapeutic Implications, (1999) *Adv. Oncol.*, 15, 3-10.
5. Druck, T., Hadaczek, P., Fu, T.B., Ohta, M., Siprashvili, Z., Baffa, R., Negrini, M., Kastury, K., Veronese, M. L., Rosen, D., Rothstein, J., McCue, P., Cotticelli, M. G., Inoue, H., Croce, C. M. & Huebner, K. Structure and expression of the human FHIT gene in normal and tumor cells. (1997) *Cancer Res.*, 57, 504-512
6. Sozzi, G., Tornielli, S., Tagliabue, E., Sard, L., Pezzella, F., Pastorino, U., Minoletti, F., Pilotti, S., Ratcliffe, C., Veronese, M. L., Goldstraw, P., Huebner, K., Croce, C. M., & Pierotti, M. A. Absence of Fhit protein in primary lung tumors and cell lines with FHIT gene abnormalities. (1997) *Cancer Res.*, 57, 5207-12
7. Baffa, R., Veronese, M. L., Santoro, R., Mandes, B., Palazzo, J. P., Rugge, M., Santoro, E., Croce, C. M., & Huebner, K. Loss of FHIT expression in gastric carcinoma. (1998) *Cancer Res.*, 58(20), 4708-14

8. Huang, Y., Garrison, P. N. & Barnes, L. D. Cloning of the *Schizosaccharomyces pombe* gene encoding diadenosine 5',5'''-P₁,P₄-tetrphosphate (Ap4A) asymmetrical hydrolase: sequence similarity with the histidine triad (HIT) protein family. (1995) *Biochem. J.*, 312, 925-932
9. Brenner, C., Garrison, P., Gilmour, J., Peisach, D., Ringe, D., Petsko, G. A. & Lowenstein, J. M. Crystal structures of HINT demonstrate that histidine triad proteins are GalT-related nucleotide-binding proteins. (1997) *Nat. Struct. Biol.*, 4, 231-238
10. Seraphin, B. The HIT protein family: a new family of proteins present in prokaryotes, yeast and mammals. (1992) *DNA Sequence*, 3, 177-179
11. Barnes, L. D., Garrison, P. N., Sibrashvili, Z., Guranowski, A., Robinson, A. K., Ingram, S. W., Croce, C. M., Ohta, M. & Huebner, K. Fhit, a putative tumor suppressor in humans, is a dinucleoside 5',5'''-P₁,P₃-triphosphate hydrolase. (1996) *Biochemistry*, 35, 11529-11535
12. Sibrashvili, Z., Sozzi, G., Barnes, L. D., McCue, P., Robinson, A.K., Eryomin, V., Sard, L., Tagliabue, E., Greco, A., Fusetti, L., Schwartz, G., Pierotti, M.A., Croce, C. M. & Huebner, K. Replacement of Fhit in cancer cells suppresses tumorigenicity. (1997) *Proc. Natl. Acad.Sci. USA*, 94(25), 13771-6
13. Dumon, K.R., Ishii, H., Fong, L. Y., Zanesi, N., Fidanza, V., Mancini, R., Vecchione, A., Baffa, R., Trapasso, F., During, M. J., Huebner, K., & Croce, C. M. FHIT gene therapy prevents tumor development in Fhit-deficient mice. (2001) *Proc. Natl. Acad. Sci. USA*, 98(6), 3346-51

14. Herzog, C. R., Crist, K. A., Sabourin, C. L., Kelloff, G. J., Boone, C.W., Stoner, G.D., & You, M. Chromosome 3p tumor-suppressor gene alterations in cervical carcinomas. (2001) *Mol. Carcinog.*, 30(3),159-68
15. Lee, J. I., Soria, J. C., Hassan, K., Liu, D., Tang, X., El-Naggar, A., Hong, W. K., & Mao, L. Loss of Fhit expression is a predictor of poor outcome in tongue cancer. (2001) *Cancer Res.*, 61(3), 837-41
16. Ishii, H., Dumon, K.R., Vecchione, A., Trapasso, F., Mimori, K., Alder, H., Mori, M., Sozzi, G., Baffa, R, Huebner, K., & Croce, C. M. Effect of adenoviral transduction of the fragile histidine triad gene into esophageal cancer cells. (2001) *Cancer Res.*, 61(4):1578-84
17. Ji, L., Fang, B., Yen, N. , Fong, K. , Minna, J. D. & Roth, J. A. Induction of apoptosis and inhibition of tumorigenicity and tumor growth by adenovirus vector-mediated fragile histidine triad (FHIT) gene overexpression. (1999) *Cancer Res.* 59, 3333-3339
18. Sard, L., Accornero, P., Tornielli, S., Delia, D., Bunone, G., Campiglio, M., Colombo, M. P., Gramegna, M. ,Croce, C. M. , Pierotti, M. A. & Sozzi, G. The tumor-suppressor gene FHIT is involved in the regulation of apoptosis and in cell cycle control. (1999) *Proc. Natl. Acad. Sci. USA*, 96, 8489-8492
19. Hinds, P. W., & Weinberg, R. A. Tumor suppressor genes. (1994) *Cur. Opin. Genet. and Devel.*, 4, 135-141
20. Hadaczek, P., Siprashvili, Z., Markiewski, M., Domagala, W., Druck, T., McCue, P.A., Pekarsky, Y., Ohta, M., Huebner, K., & Lubinski, J. Absence or reduction of Fhit expression in most clear cell renal carcinomas. (1998) *Cancer Res.*, 58(14), 2946-51

21. Campiglio, M., Pekarsky, Y., Menard, S., Tagliabue, E., Pilotti, S., & Croce, C. M.

FHIT loss of function in human primary breast cancer correlates with advanced stage of the disease. (1999) *CancerRes.*, 59, 3866-3869

22. Sozzi, G., Pastorino, U., Moiraghi, L., Tagliabue, E., Pezzella, F., Ghirelli, C.,

Tornielli, S., Sard, L., Huebner, K., Pierotti, M.A., Croce, C.M., & Pilotti, S., Loss of FHIT function in lung cancer and preinvasive bronchial lesions. (1998) *Cancer Res.*, 58(22), 5032-7

VITA

Minoo Askari Dermenaki Farahani was born July 5th, 1959 in Tehran, Iran. She received her primary and secondary education in her native country, Iran. In pursuit of higher education, Minoo moved to the USA following High School graduation in 1977. She received her B.S. degree in Biology in May of 1982 from Worcester State College. After accepting a graduate assistantship, the author started her graduate study program in the department of Biological Sciences at the University of Massachusetts at Lowell where she received her M.S. degree in May of 1984. The main focus of her graduate project was on plant physiology and mechanisms involved in culmination of plant senescence. In the ensuing period until 1997, Minoo gained employment in various biological research laboratories, where she made contributions to numerous research projects in fields of immunology, genetics, molecular biology, toxicology, dermatology and photo medicine. The author started her Ph.D. program in the school of Biomedical Sciences at the University of Tennessee at Knoxville in 1997. Her investigations focused on application of various nanosensor technologies for cancer detection. Under direction of Dr. Tuan Vo-Dinh, she applied the biochip technology and synchronous luminescence spectroscopy to gain more insight into tumor suppressor activity and apoptotic role of the FHIT gene in inhibition of carcinogenesis. Minoo completed her Ph.D. degree in the summer of 2001 with a thesis entitled "Characterization of the Tumor Suppressor Activity of the FHIT Gene in Association with Application of Innovative Detection Technologies".